Deltares

Enabling Delta Life

Analysis report coarse sand barrier

Delta Flume tests (phase 2c)

Deltares

Analysis report coarse sand barrier

Delta Flume tests (phase 2c)

Esther Rosenbrand
Ane Wiersma
Ulrich Förster

Deltares

Analysis report coarse sand barrier

Delta Flume tests (phase 2c)

Esther Rosenbrand
Ane Wiersma
Ulrich Förster

Deltares

Title
Analysis report coarse sand barrier

Client	Project	Attribute	Pages
Waterschap Rivierenland	11200952-012	11200952-012-GEO-0001	92

Trefwoorden
Piping, preventive measure, coarse sand barrier, innovation, large-scale, scale effects, Delta Flume

Summary
Piping is one of the most important threats for the safety of Dutch levees, especially for the sections that are located along the main rivers. Based on research conducted in the past years several piping mitigating measures have been developed that prevent the pipe from progressing towards the river. One of these measures is the coarse sand barrier. The coarse sand barrier is a trench of coarse sand that prevents fine sand from upstream of the barrier from being eroded, and thereby hinders the pipe from progressing upstream below the dike.
The coarse sand barrier seems to be a promising measure based on preliminary and small-scale (phase 2a) and medium-scale (phase 2b) experiments, but additional research is required to assess the feasibility of this measure in practice.
The report at hand describes the research conducted in the third experimental phase (2c) of a larger research programme in which the feasibility of this method is assessed through the analysis of two large-scale experiments in the Delta Flume.

The current phase, similar to the previous phases, shows that the coarse sand barrier can provide a significant amount of resistance against piping. Two tests were conducted, using the same type of background- and barrier material. In the first test, the barrier protruded into the cover layer, in the second test, the top of the barrier was level with the background sand. The first Delta Flume test had to be abandoned because of leakage problems attributed to imperfections in the sealing of the joints between the flume wall and the bulkhead and an insufficient embedding of the bulkhead in the blanket layer. During this test, the pipe did not cause a clear failure of the barrier. Because of this, the distance of the coarse sand barrier with respect to the entry point was shortened in the second test, in order to be certain that failure of the barrier will be reached at head differences attainable in the flume. Indeed, the barrier collapsed at the end of the second test.

Both tests indicate that the pipe in front of the barrier did not progress along the entire width of the model, which is an important factor affecting the concentration of flow inside the barrier. Less progression parallel to the barrier is unfavourable for the critical head drop.

In test 1, the barrier crumbled into the pipe. It is most likely that a slope established in the barrier that reached all the way to the upstream end of the barrier at the point that the test was first interrupted to make repairs against leakage. The stability of the slope, and the hydraulic gradient at the upstream side of the slope probably govern the barrier strength in this case. A probable failure mechanism is that erosion of the slope reduces the slope inclination until vertical gradients on the upstream side cause heave and background sand washes over the barrier. This mechanism requires further analysis. Furthermore, excavations after the test indicate that the pipe cut into the blanket layer, which is remarkable.

In test 2, the barrier was level with the background sand and the failure mechanism appears to be the same as in the medium-scale tests: erosion of the barrier occurs when a critical local gradient inside the barrier is exceeded. Measurements indicate that a progression step (long growth step) occurred and that additional head increases were required to cause failure.

Deltares

Title
Analysis report coarse sand barrier

Client	Project	Attribute	Pages
Waterschap Rivierenland	11200952-012	11200952-012-GEO-0001	92

Pore pressure measurements were effective in analysing the arrival of the pipe at the barrier, and, to some extent, the progression of the pipe parallel, into, and through the barrier. Tracer particles with a density lower than water were not effective for identifying the pipe location as these were not always transported to the ditch directly but appear to have been trapped in the pipe.

For test 1, the stability of the slope, and the vertical gradients in the protrusion were analysed using a 2D model. The computed gradients on the slope face and the vertical gradient at the upstream end of the slope are low. This is in accordance with the observation that a complete failure did not occur during this test.

For test 2, the gradient inside the barrier at the progression step was modelled using a 2D and a 3D model. Using a 2D model, the hydraulic conductivity of the barrier had to be very low, and therefore the relative density (RD) very high, to fit the measured heads. The 3D model showed that this was due to 3D flow effects. Due to a larger number of unknowns in the 3D model, there is no unique combination of pipe length and RD of the barrier. This means that the RD of the barrier cannot be determined based on modelling, and that the RD estimated from preparation of the first test is the best estimate for the second test as well. The 2D and 3D model result in approximately the same strength criterion, because both models are fit to the measured heads.

The modelled strength criterion for test 2 is lower than for the medium-scale tests on GZB2. A value of 0.59 was computed, whereas the medium-scale tests had values of 0.72 and 0.86. This difference could possibly be due to: a lower RD of the barrier in the Delta Flume test; progression of the pipe at a greater distance from the transducers or the uncertainty regarding the variation among tests. Therefore, the result indicates that the strength criterion derived based on medium-scale tests is indeed valid at larger scale, but it does not prove the hypothesis conclusively.

The strength of a barrier which protrudes into the cover layer could be expected to exceed the strength of the situation where the barrier is level with the background sand. However, due to the different location of the barrier in tests 1and test 2, and due to leakage in test 1, it is not possible to conclude this based on these two tests alone. The failure mechanism in the case of a protruding barrier has been speculated on but requires further analysis and quantification of a strength criterion.

Versie	Datum	Auteur	Paraaf	Review	Paraaf	Goedkeuring	Paraaf
2.0	juni 2019	Esther Rosenbrand		Vera van Beek		Leo Voogt	
		Ane Wiersma					
		Ulrich Förster					

Status
final

Deltares

Title
Analysis report coarse sand barrier

Client	Project	Attribute	Pages
Waterschap Rivierenland	11200952-012	11200952-012-GEO-0001	92

Contents

1 Introduction

The current safety assessment method for piping, applied in the Netherlands, results in a large amount of sections to be reinforced. One of the sections that failed the safety assessment criteria is located at the river Waal nearby the village of Gameren. A dike stretch of 0.3 km failed the safety assessment criteria in the third safety assessment round, that was conducted in the period 2006-2011, and will need to be reinforced within short term. However, this is not the only dike section that will need to be reinforced. Indicative studies show that approximately half of the levees that are operated by Dutch Water Authority Rivierenland will not pass the current safety assessment criteria for piping.

Traditional reinforcement methods, like berms to increase seepage length, become less and less attractive due to the large required seepage length and the dense population and building development in this area. Several alternative (and innovative) methods are available that require less space. A new alternative method is the coarse sand barrier. This method entails the replacement of existing sand with coarse sand in a trench on the landside of the levee directly below the blanket layer. The blanket layer is restored after trenching.

The Dutch Water Authority Rivierenland intends to apply the coarse sand barrier at the pilot location Gameren as an innovative measure. Although experiments in the laboratory and at the IJkdijk (a former full-scale test facility in the North-Eastern part of the Netherlands) indicate the potential of the method, it is required to conduct a feasibility study to investigate whether the method offers sufficient resistance against piping in the field, both for the intended pilot location and for other, comparable locations. Based on the result of this feasibility study and the exploration of alternative measures, a preferential measure will be selected for the pilot location.

The purpose of the study is to assess the feasibility of the application of a coarse sand barrier as a piping measure for the location of Gameren, and for other locations along the Dutch main rivers in a more generic sense. To quantify the strength of the barrier, a criterion needs to be identified that predicts pipe formation into the barrier.

Based on analysis of small- and medium-scale experiments (Deltares, 2017d,e; Deltares, 2018a,b,c,d) the hypothesis is that the local horizontal gradient in the barrier near the tip of the pipe characterises the strength of a given barrier material at a given relative density, i.e. implying that different tests with the same material show the same local critical gradient in the barrier, regardless of the configuration or dimensions of the barrier. The feasibility of a coarse sand barrier at larger scale is analysed in this report, using the Delta Flume experiments described in (Deltares, 2019a).

The approach to the feasibility study is described in (Deltares, 2017a) and consists of the following phases:

- Phase 1: Literature study filter requirements and selection of barrier material.
- Phase 2a: Small-scale experiments and numerical simulation.
- Phase 2b: Medium-scale experiments and numerical simulation.
- Phase 2c: Large-scale experiments and numerical simulation.

The feasibility study is oriented towards one pilot location, but much of the knowledge developed in this study will be applicable in a more generic sense (at other locations). The

study focuses explicitly on the technical feasibility of the measure and will not address the practical aspects of installing the coarse sand barrier in the field. Phase 1 involved a literature study concerning applicable filter criteria for the design of a coarse sand barrier and was reported (Deltares, 2017b). This has led to the selection of barrier materials used for the small-scale experiments reported in (Deltares, 2017c). The report at hand presents the analysis of the experiments conducted in phase 2c of the feasibility study. The research questions for phase 2, which contains: the small-scale tests in phase 2a, and the medium-scale tests in phase 2b, and the Delta Flume tests in phase 2c (this report), are:

- What characterises the piping process in the presence of a (protruding) coarse sand barrier
- What is the local gradient upstream of the pipe, at which the pipe progresses into the barrier, in small-, medium- and large-scale experiments?
- What is the influence of the hydraulic conductivity contrast and grain size contrast of the chosen barrier material and original material on the resistance to piping?
- How can we monitor pipe formation through the barrier (failure of the barrier)?

2 Experiments

The experimental set-up including the details concerning the installed monitoring system containing pore pressure transducers and coloured tracers, the experiments and the observations of the two Delta Flume tests are reported in de Factual Report Delta Flume Experiments Coarse Sand Barrier (Deltares, 2019a). A general impression of the set-up is shown in Figure 2.1.

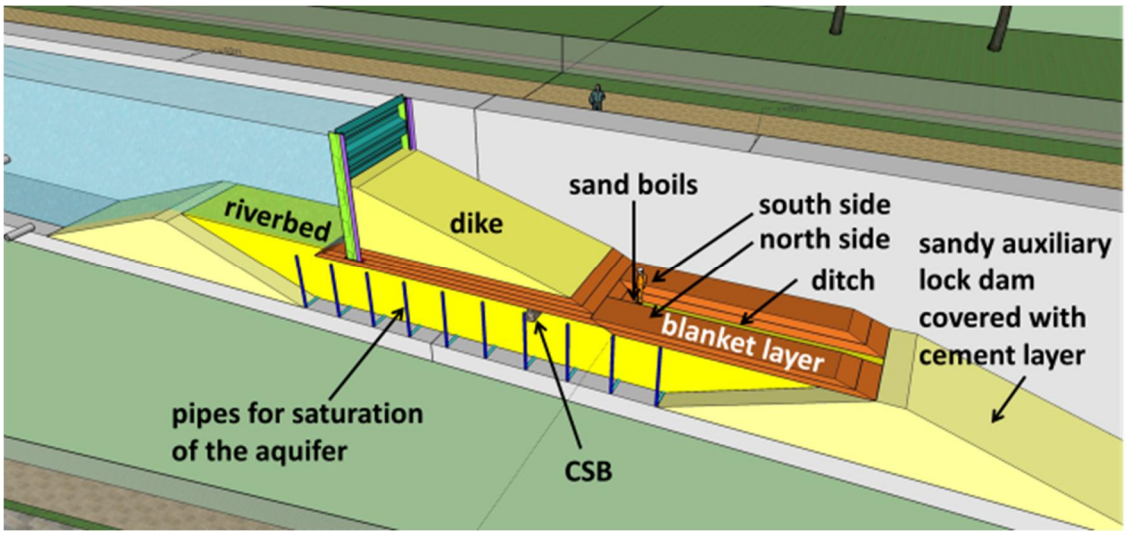

Figure 2.1 Schematic overview of the set-up of the Delta Flume experiments (Barrier (CSB) locations in the tests were different from shown in this sketch. The trapezoidal sand body has a width of 5 m and a length of 34. South and north side of sample are indicated for reference.

Figure 2.2 and Figure 2.3 present longitudinal sections and top views of the set-up of the two tests.

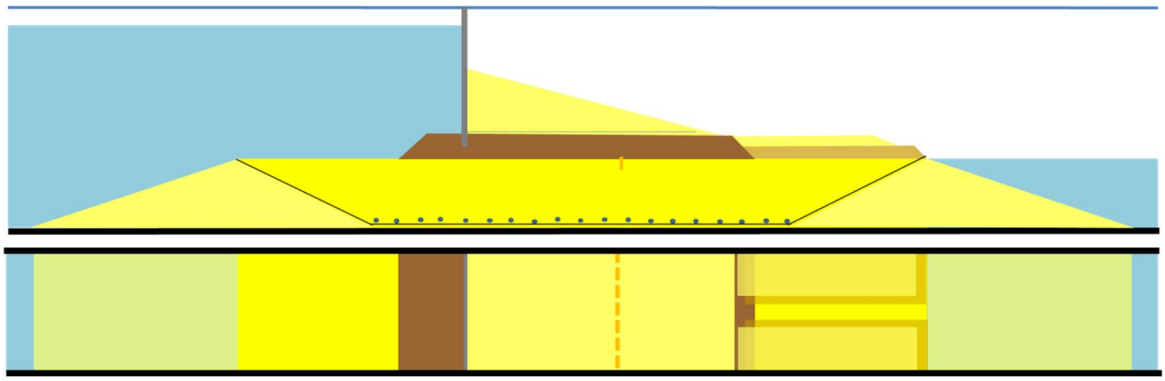

Figure 2.2 Longitudinal section and top view of first test (to scale): aquifer (bright yellow) is 3.0 m thick, clay top layer (dark brown) 1.0 m thick and 15.5 m long, the flume width is 5 m

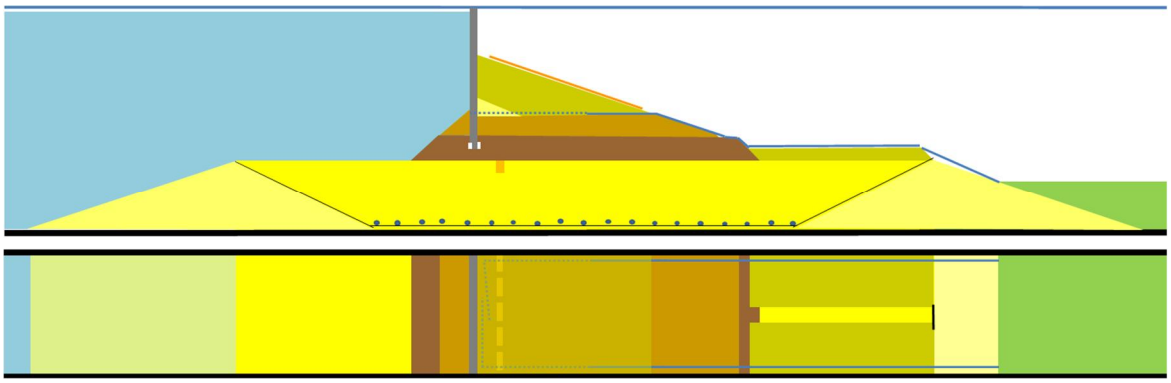

Figure 2.3 Longitudinal section and top view of second test to scale): aquifer (bright yellow) is 3.0 m thick, clay top layer (dark brown) 1.0 m thick and 15.0 m long, the flume width is 5 m

The width of the Delta Flume is 5.00 m. The sand layer prone to piping, the background sand, is 3.0 m thick. The sand body is trapezoidal with a length of 34.1 m at the top surface and 18 m on the bottom surface. The background sand is separated from the bottom of the flume and the supporting dikes by means of a foil. On top of the test sand layer, a continuous clay layer has been placed over a length of 15.50 m in the first, and 15 m in the second test, ending at a small ditch (0.50 m bottom width) in the centreline of the flume with a clay cover on both sides over the full length of the outflow section. The thickness of the clay layer is 0.50 m. The inflow section is uncovered. During the first Delta Flume test the barrier is placed 6 m from the upstream tip of the ditch, during the second test this distance is increased to 11 m in order to be able to fail the barrier.

The coarse sand barrier extends 0.50 m deep into the sand layer in both tests. In test 1, its top also extends 0.20 to 0.25 m into the clay cover. In test 2, the top of the barrier is level with the top of the background sand. The thickness of the barrier is ca. 0.30 m. The barrier is not applied over the full width of the Delta Flume: near the concrete walls pockets of swelling clay (Mikolit) have been installed over a distance of approximately 20 cm on both sides over the full thickness and depth of the coarse sand barrier, in order to prevent leakage or preferential flow along the sides.

The coordinate system in this report has its origin at middle of the tip of the ditch, i.e. 2.50 m from each wall, at the top of the sand layer. Thus, the barrier is placed from x = -6.00 m to x = -6.30 m in the first test and x = -11.00 m to x = -11.30 m in the second test.

In both tests the same combination of background sand and coarse sand barrier material is applied. For the barrier GZB2 is used (d_{50} = 0.87 mm, Cu= d_{60}/d_{10} = 2.5), for the sand bed a batch of sand from the Western Scheldt Estuary (d_{50} = 0.23 mm, Cu= d_{60}/d_{10} = 1.7; these values are averages of the samples taken, refer to Deltares (2019a)).
The background sand was constructed in 10 layers of 30 cm thickness. Each layer was compacted by vibrating compacting equipment. From all layers except for the eighth layer, three samples were taken to determine the relative density. The achieved relative density for the background material varied between 0.35 and 0.65. Two samples were taken from the coarse sand barrier. For these samples a relative density of 0.73 - 0.74 was found (refer to Deltares (2019a) for the method used to determine RD).

In test 1, there are 28 pore pressure transducers (PPTs) in the sand bed. The measurement uncertainty of these transducers is 0.1% of the full measurement range. The measurement

ranges used are 60 kPa (for transducer numbers 15 through 68) and 100 kPa (transducer numbers 10 and 67 through 97). Two transducers have been placed at a depth of 2.0 m with respect to the sand-clay-interface and the others were placed directly at the sand-clay interface, including those in the coarse sand barrier. The positions of the pore pressure transducers (PPTs) of test 1 are depicted to scale in Figure 2.4 and Figure 2.5.

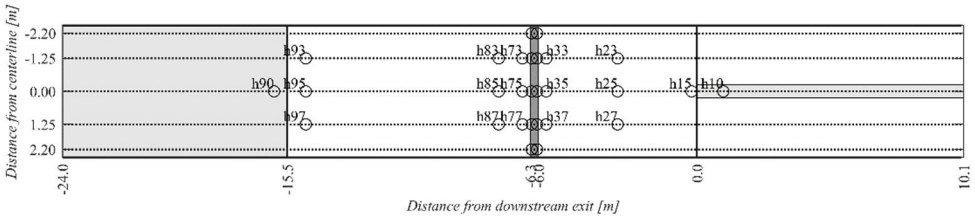

Figure 2.4 Top view of the sand bed with positions of all PPTs along the aquifer in Delta Flume test 1, distances are relative to the tip of the ditch in the centre of the model.

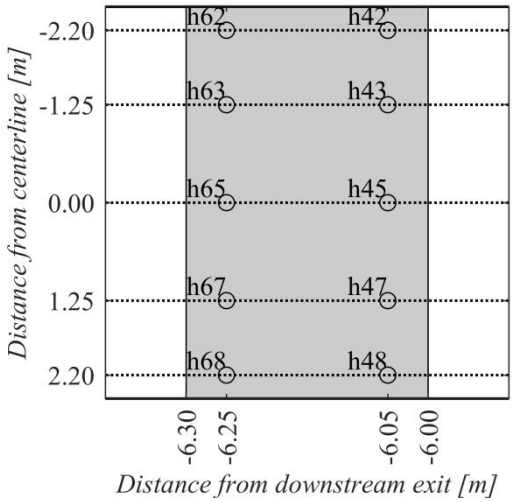

Figure 2.5 Top view of the sand bed with positions of all PPTs along the aquifer in Delta Flume test 1, distances are relative to the tip of the ditch in the centre of the model, close-up of the barrier.

The system of naming transducers is such that transducers with the same x-coordinate have the same first digit e.g. h6#, and transducers with the same y-coordinate have the same second digit, e.g. h#5.

Five rows of tracer particles, ca. 0.003 m diameter Polystyrene foam balls In Gelatine (PIGs), are built in. These tracer particles have a density lower than water, therefore these were expected to flow to the exit point as soon as they are reached by the pipe(s). The tracer particles have different colours depending on their position in the set-up, which means that they might give an indication of the progress of pipe development. The distance of the rows with tracer particles with respect to the position of the downstream exit at the edge of the ditch is given in Table 2.1.

Table 2.1 Positions rows of coloured tracer particles in test 1

Colour of tracer particles	Distance x from ditch [m]
white	5.95
green	6.05 (5 cm in barrier)
blue	6.25 (25 cm in barrier)
black	6.40
red	8.00

The positions of the pore pressure transducers (PPTs) in test 2 are depicted in Figure 2.6 and Figure 2.7. In the second test, 37 instruments were used. The measurement uncertainty of these transducers is also 0.1% of the full measurement range. The measurement ranges used are 60 kPa (for transducer numbers 09 - 68) and 100 kPa (transducer numbers 72 - 99). Based upon the experience of the first test, where much piping activity took place near the walls of the flume, most additional instruments have been installed close to the walls (numbers 22-28-32-38-72-78). Another additional instrument has been placed at a depth of approximately 35 cm inside the barrier, near the downstream side and close to the middle (number 246).
The PPTs 10 and 90 are installed at around 2.0 m depth below the sand surface. The instruments 09 and 99 are located near or at the surface. Furthermore, a pore pressure transducer is added in the upstream reservoir (number 99) to reliably measure the reservoir level once the basic instrumentation of the Delta Flume does not register properly anymore (at a level of approximately 5.9 m above the sand-clay interface). At the downstream side, an additional pore pressure transducer is placed inside the ditch, near the top of the sand (number 09), to enable calculation of the hydraulic head over the structure.

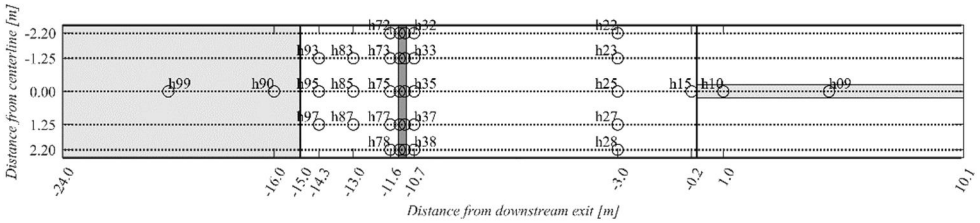

Figure 2.6 Positions of all PPTs along the aquifer in test 2 with respect to the position of the downstream exit

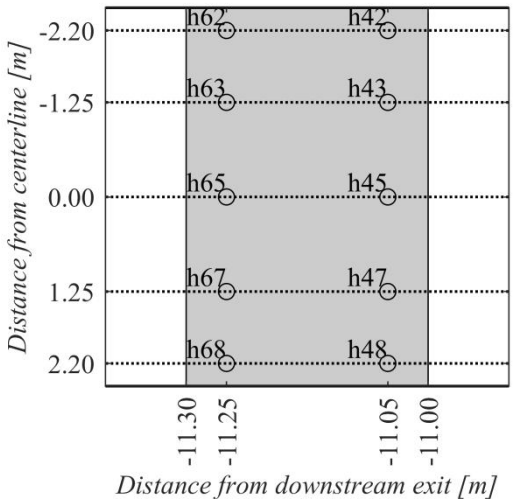

Figure 2.7 View on positions of PPTs in coarse sand barrier in test 2 with respect to the position of the downstream exit

In addition to these instruments, also four rows of tracer particles and an additional line of red coloured Metselzand were built in as tracers. The distance of the rows with tracer particles and the coloured sand with respect to the position of the downstream exit at the edge of the ditch is given in Table 2.2.
One thin line of red-coloured Metselzand (normally constituting 20% of the coarse sand barrier) was added 8 cm upstream of the downstream end of the coarse sand barrier in order to serve as an extra tracer and to test its suitability as a tracer in field situations.

Table 2.2 Positions rows of coloured tracer particles and coloured Metselzand in test 2

Tracer	Distance x from ditch [m]
black (southern side) / red (northern side) tracer particles	10.95
green tracer particles	11.05 (5 cm in barrier)
red Metselzand	11.08 (8 cm in barrier)
white tracer particles	11.25 (25 cm in barrier)
purple tracer particles	11.40

In test 2, a fibre optic cable for temperature measurement (Active Heating Distributed Temperature Sensing, AH-DTS also referred to as ADTS) combined with copper wire heating was installed to give an indication of the groundwater flow. These data are reported in Deltares (2019a) and analysed further in Appendix A.

During the tests the head drop across the dike is increased according to a certain load scheme, which is described in detail in Appendix E of de factual report (Deltares, 2019a).

During the tests the following data is collected:

- Hydraulic head in the upstream reservoir. The actual water level is automatically measured by a gauge at the upstream side of the bulkhead. This system works accurately until a water level of 8.927 m above flume floor level (at a level of approximately 5.9 m). Beyond this, the actual water level has to be controlled by hand, using a tape rule or a folding rule, based on the height of the edge of the flume wall of 9.50 m. The accuracy of the automatic measurements is 1 cm.

- The water level in the ditch is variable and therefore measured throughout the test.
- Observations concerning sand boil forming in the ditch and the discharge of tracers (tracer particles).
- Photographs are taken during every patrol of inspection.
- Flow is recorded manually regularly at the downstream side of the ditch by weighting the mass of water flowing through a pipe at the end of the ditch within a certain time, using a 5 l bucket or a measuring jug, a stopwatch and a balance with an estimated uncertainty of ca.1% during the tests (uncertainty arising from time taken to collect sample and uncertainty in weight of the sample).
- Samples of sand originating from the sand boils were collected in frequent intervals. It was the intention to use these samples for tentative sieve analyses determining the percentage of coarse sand in case of inconsistencies concerning the erosion development of the barrier itself. Afterwards, it turned out that this was not necessary. It was possible to detect the output of coarse sand in the sand boils visually. Thus, it was decided to omit further sieve analyses.
- During test 2, a fibre optic cable for temperature measurement (Active Heating Distributed Temperature Sensing, AH-DTS) combined with copper wire heating was installed to give an indication of the groundwater flow.
- Pore pressure transducers measure heads at the top of the aquifer with a measurement uncertainty of 0.006 to 0.01 m in the transducers (0.1% of the maximum measurement range; the measurement ranges of the individual transducers are reported earlier in this Chapter). Measurements are made with a frequency of 1 Hz. Because there were fluctuations in the head measurements, the raw data are smoothed with a moving mean filter of 1 minute before analysis. Computed gradients, based on the head measurements, show a large degree of variation and are therefore smoothed with a moving mean filter of 10 minutes.

The temperature during test 1 was ca. 10-12°C, and during test 2 ca. 15-16°C.

Concerning the recorded flow, there are several things to be aware of for test 2:

- A few hours after the start of the test, a heavy rainfall occurred (approximately 30 to 70 mm in less than half an hour, not measured locally). Long, steady rain for about 10 hours roughly from t=32 to t=42 hours, with a strong variation in total amount perpendicular to the wind direction within a few miles only, total amount at the Delta Flume again roughly between 30 and 70 mm.
- The ditch had not been dug deep enough; therefore, a layer of clay was removed from the bottom of the ditch at 10:00 on June 1st (ca. 1 day after the start of the test).

The test characteristics of the two tests are presented in Table 2.3 and Table 2.4.

Table 2.3 Test characteristics test 1

Delta Flume test 1		
Type of background sand and barrier	**Western Scheldt sand**	**GZB 2**
Relative density	35-65%	74%
d_{50}	0.23 [mm]	0.87 [mm]
d_{70}	0.27 [mm]	0.99 [mm]
d_{60}/d_{10}	1.7	2.5
Seepage length	15.5 [m]	

Table 2.4 Test characteristics test 2

Delta Flume test 2		
Type of background sand and barrier	**Western Scheldt sand**	**GZB 2**
Relative density	not measured	not measured
d_{50}	0.23 [mm]	0.87 [mm]
d_{70}	0.271 [mm]	0.99 [mm]
d_{60}/d_{10}	1.7	2.5
Seepage length	15.0 [m]	

During test 1, the bulkhead, embedded in the top of the blanket layer of the test dike for enabling a maximum hydraulic load, showed some leakage problems. For this reason, test 1 had to be interrupted at an upstream water level of 4.0 m (relative to the surface of the sand body) in order to take additional sealing measures. After this the test was restarted. Test 1 was abandoned at an upstream water level of 6 m, because of reoccurring leakage damages. The pipe did not progress through the barrier in this test.

Test 2 was terminated at a head drop of 3.3 m between the measurement h99 in the upstream sand bed and h09 in the ditch. At this head drop failure had clearly occurred. Erosion was already observed at a lower head drop; the critical head, which is defined as the head drop at which the pipe progresses inside the barrier, is determined based on the head measurements and will be discussed in Chapter 6.

A detailed record of the observations at the different load steps is given in Appendix E of the factual report (Deltares 2019a).

3 Methodology for analysis of the piping process based on measured heads

Due to the presence of a clay cover, the piping process in the Delta Flume experiments cannot be directly observed. But it can be described by interpretation of pressure transducer measurements, Active Distributed Temperature Sensing (AH-DTS) measurements (only for the second test), observations made at the ditch during the experiments, and observations made during the excavation after the tests.
The interpretation of the head measurements is aided by experience gained in the medium-scale experiments, this is summarised in this Chapter.

3.1 Analysis of measured heads and observations in medium-scale tests

During the medium-scale experiments, the progression of the pipe could be observed through the Perspex plate, and monitored using the pore pressure transducers (PPTs). It was noted that several steps of the pipe progression were distinguished in the pore pressure profile, and that these can typically be most clearly observed when considering the gradient that is computed parallel to the flow direction between the transducers on the upstream side of the barrier and the transducers on the downstream side of the barrier. The locations of the transducers inside the barrier in the medium-scale tests are shown in Figure 3.1. The transducers that are close to the upstream and downstream interface of the barrier (h8 - h10 and h15 - h17 respectively) are used to compute the local gradient inside the barrier at three locations along the width of the model.

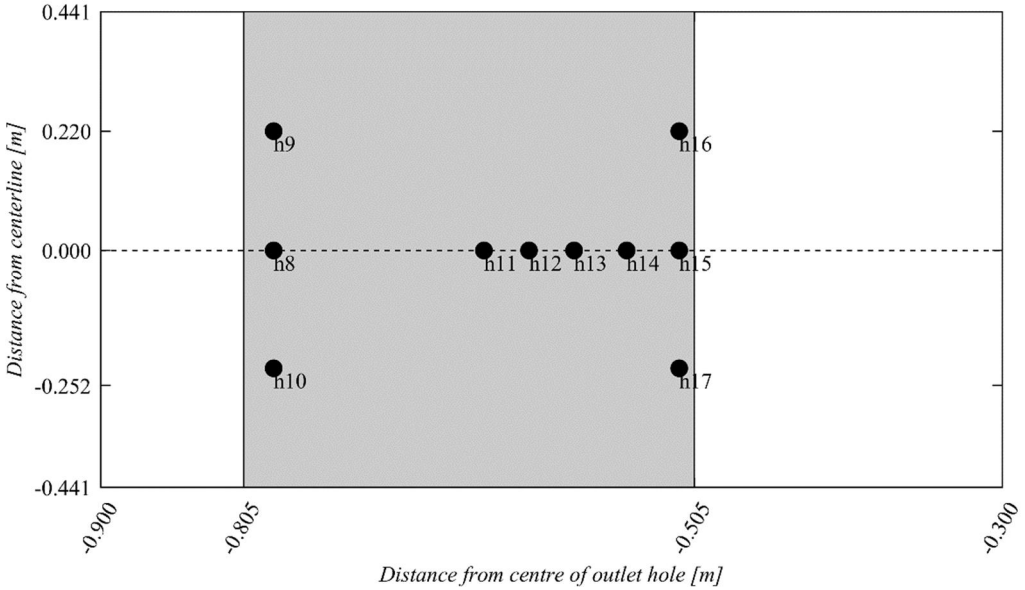

Figure 3.1 Locations of pore pressure transducers in medium-scale set-up

Steps in the process that were detected by visual observations and in PPT measurements during the medium-scale experiments are:

- The pipe reaching the barrier; when the head drop was increased the pipe progressed in the background sand parallel to the barrier along the entire width of the model. This was observed in all tests with one exception. In that test it appears that the resistance to primary erosion in the background sand might have been comparable to that of the barrier, as the coefficient of uniformity ($Cu = d_{60}/d_{10}$) of the two materials is comparable and the relative density (RD) of the barrier was lower than the RD of the background sand;
- The long growth step, where one pipe typically progresses approximately past half way in the barrier but does not lead to failure. In one test the pipe progressed upstream and caused failure during the step which would otherwise be considered the long growth step. The presence of the residual strength after a long growth step is subject of investigation in additional medium-scale experiments.

In between these two steps, there was a step where the pipe first damaged the barrier. This step was difficult to establish clearly as there was also crumbling of the barrier into the pipe at the interface between the barrier and the background sand. This damage also did not show in the PPT measurements. The crumbling did not extend very far into the barrier, a stable slope was established that progressed ca. 1 cm into the barrier, the distance is limited by the limited depth of the pipe downstream of the barrier. For damage, and the formation of a pipe to occur inside the barrier, it was necessary to raise the head drop significantly above the head drop at which the pipe first reached the barrier. This increased the gradients in the barrier and resulted in the mobilisation of a group of particles, resulting in a pipe shape in the barrier at one or more locations.

There were often several steps between damage and the long growth, during which one or multiple pipes progressed a discrete distance into the barrier. One of these steps is referred to as the short growth step in the Analysis Report for the medium-scale tests (Deltares, 2018c). These steps are not considered here, because they do not clearly affect the PPT measurements, and are thus indistinguishable for the Delta Flume tests.

The outline of the pipe at damage and at different progression steps, the heads measured in the transducers along the upstream and downstream interfaces of the barrier, and the measured gradient profile in the barrier are shown for medium-scale test MSP 26 in Figure 3.2 through Figure 3.4.

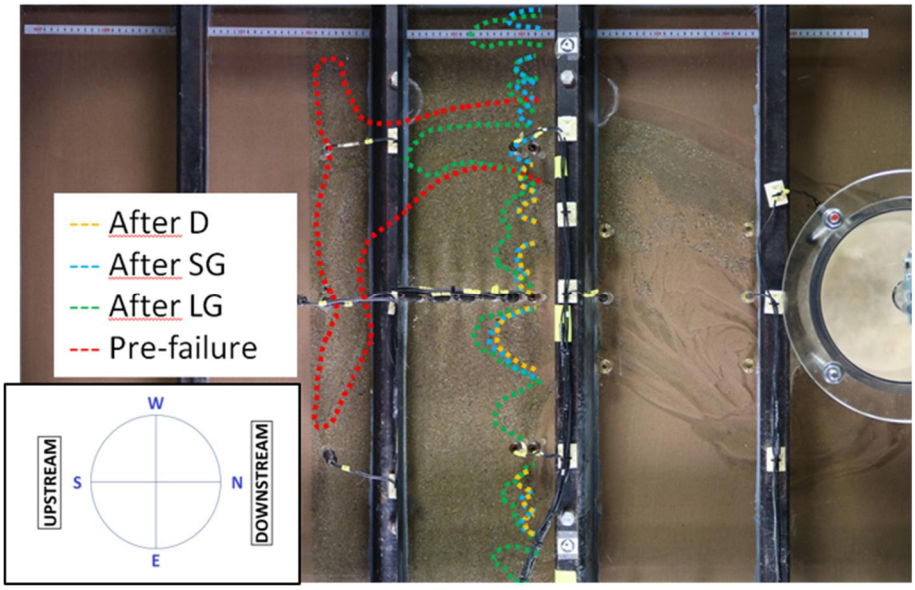

Figure 3.2 Indication of the extent of the pipe after characteristic growth steps and prior to failure based on visual inspection for medium-scale test MSP 26 (GZB 1 and Baskarp 25). Abbreviations D = damage, SG = short growth, LG = long growth.

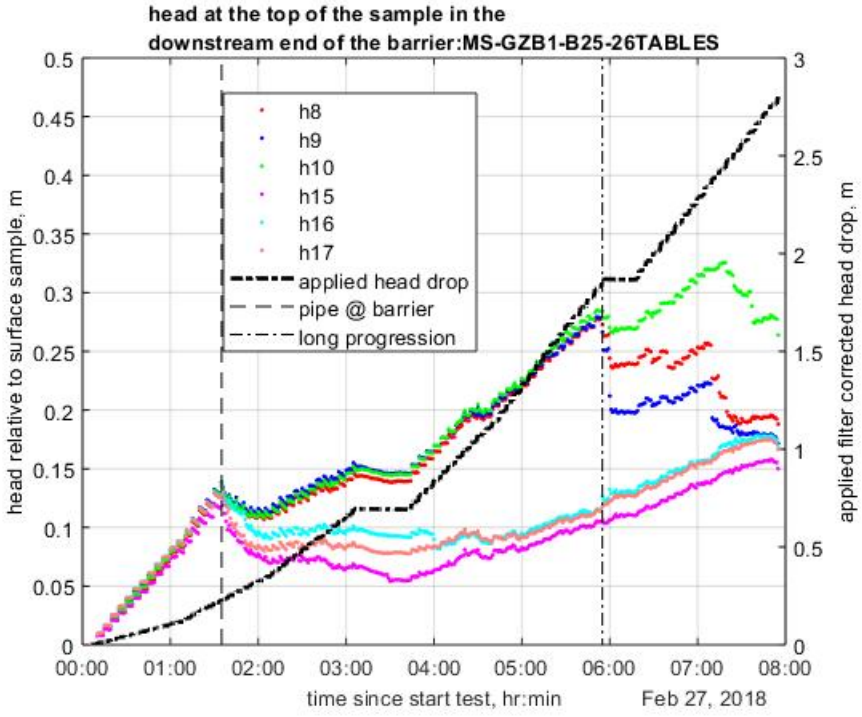

Figure 3.3 Heads at the upstream and downstream interface of the barrier for medium-scale test MSP 26 (GZB 1 and Baskarp 25)

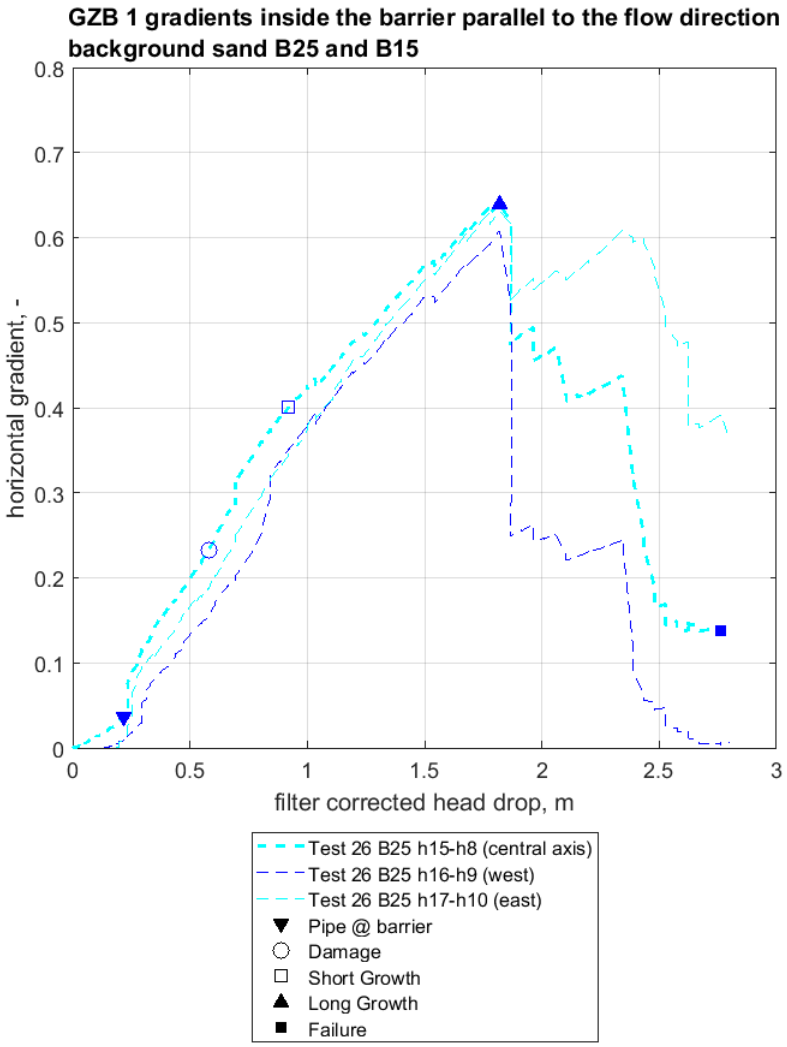

Figure 3.4 Gradients parallel to the flow direction inside the barrier (over distance 27 cm) and critical conditions resulting in the pipe reaching the barrier, damage, short growth, long growth and failure, for medium-scale test MSP 26 (GZB 1 and Baskarp 25)

These figures indicate that:

- The pipe reaching the barrier causes the heads throughout the set-up to fall, and the gradients in the barrier to increase. The head in the downstream side of the barrier that is closest to the location where the pipe arrives at the barrier (h15 in the example of MS 26) falls most.
- The long growth step causes the heads on the upstream side within the barrier to fall, and the effect is most pronounced in the transducer closest to the location at which the pipe progresses (h9 in the example above). This also results in a sharp fall of the gradient at this location. The effect is visible, but less pronounced in the transducer pairs that are further away from the location at which the pipe progresses. The reason for this fall is that the long growth step causes a sudden increase of the pipe length and thus a sudden increase in the outflow area from the barrier into the pipe. This leads to a reduction of the flow resistance and therefore lower heads.

It is important to emphasise that this fall in the gradients does not mean that the barrier has failed. The overall head drop is increased further after this step, which may cause the gradient to rise again. However, as there is a negligible resistance in the pipe, the gradient at the location closest to where the pipe is present remains relatively low compared to the situation before the long growth step.
After the long growth step, there is another step in which the pipe lengthens, approaching the upstream barrier interface but not breaching the barrier yet. This causes a second drop in the measured gradients. Subsequently the pipe progresses gradually parallel to the barrier interface, again increasing the outflow area leading to lower heads in the barrier.

3.2 Application of the methodology to the Delta Flume tests

In the Delta Flume tests, the set-up is significantly wider than in the medium-scale tests, therefore the distance between transducer pairs is also larger. This means that there is less chance of a pipe progressing close to a transducer and therefore it can be expected that measured pore pressure changes are less pronounced than in the medium-scale tests.

The head measurements made on the upstream and downstream side of the barrier, in rows h6# and h4#, are used to compute the gradient inside the barrier. These transducers are further away from the barrier interfaces than the transducers in the medium-scale tests are. In the medium-scale tests, transducers are situated 1 cm on the downstream side, and 2 cm on the upstream side away from the interface. In the Delta Flume tests the respective distances are ca. 5 cm. Although the critical gradient in the barrier will therefore not be directly comparable for the two scales, the measured gradients during the Delta Flume tests should give an impression of when the critical point is reached.

Medium-scale tests with GZB 2 at a high relative density indicate that the critical gradient over the barrier (i.e. over 0.27 m) that causes the long growth step is in the order of 0.4 (Deltares 2018c).

As transducers are numbered so that transducers with the same x location have the same first digit, the rows can be identified based on these numbers, i.e. we speak of row 4# indicating measurements in the row of transducers h 42-h48 inside the barrier. Similarly, perpendicular to the barrier transducer at the same y location have the same second digit, so we can for instance refer to side #2 when speaking of the transducers on the south side of the model. This is illustrated in the figures below.

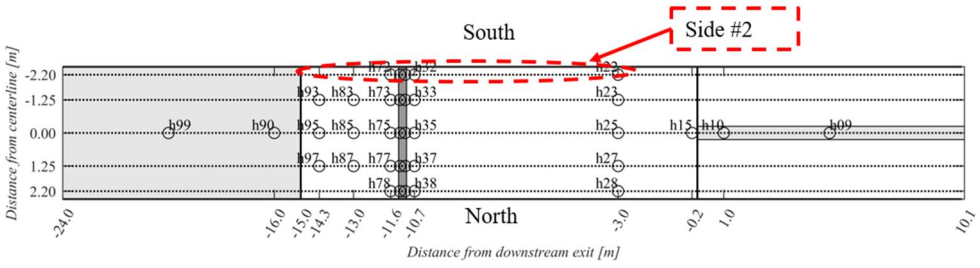

Figure 3.5 Top view of second Delta Flume test indicating the side #2, which refers to the area where the PPTs with the same y coordinate that are labelled h22, h32, h42, h62, h72, h82 and h92 are located.

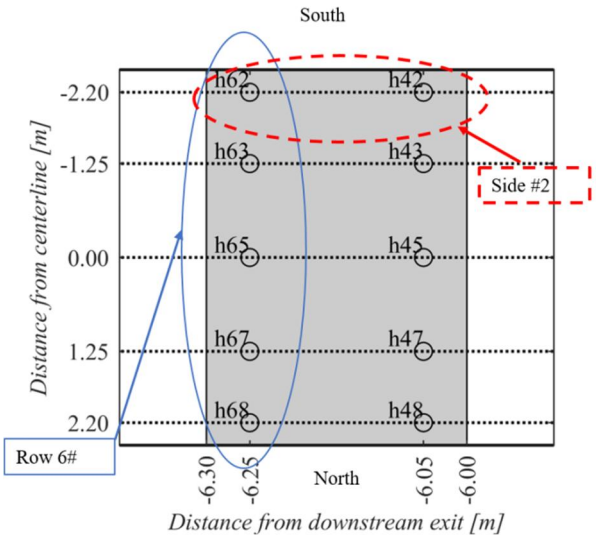

Figure 3.6 Top view of second Delta Flume test close-up of the barrier indicating the side #2, which refers to the area where the PPTs with the same y coordinate that are labelled h42 and h62 are located. Also, the row 6# is indicated, referring to transducers with the same x coordinate which have numbers h62, h63, h65, h67 and h68.

4 Piping process during the first Delta Flume test

This chapter combines the data that was collected during the first Delta Flume test: PPT measurements, observations during the test, and observations from the excavation after the test in order to analyse the piping process. The factual data has been presented in Deltares (2019a), therefore this chapter only shows those data that are most relevant to the interpretation.

As described in Chapter 3, the horizontal gradients in the barrier (for the Delta Flume test measured over 20 cm – computed using transducer pairs 4# and 6#, as indicated in Figure 3.5 and Figure 3.6), are used for the analysis of the piping process. The measured gradients inside the barrier during the entire test are shown in Figure 4.1. The measured heads on the upstream (h6#) and downstream (h4#) side of the barrier provide additional insight relevant to the interpretation of the gradients. These are shown in Figure 4.2 and Figure 4.3.

During this test, the measurement data was not recorded on April 20th between 11:11 and 18:00. During this time, the upstream head was maintained at a level of 4.0 m until 16:30, then the head upstream was reduced to ca. 0.2 m for repair activities to mitigate leakage at the sheet pile and the Delta Flume wall. After repairs, the head drop was increased again, however, due do further leakage the test was stopped again after an upstream head of ca. 6 m was applied.

The experiment was thus carried out in two loadings, due to leakage issues during the test. During the experiment, the first loading appeared to predominantly affect the south side of the set-up. After the upstream head was reduced for leakage mitigation measures, the second loading predominantly affected the north side. The two loading steps are analysed in the next sections, followed by a summary and discussion of implications.
Note that the last head increments after 18:00 on April 23rd are not registered in the upstream head sensor: the upstream water level was raised to 5.8 m at 18:00 and to 6.0 m at 20:33.

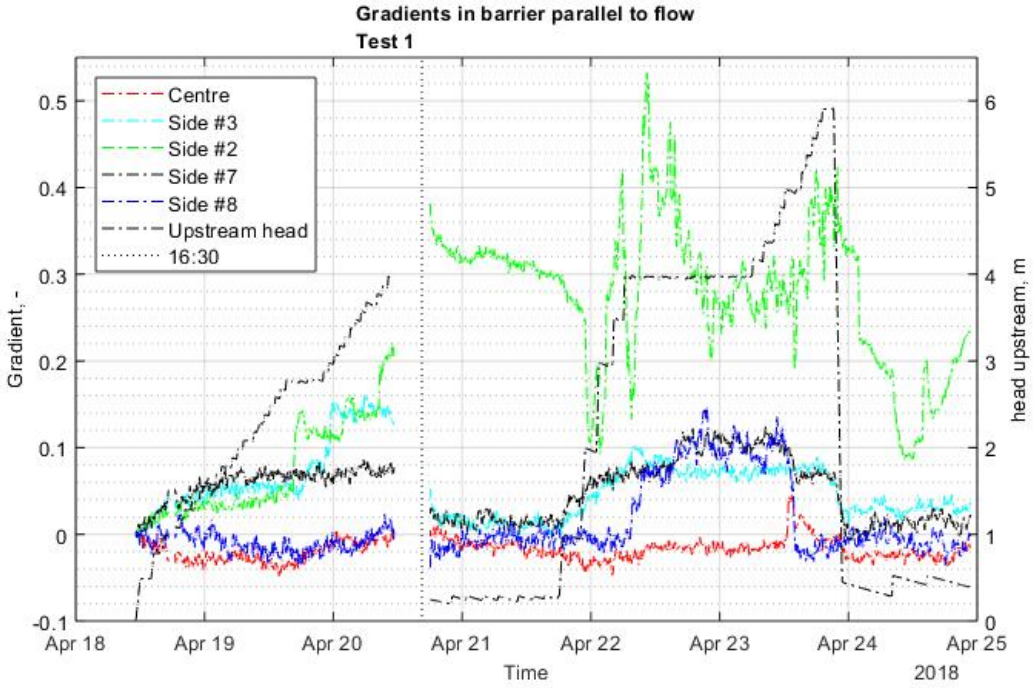

Figure 4.1 Measured gradient inside the barrier during the first Delta Flume test. The upstream head was maintained at 4 m until 16:30 on April 20th, and subsequently reduced for carrying out maintenance.

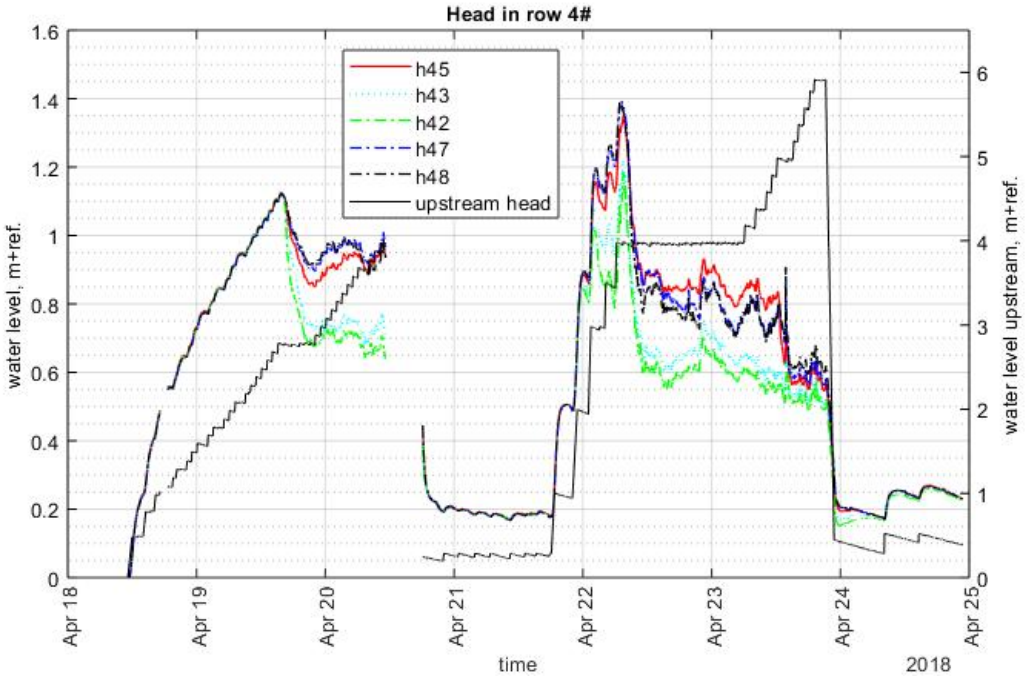

Figure 4.2 Measured heads in row h4# at the downstream side of the barrier.

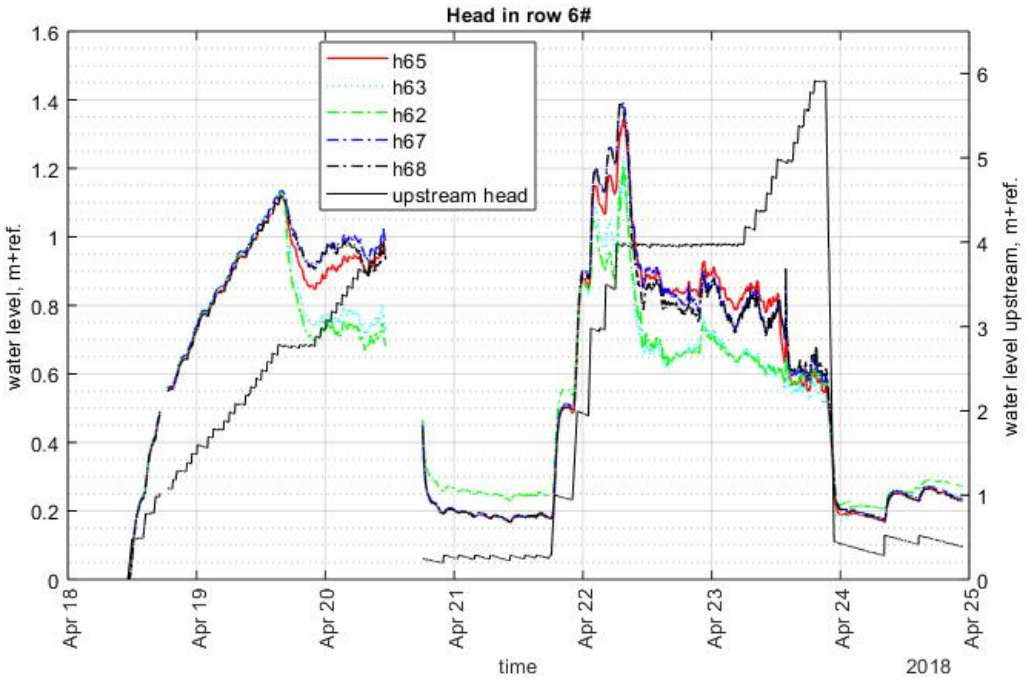

Figure 4.3 Measured heads in row h6# at the upstream side of the barrier.

4.1 First loading

The analysis is split up into the chronological presentation of evidence obtained during the test, followed by the results of the excavation after the test was completed.

4.1.1 Evidence during the test

Initiation of piping and development of pipe to the barrier on the south side of the set-up

The first sand boils are observed at the tip of the ditch and on both sides of the ditch at 19:15 on April 18th. This indicates that several pipes form and progress upstream rather than only one pipe. On April 19th, around 08:00, the progression of the pipes in the vicinity of the row of transducers h2# is likely as suggested by the reduction of the measured heads, whilst the upstream head is being increased. The heads in the centre and north fall before the head in the south.

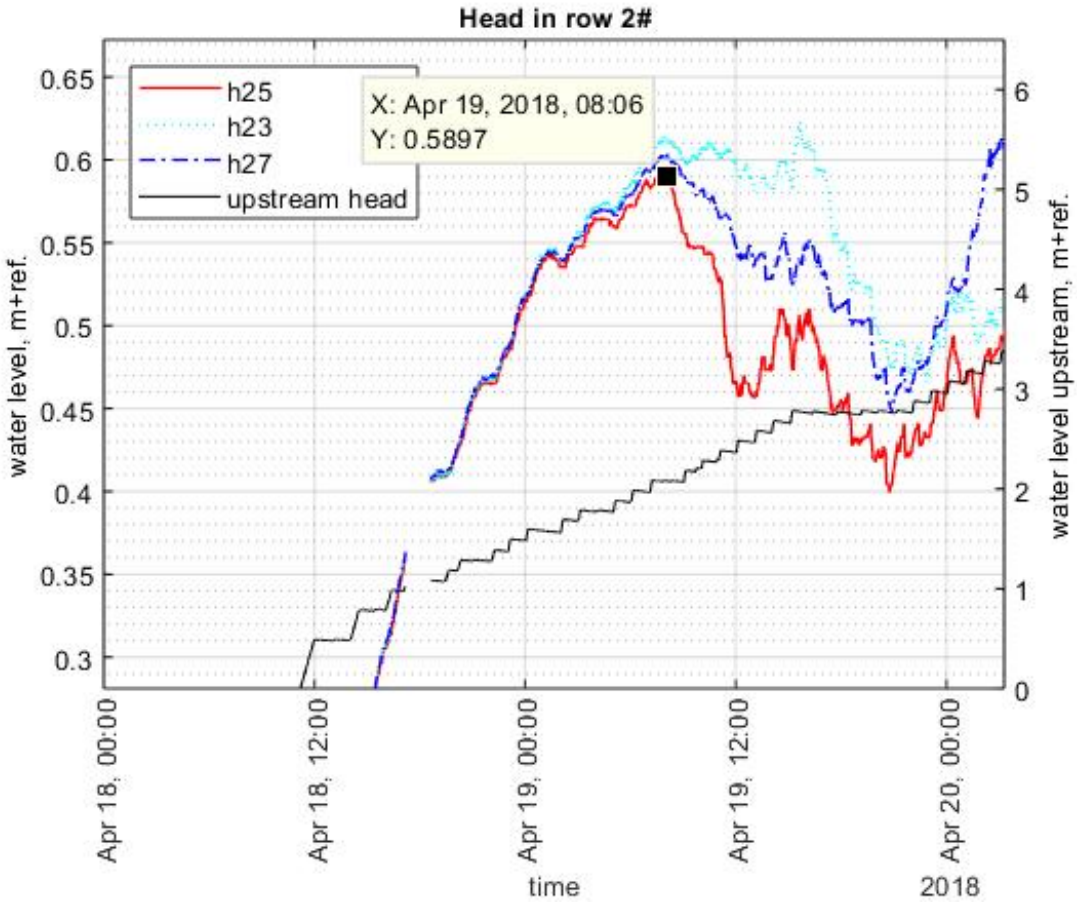

Figure 4.4 Heads measured during the first Delta Flume test in row h2# indicate the progression of pipes (time of critical situation before progression denoted by black square).

A pipe appears to reach the south side of the barrier on April 19th at ca. 16:00. The arrival of the pipe at the barrier causes a reduction in the heads measured throughout the set-up, as was also the case in the medium-scale tests. This is due to the lower resistance in the pipe as compared to the background sand. The pipe appears to arrive closest to the side of h#2, this is reflected by the sharpest reduction in h42, and by the steep increase of the local gradient at h62-h42. There are no observations recorded directly at this time, but at 19:40 it is reported that a full bucket of sand is removed from the ditch, which could be related to the increased erosion in the pipe, after reaching the barrier.

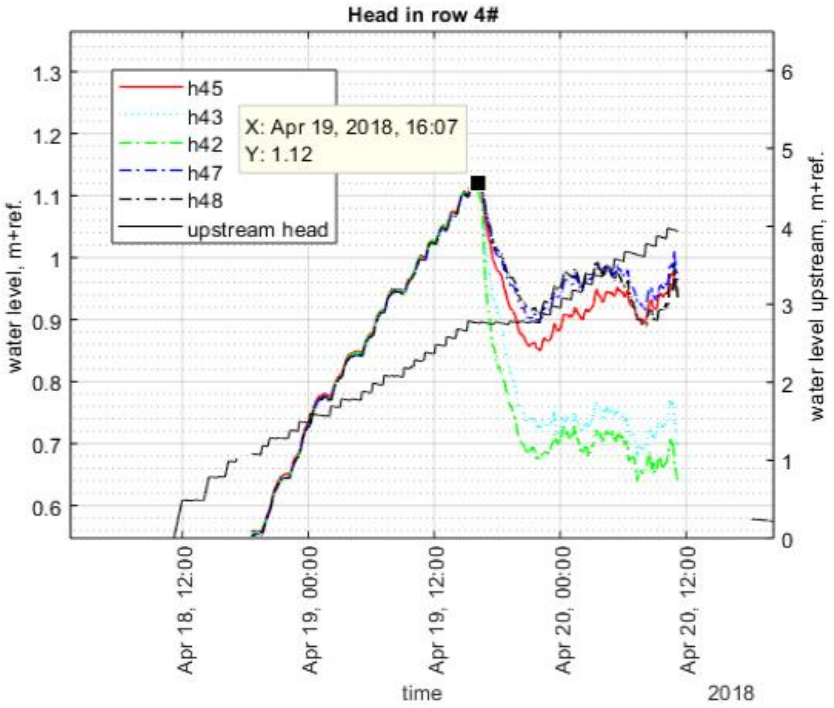

Figure 4.5 Heads measured during the first Delta Flume test in row h4# indicate the arrival of the pipe at the barrier. Critical conditions leading to the arrival of the pipe are indicated by the black square.

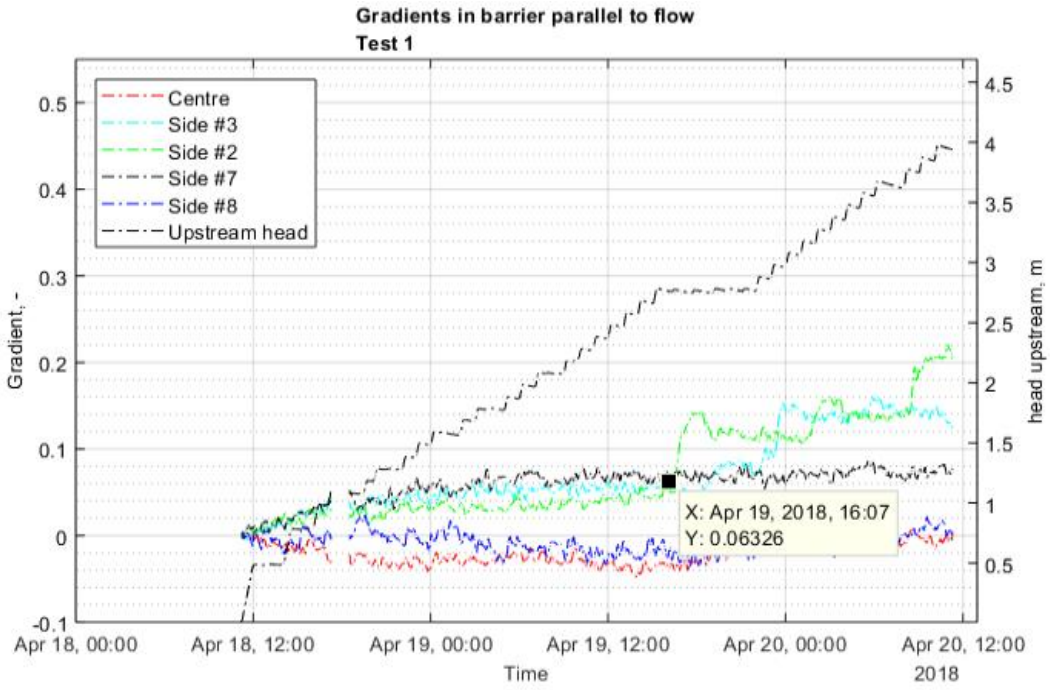

Figure 4.6 Measured gradients in the barrier during the first Delta Flume test indicate the arrival of the pipe at the barrier (measured between transducers in rows 6# and 4#).

The development in the overall conductivity of the sample can be visualised by dividing the measured flow rate over the head drop. This is shown in Figure 4.7, considering the head drop from the upstream water body to the measurement in h15 (just at the tip of the ditch). The flow rate over head drop slowly increased, which means that the total flow resistance of the set-up decreased during the test due to the erosion of sand particles and the resulting permeable pipes. There is no clear jump when the pipe is considered to have reached the barrier. When the test is restarted April 21st, the flow resistance appears to be increased, probably due to sedimentation of sand in erosion pipes or settlement of the clay. Just before April 22nd 11:00 the resistance is decreased to the level of the first part of the test and during the test in decreased further. The decrease in resistance is relatively limited compared to what is measured in traditional piping set-ups. The reason is that the flow resistance is mainly caused by the flow through the upstream background sand and this is only affected at the very end of the test but results in a constant flow resistance during most of the test duration.

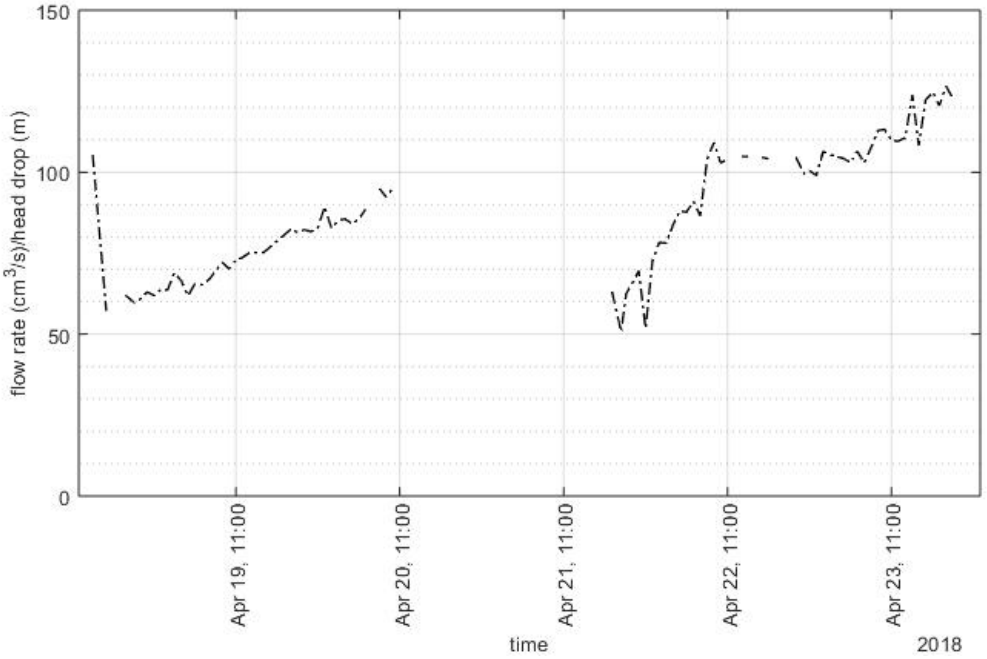

Figure 4.7 Flow rate divided by head drop between upstream water body and h15.

Development of the pipe in the downstream sand along the barrier on the south side of the set-up

The heads in row h4# (Figure 4.5) indicate that the pipe is closest to side #2 (south) but all heads in this row fall over the entire period that the upstream head is maintained constant at 2.8 m. This suggests that the pipe between the barrier and the ditch is getting deeper and wider and the resistance downstream is decreasing. Accordingly, sand is produced by the sand boils in the ditch during this time. The sand boils on the north side of the ditch also produce sand, indicating that pipes at the north side are also eroding material.

The local gradient at side #3 increases first around 18:30, and again around 23:00 suggesting that the pipe progresses parallel to the barrier in this direction, but it is not clear if the pipe actually progresses all the way up to the location of h43 (which is ca. 0.9 m away from h42). Excavations after the test suggest that the pipe did not progress all the way to h43.

The upstream head is increased at 22:00 on April 19th, which causes the heads in h45 – h48 to rise, whereas the heads in h42 and h43 rise a bit but fluctuate. This suggests that erosion in the pipe between the ditch and the south side of the barrier reduces the effect of the higher upstream head on transducers h42 and h43, and that there is no direct pipe from the ditch to the north side of the barrier yet.

Leakage occurred during this test. The first observation of this is recorded on April 19th at 22:20, water coming out of the slope on the south side of the model. The leakage continued and led to the upstream water level being lowered on April 20th at 16:30 for repairs. This leakage may have contributed to a decline in the heads in the barrier. However, as sand is being produced as well by the sand boils on the north and on the south side in the ditch it appears likely that erosion also contributes to the decline in the measured heads.

The gradients in the centre and at the north side of the barrier remain low. The measured gradients (between transducers in rows 6# and 4#) are in the order of 0 for the centre and side #8 and around 0.07 for side #7. It is not clear why the gradient in side #7 is higher than the gradients on both sides of this transducer pair. The gradient of 0.07 corresponds to a head difference of only 0.014 m between the transducers. Possibly the pipes that formed on the north side of the ditch reached closer to side #7 than to #48 or #45, without actually reaching all the way to the barrier.

Erosion of the barrier on the south side of the set-up

At ca. 08:30 on April 20th, the gradient at the side #2 (south) starts to rise steeply and continues to rise until the point where the data storage is interrupted at 11:00. The gradient increases to a value of 0.22. This is lower than the critical gradient for medium-scale tests where the barrier does not penetrate into the cover layer, where the critical gradient for progression is in the order of 0.4.

During this period, the measured heads in the barrier at sides #2 and #3 show fluctuations. This behaviour could indicate crumbling or erosion of the barrier into the pipe downstream. Just prior to the gap in the data, the measured heads show a reduction. The significance of this this is unclear as there are always fluctuations during the test.

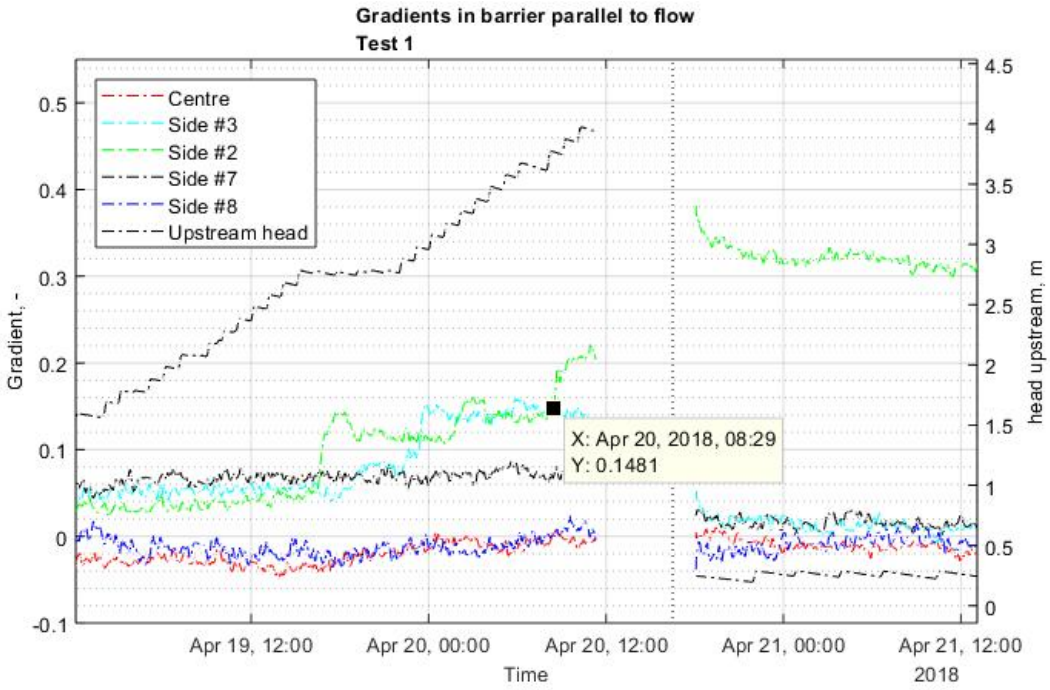

Figure 4.8 Measured gradients in the barrier during the first Delta Flume test indicate erosion near side #2 at the barrier.

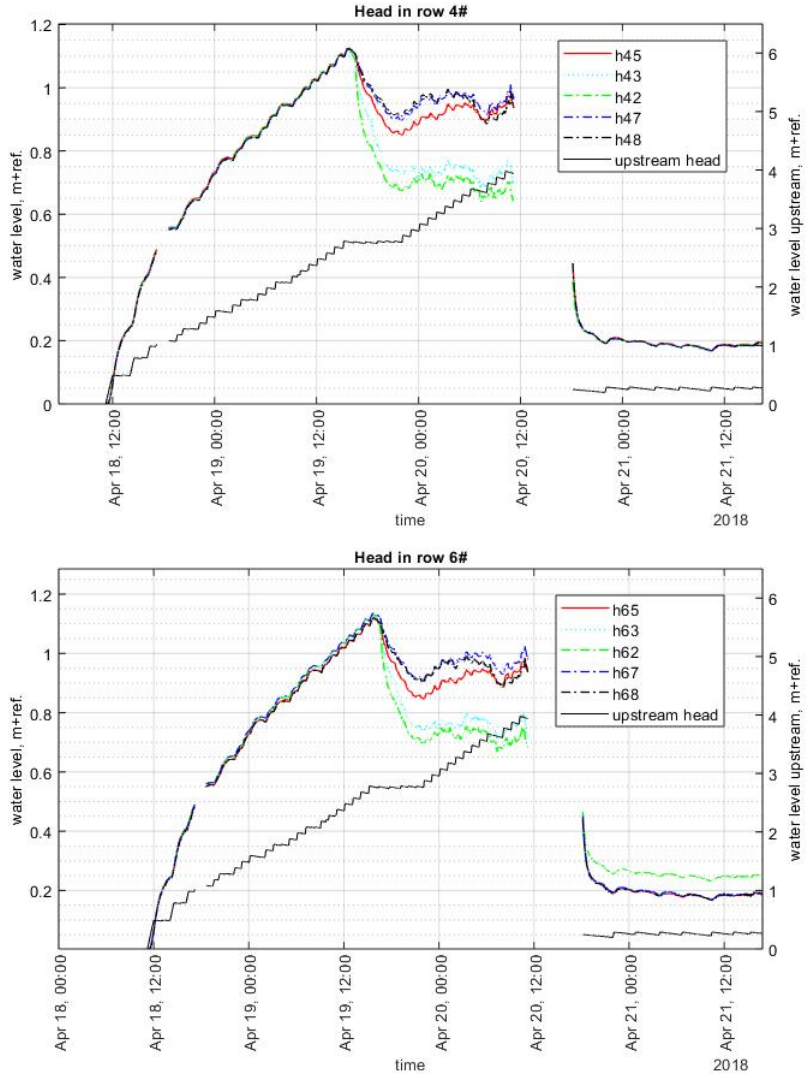

Figure 4.9 Prior to the gap in the data, the heads measured in the transducers inside the barrier show a sharp fall. After the data gap and the repairs, h62 shows a 5 cm higher value than the other transducers at the same applied head drop.

At 12:30 on April 20th, barrier material was observed in the sand boils. Although this might possibly be due to coarse sand having been spilled during the construction phase, the measurements strongly suggest that barrier material has been eroded and transported through the pipe to the sand boils. No white tracer particles, which were placed in front of the barrier are observed at this point.

Erosion in the barrier on the south side and deformation of the cover layer?

During the period in which data is missing, the head drop was maintained constant at 4 m head upstream. Prior to the gap in the data, the head in h62 was less than in the other transducers in row h6#, and erosion appeared strongest on the side of #2. After the data gap, during which the upstream head was first constant at 4 m and then lowered to ca 0.2 m for repairs at 16:30, the head in h62 is ca. 0.05 m higher than the head in the rest of row 6#. This higher measured head suggests that during the period of repairs h62 was displaced downwards. If the transducer is actually 0.05 m deeper than the elevation at which it was referenced to, this would result in a 0.05 m higher head measurement at hydrostatic pressure. The displacement of h62 might

possibly have occurred if the erosion of the barrier material resulted in a void above the barrier, into which the cover layer clay could subside. During the repair works, there was a considerable load placed on top of the sample, which might have affected this displacement.
The measurements in h42 do not indicate displacement of this transducer. This does not mean that the cover layer at this location was not displaced. The transducers are connected to relatively stiff cables and the cable might have kept the transducer in its original place, whilst the clay settled around it.
This would imply that, before or during the period of constant head drop in which there is no data, there was significant erosion of the barrier, which is supported by the last measurements indicating an increasing gradient at side #2, a fall in the heads in the barrier, and the observation of barrier material in the ditch. This raises the question whether the pipe even breached the barrier.

4.1.2 Evidence from excavation in front of the barrier after the test

The head measurements during the first loading indicate erosion of the barrier occurred at the south side of the sample. Therefore, here we describe the evidence from the south side of the excavations that were done after the entire first Delta Flume test. The remainder of the excavations are described after describing the results of the second loading.

The excavations of the south side after the entire test indicate that there was significant erosion in front of the barrier on the south side, the cover layer has settled ca. 0.05 m over an area that was ca. 0.4 m wide. A channel (pipe) was eroded into the cover layer and this was filled with coarse barrier sand. This indicates that the pipe did not only erode the sand body, but also the clay that composed the cover layer. White tracer particles were observed in this pipe. This pipe was also observed close to the ditch (as discussed in Section 1.1.1).

These excavations indicate that there was erosion of the barrier itself at the location where h42 and h62 were. Barrier sand and the blue tracer particles (that were in line with h62, 0.05 m away from the upstream barrier edge) are encountered scattered through, and also in front of the barrier. Erosion of the barrier would have created a void above the barrier, which might have trapped the buoyant blue and green tracer particles that were present in the barrier. This would explain why these are found above and in front of the barrier during the excavation, and not in the pipe downstream or in the ditch.

The cover layer above the barrier had settled over an area of ca. 0.5 m wide close to the wall of the set-up (i.e. at the location of h#2 but not at h#3). In order for the cover layer to be able to settle, there must have been erosion of the barrier material below the cover layer. Settlement of the cover layer was also indicated by measurements in h62 after repairs.

The pipes filled with sand in the cover layer indicate that flow rates were high enough to erode the cover layer, and to transport the barrier sand.

During excavation a fine layer of fine sand was observed on top of the barrier at the location where the barrier was eroded. The origin of this fine sand is not clear. If the pipe had progressed through the upstream interface, this could be the fine sand from upstream. This would be expected to lead to failure at constant head drop, but failure was not observed. However, as the head drop was lowered rapidly during the critical period of erosion in the south side, it cannot be ruled out that indeed the pipe progressed through the upstream barrier interface. When the head was lowered, and repair works were conducted, the deformation of the cover layer may have clogged the pipe that had formed, so that when the head upstream was raised again there was no further pipe progression at the side h#2.

However, the amount of sand observed on top of the barrier is very small, less than would be expected if the pipe had breached the barrier. It is also possible that there is another source of the fine sand, this might have been spilled during the preparation of the test.

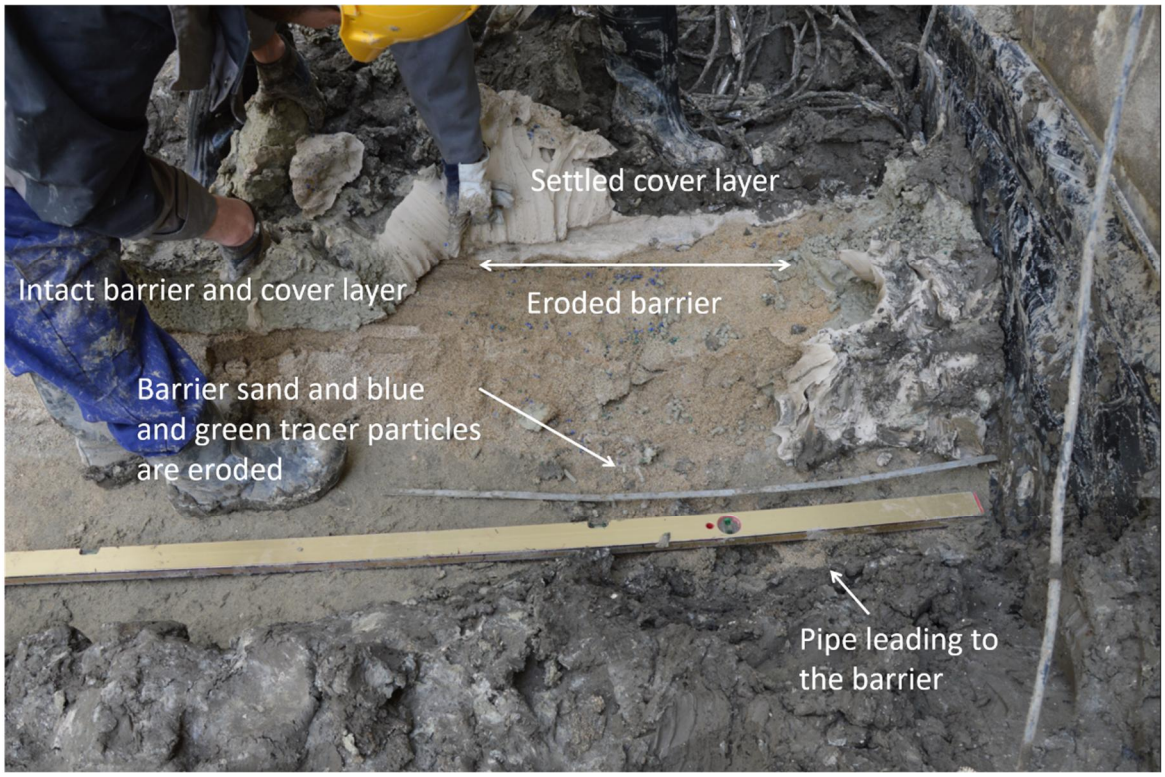

Figure 4.10 Excavation indicating erosion of the barrier at south side of the set-up (in the zone containing h42 and h62).

Figure 4.11 Excavation indicating intact barrier on the north side of the model, top view of the barrier

The findings indicate erosion of the barrier material, and deposition of eroded barrier material into the pipe in front of the barrier. The medium-scale tests showed that erosion of the barrier material and the deposition of barrier material in the pipe directly in front of the barrier causes the pipe, which was originally in the background sand in front of the barrier, to shift further downstream, as the background sand is easier to erode than the deposited barrier grains. That would account for the formation of a larger eroded zone in front of the barrier, which is observed in the excavations. The observations during the test indicate that some barrier material was transported to the sand boil in the ditch as well, showing that flow velocities in the pipe were high enough to transport barrier sand. This is in accordance with the coarse sand, which was observed to have filled the pipe in the cover layer in the excavations.

Further away from the wall, towards the centre and the location of side #3 the barrier and overlying clay layer are still intact. This indicates that the pipe did not erode barrier material close to h#43, as also indicated by the measurements. There is also no evidence that the pipe has progressed parallel to the barrier in the background sand along the width of the model.

4.2 Second loading

4.2.1 Evidence during the test

When the load was re-applied, the measured gradient on the side #2 is high, due to the higher pressures measured in location h62, which is probably due to displacement of this transducer. If the transducer was displaced due to subsidence of the cover layer, this could have filled the pipe and also contribute to a higher gradient between h62 and h42. Both these effects imply that the measured gradient at this location cannot be considered to represent the barrier strength in terms of a critical gradient for pipe progression.

The head upstream is increased to 2 m in one step, causing the heads in row h4# to increase. The next increments to ca. 4 m caused less increase in h42 and h43 than in h45-h48, which would be expected due to the pipe leading to the south side of the barrier from the ditch. Possibly the first increase had a similar effect in h42-h48 due to the sand that had settled in the pipe and sand boils, increasing resistance to flow. Erosion of this material at a higher head drop would reduce the resistance to flow and results in the lower heads in h42 and h43. When the head increments are applied, the heads rise, but during the periods of constant head following each increment, heads fall indicating active erosion.

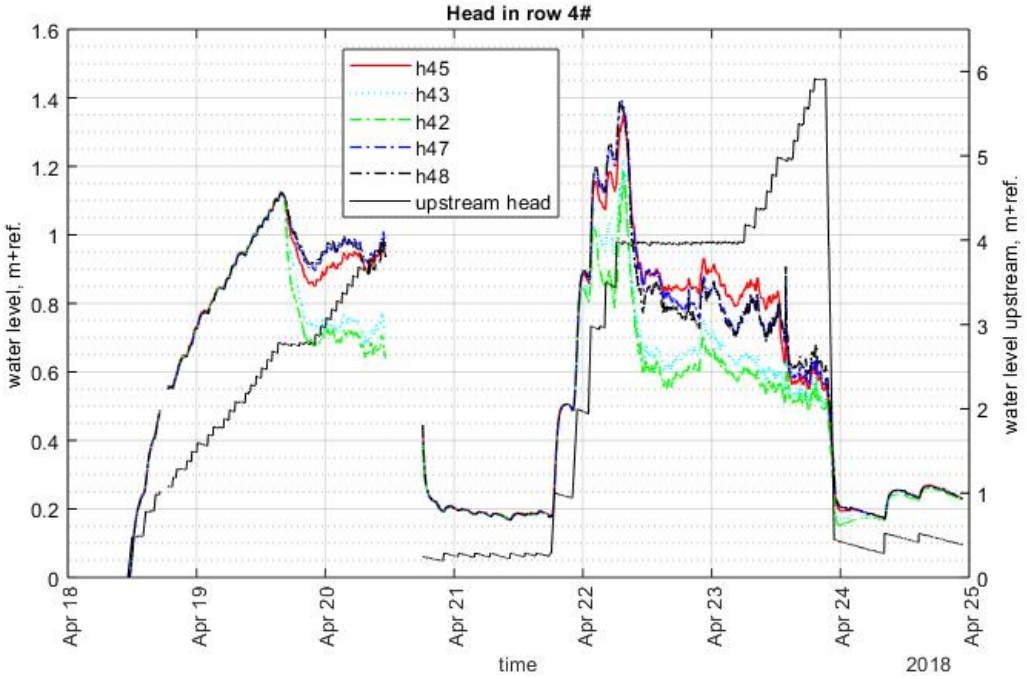

Figure 4.12 Heads measured in row h4# in the downstream side of the barrier.

On April 22nd at ca. 06:04 the gradient in side #8 increases sharply, suggesting the arrival of a pipe at the barrier close to this location. At this time, the head upstream is maintained constant for a longer period than between the prior increments, and the heads in all transducers in rows 6# and 4# fall significantly. This fall indicates erosion downstream, although leakage might possibly also play a role. At side #8 the fall in h48 is greater than in h68, raising the local gradient, the fall of h48 indicates the proximity of a pipe at this transducer.
The head that is measured in h48 is lower than the heads h47 and h45 in the same row but remains higher than the heads on the south side of the set-up in h42 and h43. This suggests that there is more resistance in the pipe downstream on the north side of the set-up, compared to the pipe in the south side. That might be expected if the pipes were smaller. With multiple pipes at the barrier, flow is being distributed amongst them whereas the south pipe first formed as the only pipe that reached the barrier. The presence of a larger network of smaller pipes in the north side of the model, and one larger pipe on the south side is observed during the excavations at the end of the experiment.

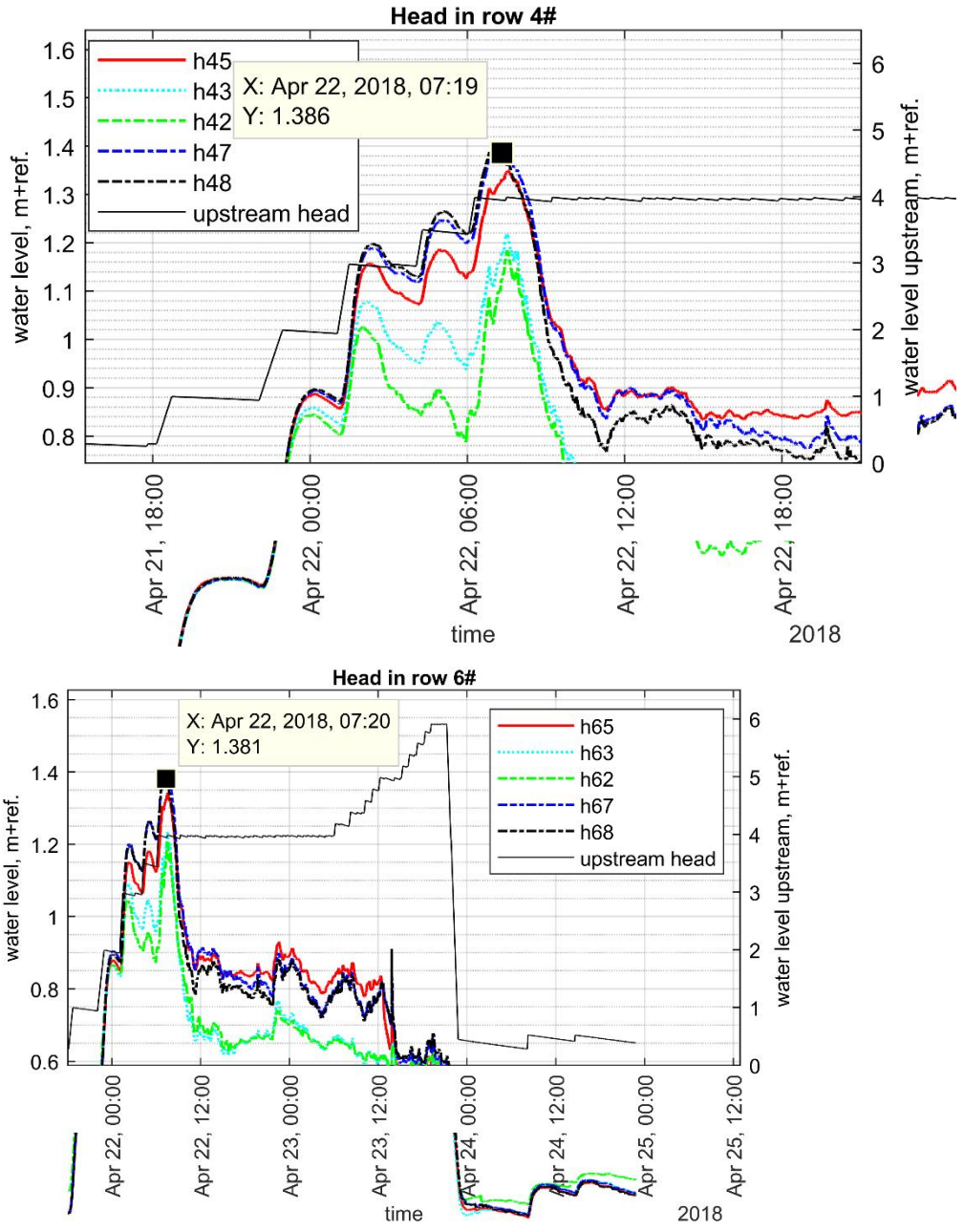

Figure 4.13 Heads measured in row 4# and row 6# during the first Delta Flume test.

The effective hydraulic conductivity of the sand bed does not change significantly during the period in which the head drop is maintained constant (Figure 4.7).
During this time, observations report that wells both on the north and on the south side of the ditch are active in transporting sand. This means that erosion is occurring in all the pipes downstream of the barrier. It is also observed that leakage occurs at the north side of the ballast sand on top of the cover layer and at the north wall nearby the ditch.

At 09:40 on April 22nd a white tracer particle is observed to come from the south well. Those tracer particles are present at a distance of 0.05 m in front of the barrier. As all evidence indicates that the pipe has passed this point already during the first loading, it appears that

these tracer particles get stuck somewhere in the pipe and do not reflect the progression of the pipe well. This would be quite probable considering their density which is much lower than that of water. At 10:00 it was observed that clay lumps were transported through the pipes, this indicates that the cover layer was also subject to erosion.

At 14:15 on April 22nd it was observed that coarse sand (likely barrier material) was produced by the well in the northern side of the ditch, and some white tracer particles were also observed.

At 14:50 on April 22nd there is another increase of the gradient over the barrier in side #8, and also in side #7 which suggests further erosion close to these transducers. There might be some erosion of the barrier at #8 as well as progression from #8 parallel to the barrier towards the centre of the model, or possibly the arrival of another pipe at the barrier at side #7.

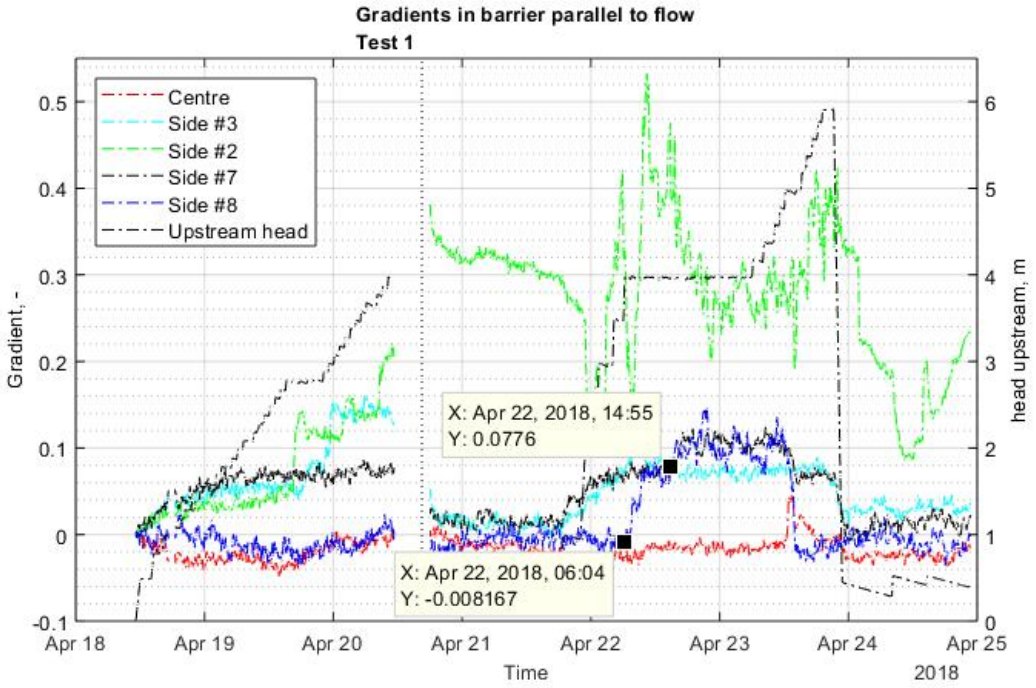

Figure 4.14 Measured gradients in the barrier, black points indicate rise of the gradient at side #8

At April 23rd ca 12:00 the gradients in side #7 and #8 fall sharply despite the increase in head drop. The gradient at #8 even reduces to approximately zero. The observations indicate that white tracers are transported from the north side and intensive sand boiling at this time. No blue or green particles are observed. A fall in the gradients would suggest progression of the pipe in the barrier, however, excavations after the test do not indicate significant erosion of the barrier on the north side of the model.
It is also observed that water is seeping from the northern edge of the flume wall. This leakage may contribute to the overall falling heads and the drop in the gradient at side #8.

During the remainder of the test, the observations do indicate more sand transport and erosion of white tracer particles, indicating more erosion occurs downstream. However, leakage at the sheet pile wall and failing of the sand slope at the sheet pile wall were the reason to stop the test.

4.2.2 Evidence from excavation in front of the barrier after the test

In this paragraph the excavation results of the north side of the test are described, since this was the area that appeared active during the second loading. Excavations at the ditch indicate that the sand boil was fed by a few meandering channels of about 1 m length cut into the cover layer. Further upstream, these channels diverged into a wider area without clear channels but with braid plain like flow structures in which the cover layer was subsided for ca. 0.10 m in an area over 1m wide. Hence, the sand under the cover layer was eroded. White tracer particles were observed spread below the cover layer in this area, indicating the tracer particles were not transported all the way to the ditch after having been eroded. This corresponds to measurements that indicated erosion occurs downstream of the barrier in the north side of the model. The presence of the white tracers suggests that one or more pipes on the north side of the barrier reached at least up to 5 cm from the barrier.

Excavation of the barrier revealed that the barrier was intact on the north side of the model. The green tracer particles that were placed in line with row of transducers h4# are still in place. Whereas in the south side of the model the pipe could clearly be traced in the vicinity of the barrier, and an eroded zone with barrier material and tracer particles from the barrier indicated the damage of the barrier, this was not observed in the north side of the model. The measured heads indicate the presence of pipes close to h48 and h47, however, these appear not to have affected the barrier stability. It cannot be ruled out that pipes did reach the barrier, however, these would have been significantly smaller than the pipe that was excavated on the south side of the model, and therefore may not have caused erosion of the barrier. It is also described that the white tracer particles are still in place at the barrier in the north, at some locations. The top of the barrier on the north side was excavated partly, and subsequently the south side was excavated as the south side showed the clearest sign of erosion.

Figure 4.15 Intact barrier on the north side of the set-up.

During the excavation, it was observed that the cover layer could easily be removed at the north side upstream of the ditch around the zone of transducers in row 2#. The observations of clay in the sand boils during the test also indicate that the clay could be eroded by the high flow rates in the pipes.

4.2.3 Evidence from excavation in the vicinity of the ditch and towards the barrier

It was observed that pipes had eroded into the cover layer and were filled with sand both at the north side close to the ditch and at the south side of the model close to the ditch and at the barrier. This corresponds to the observations of clay transport during the test, the clay was eroded, forming a pipe in the cover layer.

The pipe that formed on the south side of the model was most distinct, and significantly larger than the pipes on the north side of the model. Close to the barrier, the south channel had a height of 5 cm and width of 8 cm. The pipe on the south side of the model, was filled with coarse (barrier) sand, and white tracer particles were observed in this pipe. It appears that only a single pipe formed on the south side of the model.

A larger pipe in the south side would be expected if the pipe on the south side reached the barrier first and was therefore subject to a large amount of flow concentrating in the barrier. Pipes that reached the barrier at a later point would cause a redistribution of flow, but the flow in each individual pipe would be lower. The total flow rate during the second loading was higher at the end of the test, due to the higher upstream head, however, the wide delta of pipes and eroded material near the ditch observed at the north side of the ditch suggests that this was distributed over a significantly larger area than in the south side of the model.

In the south side of the model, the clay surrounding the pipe in the cover layer was softer and more saturated with water than the other clay in the cover layer.

4.3 Summary and discussion

Substantial erosion appears to have occurred inside the barrier on the south side of the model; possibly at gradients much lower than the critical gradient found in tests where the barrier does not protrude above the height of the aquifer.

The excavation indicates that barrier material was eroded at least up to the line of tracers that was 5 cm from the upstream barrier edge on the south side of the model (side #2). The head measurements also indicate a displacement of the transducer h62 at this location, which is most probably due to erosion of the barrier material below this location. The film of fine sand on top of the barrier even suggests that the pipe may have breached the barrier, although the sand may also originate from the initial preparation.

Measured gradients in the barrier at this location remained significantly below critical gradients over the barrier that were measured for the ‘long growth step’ of this barrier material in medium-scale tests. The highest gradient that is measured on the side #2 is 0.22, prior to the reduction of the upstream water level and the apparent displacement of transducer h62 (later measured gradients on this side are not considered representative as these are affected by the transducer displacement). This is significantly less than the critical gradient of ca. 0.4 for pipe progression which was found from the medium-scale tests in which the barrier did not penetrate into the cover layer.

The erosion mechanism appears to be different in the case of a barrier protruding above the aquifer. With a barrier that is level with the aquifer, as investigated in the medium-scale tests, the grains have to be mobilised horizontally by a critical gradient. In the case of the barrier

protruding above the surface of the background sand, grains roll into the pipe under the influence of gravity and a slope would form below the roof of the cover layer. The further erosion of the barrier in this case would be affected by the space that is available in the pipe downstream, as well as by gradients in the barrier. But the heads measured by the transducers are now the heads in the void above the slope and would therefore not be representative for comparison with horizontal critical gradients in experiments without protrusion.
Failure of the barrier would also be different in a protruded barrier than for a barrier that is level with the aquifer. When the slope reaches upstream in the barrier, there would still not be a path through the barrier for transport of background sand, as the slope is above the level of the background sand. The barrier could fail when the vertical gradient below the barrier at the upstream barrier interface is sufficient to fluidize the barrier material at the upstream interface. This could create a path through which the fine sand is transported over the barrier. The steepness of the slope would be important as this controls the distance over which sand must be fluidized.
In Chapter 7 numerical analyses are conducted to verify whether it is likely that vertical gradients caused the fluidisation of the barrier.
As the upstream water level was lowered, and subsequent repairs appear to have caused displacement of the cover layer, there appears to have been no further development of the slope during this experiment. When the head was raised again there was still some erosion in the pipe on the south side of the model, but the main erosion and pipe progression appears to have been occurred on the north side of the model. That might be expected if the path thought the barrier on the south side were clogged. The eroded barrier material that was distributed in front of the barrier may also have played a role in preventing further erosion of the barrier on the south side.

During the first loading, it appears there was substantial erosion of the barrier when the pipe reached the barrier in the south end of the model. On the other hand, during the second loading, pipes appear to have reached the barrier at the north end of the model as well, based on measurements. Excavations, however, did not find pipes at the barrier, and at this location no signs of erosion were observed during the excavation. However, the excavation of the top of the barrier was not performed along the entire width of the set-up, and the presence of white tracer particles in the eroded zone in the north side of the model does indicate that at some locations the pipes on the north side of the model reached at least up to 5 cm from the barrier. The difficulty to establish whether the pipes did reach the barrier on the north side of the model, and reason that no significant erosion was observed during the excavation might be that the pipes in the north side of the model were significantly smaller than the pipe in the south side of the model.
The pipe on the south side appears to have been the only pipe that reached the barrier during the first loading, and during part of the second loading and therefore channelled all the flow that converged in the barrier towards the pipe. This resulted in significant erosion both in front of the barrier and a large pipe that also cuts into the cover layer.
There have been various pipes in the north side of the model at the ditch, and observations from the excavation indicate that erosion has occurred over a much wider area. The pipes running upstream were observed to diverge but not traced to the barrier. The distribution of flow over a wider area, and also between multiple pipes in the north and the large pipe on the south side would result in smaller, shallower pipes in the north side of the model. If one or multiple of these reached the barrier, there would be much less space for erosion of barrier material than there was in the deep pipe on the south side of the model. However, this is speculation based on the available data.

As a significant amount of leakage occurred during this test, it cannot be ruled out that this affected the results. Leakage may possibly also have caused a preferential flow that influenced pipe formation and the dimensions and growth directions of the pipes. It is notable that the pipe on the south side of the model progressed almost to the edge of the model as it grew upstream. In the north side of the model the pipes also appear to tend towards the side rather than the centre of the model.

Limited pipe progression along the barrier prior to damage of the barrier

It appears that during the first loading, the pipe had not progressed significantly parallel to the barrier prior to damaging the barrier. Two possible causes for this are: (1) the geometry, with a barrier that extends into the cover layer up to ca. 0.20 m above the aquifer surface where the barrier material protrudes above the surface of the aquifer, and (2) possibly the effect of leakage along the side wall.

The geometry of the barrier is different from the medium-scale tests where the barrier is level with the sand body. In the case of a barrier level with the sand body, the pipe first progresses parallel to the barrier before penetrating the barrier. A critical horizontal gradient has to be overcome to mobilise the barrier grains in a horizontal direction. However, if the barrier rises above the sand body, as soon as a pipe reaches the barrier, the barrier grains can collapse into the pipe, even with a low gradient inside the barrier.

It is also possible that there was some leakage flow along the side of the model, which therefore caused higher flow in the barrier at the sides. This may have contributed to the erosion at the location of side #2 and allowed for more erosion of barrier material into the pipe downstream. The possibility that there was a higher flow along the sides of the model is also suggested by the direction of pipe growth form the ditch upstream towards the walls, rather than through the centre.

Erosion of the cover layer

Erosion of the cover layer above the pipe occurred. The presence of pipes that had eroded into the cover layer was observed both close to the barrier and close to the ditch. This might be due to a lower level of compaction of the clay in the test, in combination with the high flow rates in the pipe. It was also observed that the cover layer could easily be removed at the north side upstream of the ditch around the zone of transducers in row 2.

Head drop in the pipe downstream

It is not clear whether the pipe was directly below transducers in line h3#. Therefore the head drop from these to the ditch does not indicate the head drop in the pipe. However, it appears that the pipe was present below h42 or very close to this. The head drop between the transducers in the barrier in row 4# and the head measured in h15, just upstream of the tip of the ditch is shown in Figure 4.16. This shows a substantial head drop in the pipe.

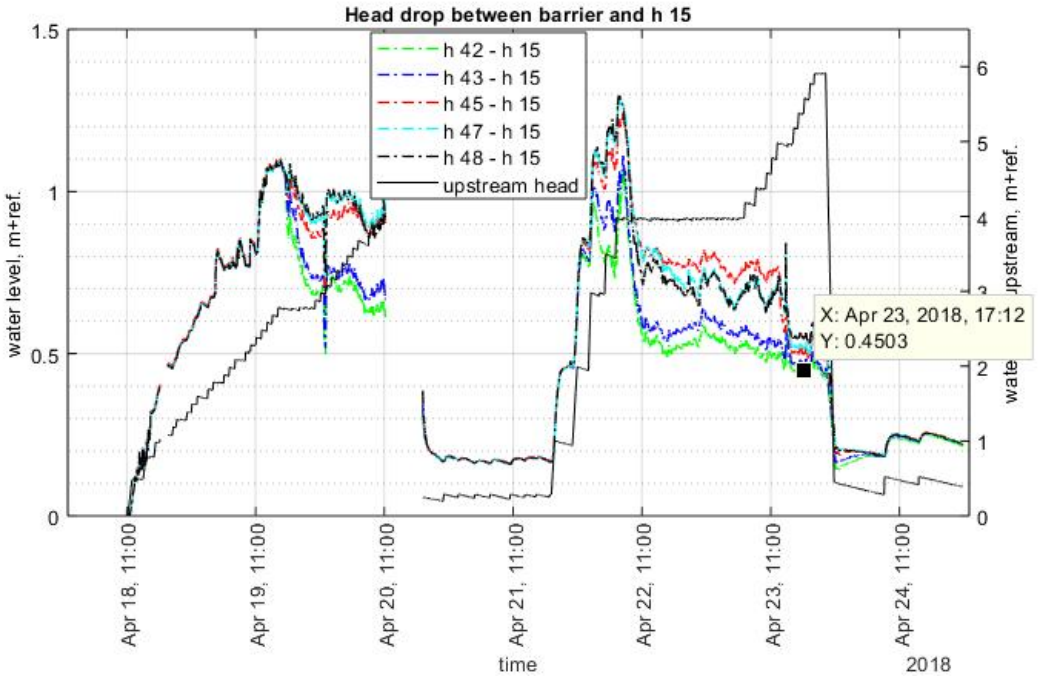

Figure 4.16 Head drop between transducers in the downstream end of the barrier and just upstream of the ditch (h15). Measurements and observations indicate that a pipe was present between h42 and the ditch from April 19th ca 16:00 onwards, therefore the head drop h42 – h15 is considered to characterise the head drop in the pipe

Considering the measurements after the head has been re-applied to a level of 4 m or more, the head drop from h42 to h15 is in the order of 0.55 – 0.45 m, corresponding to an average gradient in the order of 0.05. The pipe depth at which the grains on the bottom of the pipe would be in equilibrium is computed using the limit equilibrium by Sellmeijer, using the derivation in van Beek (2015) to compute the bedding angle. This results in pipe depths of ca. 1.5 mm (for the grain size of the background sand) or 0.8 mm (for the grain size of the barrier).

The observations during the excavation indicate that the actual pipe depth was substantially larger. In the south side of the model, the pipe had cut in the order of 5 cm height by 5 cm width or more into the blanket layer, which means that the actual pipe dimensions would have been even larger. This means that the shear stress on the walls of the pipe would be substantially above the limit equilibrium with a gradient in the pipe of 0.05, so that active erosion would be expected for the combination of discharge and head drop that were measured in the test.

The presence of suspended material, barrier material, clay, and background sand, would also increase the measured head drop in the pipe. Furthermore, turbulence can be expected to have contributed to the head drop in the pipe and to erosion.

Tracer particles do not reliably indicate pipe progression

The tracer particles appear to have been caught in the pipe, causing many to not appear downstream or only after the pipe had already passed the location of the tracers. Especially for the erosion at the barrier on the south side, the tracers appear not to have been very effective, as the observations during the excavation do indicate that the blue tracer particles from the upstream side of the barrier were displaced to the front of the barrier but not much further downstream. This might be due to erosion of the barrier leaving a void above the barrier which could collect the tracer particles rather than having the tracer particles flown downstream

through the pipe. Heavier tracer particles, with the density of water or slightly higher might have been more appropriate. White tracer particles were also found inside the pipes downstream during excavation, indicating that these got trapped somewhere inside the pipes after having been eroded, rather than that they were transported to the ditch as was intended.

Fine sand is observed on top of the barrier

The presence of fine sand on top of the barrier in the south side of the model where the barrier is eroded, and the cover layer has settled is not fully explained. This might possibly indicate that the barrier was breached, and the material flowed in from upstream, numerical modelling is used to assess this possibility in Chapter 7. As the upstream head was reduced in the period in which this breach might have occurred, the reduction of the head drop, and subsequent subsidence of the cover layer into the void in the barrier may have prevented an actual failure. This cannot be ruled out. However, the amount of sand that was observed on top of the barrier was very small, and a breakthrough of the barrier would be expected to have caused a larger inflow of background sand.

There may be another explanation for the presence of the fine sand such as a spill during preparation of the test.

4.4 Conclusion

Overall, it appears that the piping process that occurred in this test is different from what was observed in the medium-scale tests. Probably this is due to the geometry, in this test the barrier protrudes above the aquifer, whereas in the medium-scale tests the barrier is level with the aquifer. In the latter case, a pipe can reach the barrier, and first progresses parallel to the barrier. Subsequently as the pipe in front of the barrier deepens there is some crumbling to establish a stable slope. It appears that after this, a substantial horizontal gradient has to be established over the barrier in order to mobilise barrier grains and form a pipe into the barrier.

By contrast, for the barrier that extends above the aquifer top as was tested in first test in the Delta Flume, it appears that when the pipe arrived at the barrier there was only very limited lateral progression along the downstream interface of the barrier. Possibly preferential flow and leakage affected this. Due to the height of the barrier above the pipe, barrier grains will roll into the pipe under the influence of gravity. Possibly deposited grains also prevent the sideways progression to some extent, although on the other hand the pipe might still be expected to progress around such an obstacle. It appears that the pipe that was formed during the first loading was deep enough to accommodate the erosion of a substantial amount of barrier. That might also be due to the larger scale of this test, with more flow converging to the pipe than in the medium-scale tests. The erosion of barrier material will result in the formation of a slope in the barrier, and as more space becomes available, more material can roll out of the barrier. Therefore, a void is created in the top of the barrier that progresses upstream, rather than a pipe that progresses in the barrier.

This means that the critical gradient for pipe progression that was derived based on the medium-scale experiments is not directly applicable to this test.

4.5 Critical point for pipe progression

As the failure mechanism is different from the medium-scale tests, the critical point for pipe progression would be based on different considerations. It would not be the progression of a pipe in the barrier, as it is likely that a slope forms in the barrier which progresses upstream as more material is eroded. Then a critical point to determine barrier strength would be after such a slope had reached the upstream end of the barrier, creating sufficient space for fluidisation of barrier material and transport of background sand through the barrier.

For this test the progression of the slope inside the barrier in the south side of the barrier appears to have occurred at an applied upstream head of 4 m. There was no data at this point,

however, displacement of transducer h62 on the upstream end of the barrier would require the presence of a void below this transducer. This could be caused by the progression of a slope to the upstream end of the barrier. The measured gradients in the barrier rise steeply prior to the gap in the data, which indicates erosion in the barrier and the progression of the slope, although this might not have reached all the way upstream yet.
As the gradient is rising steeply in the first interval that the head drop of 4 m is applied upstream, the critical point for pipe progression is considered as the interval at which the head drop of 3.9 m is applied, from 09:00 to 10:00 on April 20th. The gradient profile at this point is shown in Figure 4.17, due to the lack of data it is not clear how the gradients developed during the period of constant head after this time.

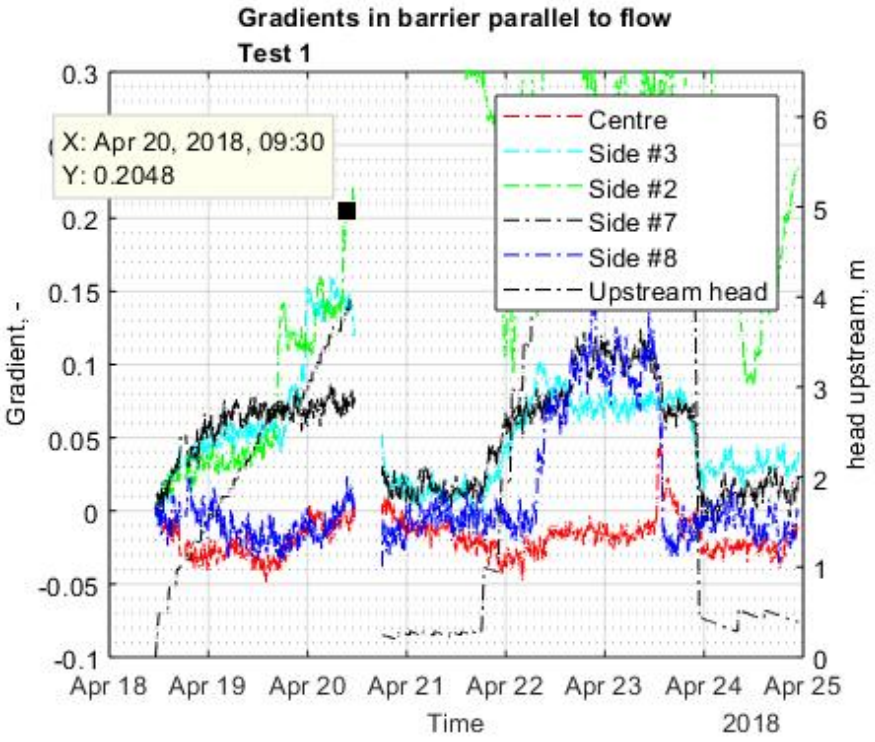

Figure 4.17 Measured gradients in the barrier in Delta Flume test 1, square indicates critical point prior to pipe progression.

The averages of the heads that were measured in the interval from 09:00-10:00 on April 20th are shown in Table 4.1. The measured profile is shown in Figure 4.18 and Figure 4.19.

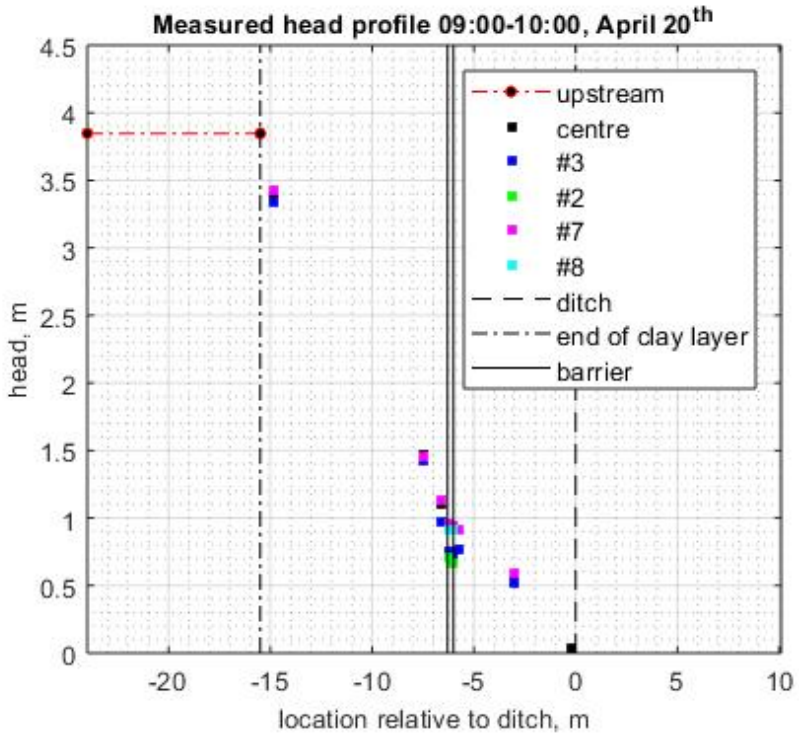

Figure 4.18 Measured head profile at critical point, average between 09:00 and 10:00 on April 20th in the 1st Delta Flume test

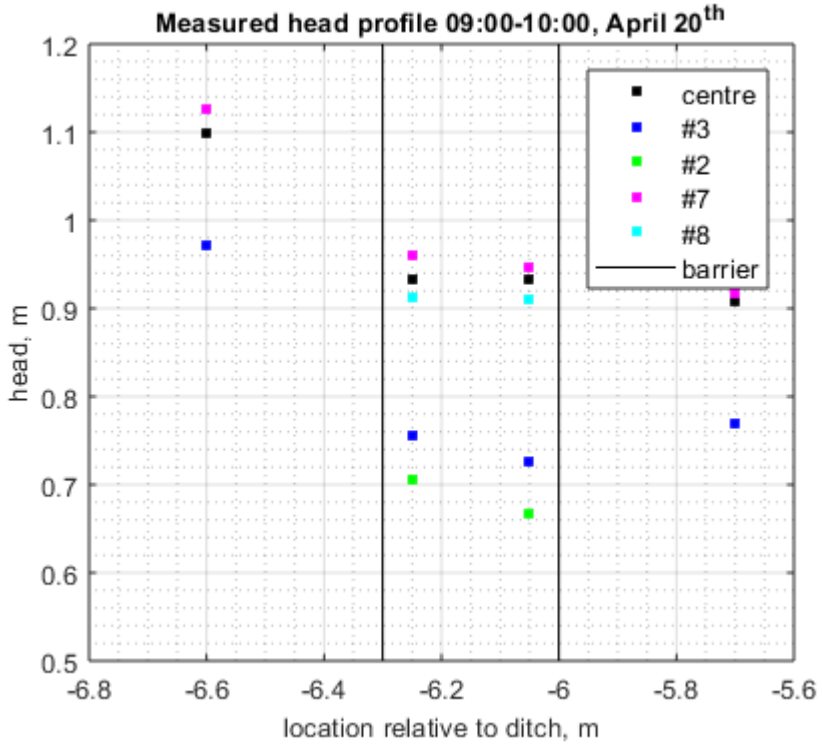

Figure 4.19 Measured head profile at critical point, average between 09:00 and 10:00 on April 20th in the 1st Delta Flume test

Table 4.1 Heads measured during the critical point (09:00-10:00 on April 20th)

DCTM01	h_93	h_95	h_97	h_90	h_10	h_15	h_23	h_25	h_27	h_33	h_35	h_37
3.85	3.34	3.39	3.43	3.52	0.33	0.03	0.52	0.55	0.59	0.77	0.91	0.92

h_42	h_43	h_45	h_47	h_48	h_62	h_63	h_65	h_67	h_68	h_73	h_75	h_77
0.67	0.73	0.93	0.95	0.91	0.71	0.75	0.93	0.96	0.91	0.97	1.10	1.13

h_83	h_85	h_87
1.43	1.46	1.45

The heads in h62 and h42 are significantly lower than the heads in rows parallel to these PPTs inside the barrier. This would be expected due to the presence of the pipe in front of the barrier at that point. The head in h33 in front of the barrier is lower than in h35 to the centre, which is probably due to the presence of the pipe and the eroded area in front of the barrier in the vicinity, but this appears to be just to the south of h33 (based the higher head at h33 than in h42, and this is also indicated by the observations after the excavation). The expected outline of the pipe is shown in Figure 4.17 at the end of this chapter. It is not clear how much of the barrier had crumbled into the pipe at the critical point, or how the erosion front in the barrier progressed over time from April 19th to April 20th.

The head drop from the upstream water reservoir to h15 just upstream of the ditch is considered as the critical head drop for pipe progression in this test, this head drop is 3.81 m.

There is still a significant head loss between the head measured in the downstream side of the barrier where the pipe appears to be, h42 and the head in h15. The head drop is ca. 0.63 m. In the medium-scale tests, the head loss in the pipe was negligible, but that is not the case here. This high head drop in the pipe might be due to the presence of suspended material, and it could indicate that the limit equilibrium for grains on the bottom of the pipe was not fulfilled, and that grains were still being eroded in the downstream pipe.

Upstream of the barrier, the head in h73 is also lower than the heads in h75 and h77, indicating that the pipe being on the south side at the barrier also affects the head profile upstream of the barrier. A sketch indicating possible pipe extents at different times during the experiment is shown in Figure 4.17. The progression of the pipe in the north side of the model occurred after what is considered to be the critical point of pipe progression, as pipe progression did not lead to a clear collapse of the barrier.

Note the uncertainty regarding:

- Progression of the pipe through the upstream barrier interface at h62, it is not clear whether this was the case.
- The progression of the pipes on the north side of the model parallel to the barrier or not. Excavations show multiple pipes progressing from the ditch towards the barrier in the north side of the model. The fall in h47 could therefore be due to one of those reaching towards that location, or to parallel progression of the pipe that progressed towards h48

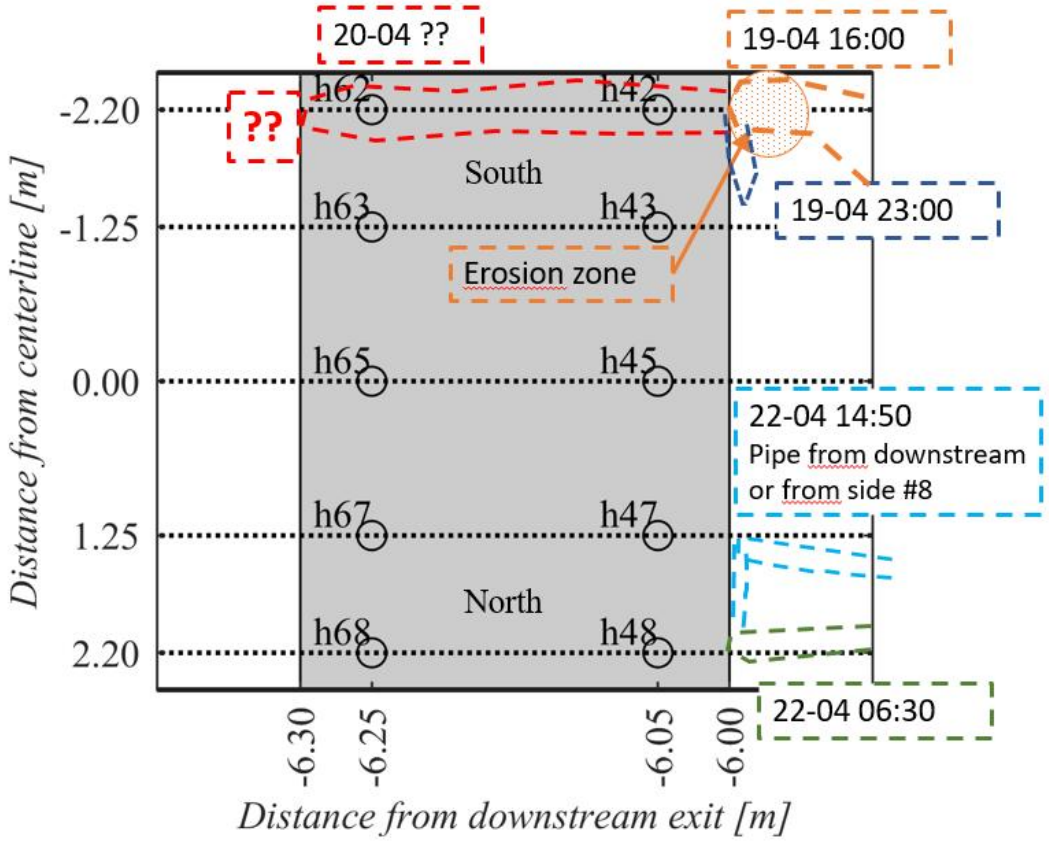

Figure 4.20 Indicative sketch of possible pipe extent during Delta Flume test 1 based on head measurements. The expected minimal extent of the pipe after the progression after *the indicated time steps is shown; it is possible that the pipe progressed further than the locations indicated here.*

5 Piping process during 2nd Delta Flume test

This chapter combines the data that was collected during the second Delta Flume test: PPT measurements, observations during the test, and observations from the excavation after the test in order to analyse the piping process.
Most data was presented in Deltares (2019a), therefore this chapter only shows those data that are most relevant to the interpretation of the piping process. The measured gradients inside the barrier during the entire test are shown in Figure 5.1. The measured heads on the upstream (h6#) and downstream (h4#) side of the barrier provide additional insight relevant to the interpretation of the gradients. These are shown in Figure 5.2 and Figure 5.3.

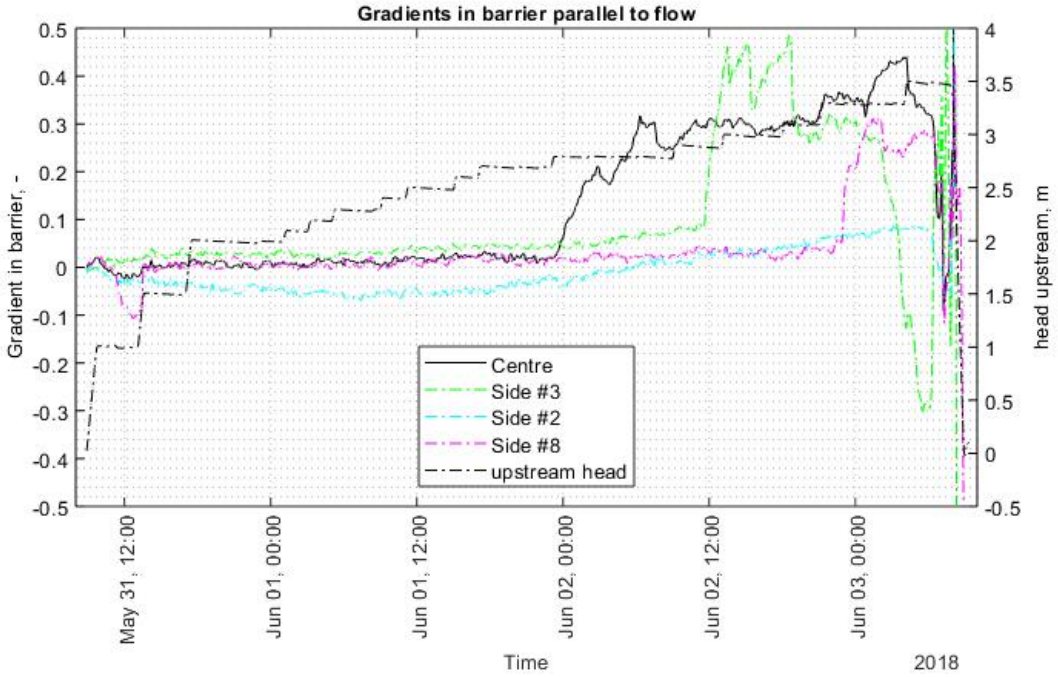

Figure 5.1 Gradient parallel to the flow direction inside the barrier (over 20 cm) during the second Delta Flume test (GZB 2, Delta Flume sand). Line 7 is not shown as the transducers P47 and P67 were both considered to be unreliable.

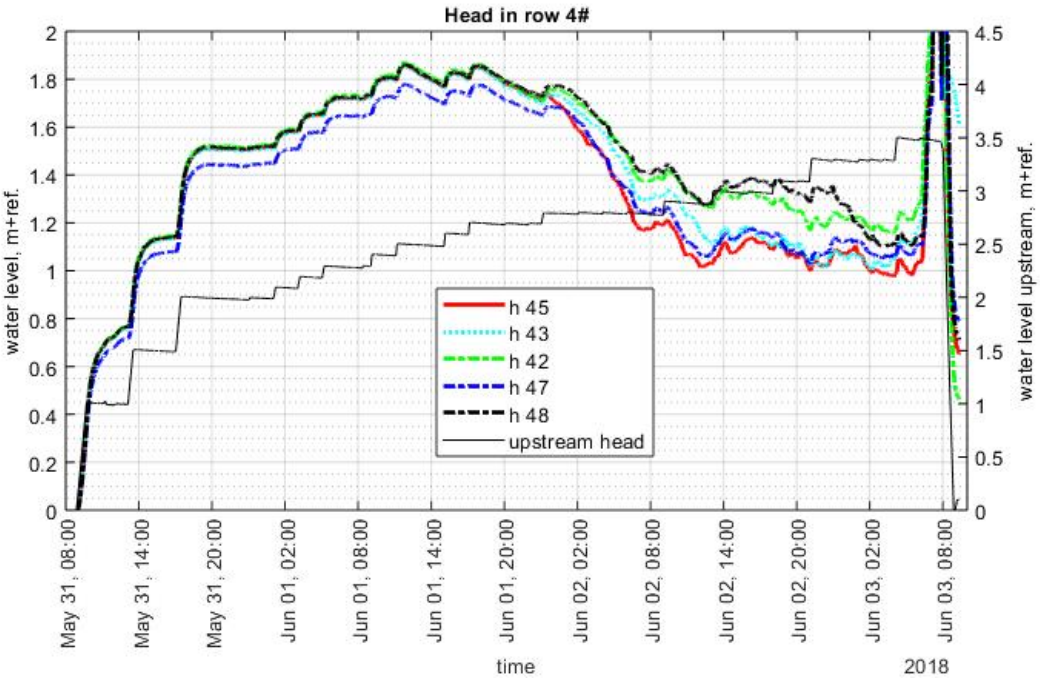

Figure 5.2 Heads measured near the downstream barrier interface during test 2, applied head drop is shown on right hand axis

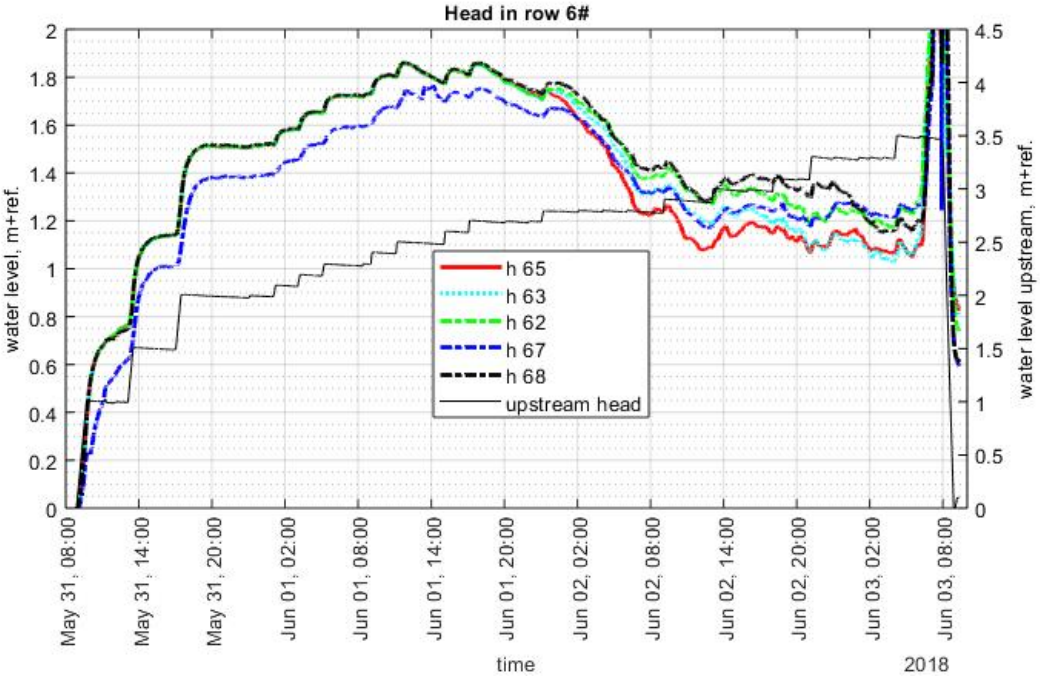

Figure 5.3 Heads measured near the upstream barrier interface during test 2, applied head drop is shown on right hand axis

5.1 Evidence during the test

During this experiment the heads measured in h47 and h67 rise less than the heads in the rest of the transducers from the start of the test. The difference between these two transducers also increases in an apparently erratic manner. Therefore, these transducers are considered to be unreliable and these are not used for the analysis.

Initiation of piping

The first sand boils are reported to form at poles stuck into the ditch which are intended to hold a screen to catch the eroded tracers around midnight on May 31st. This is remarkable as these are not at the tip of the ditch. It appeared the ditch was not dug entirely through the clay layer, which caused additional resistance. On June 1st at 10:35, the clay layer was removed which results in a fall of h15 that is at the surface closest to the ditch.
H09 is in the ditch and measures the water level in the ditch. The sawtooth pattern that can be observed in the value of h15 is probably due to the periodic removal of sand from the sand boils.
Due to these effects the initiation of piping and the progression of the first pipes cannot be clearly identified.

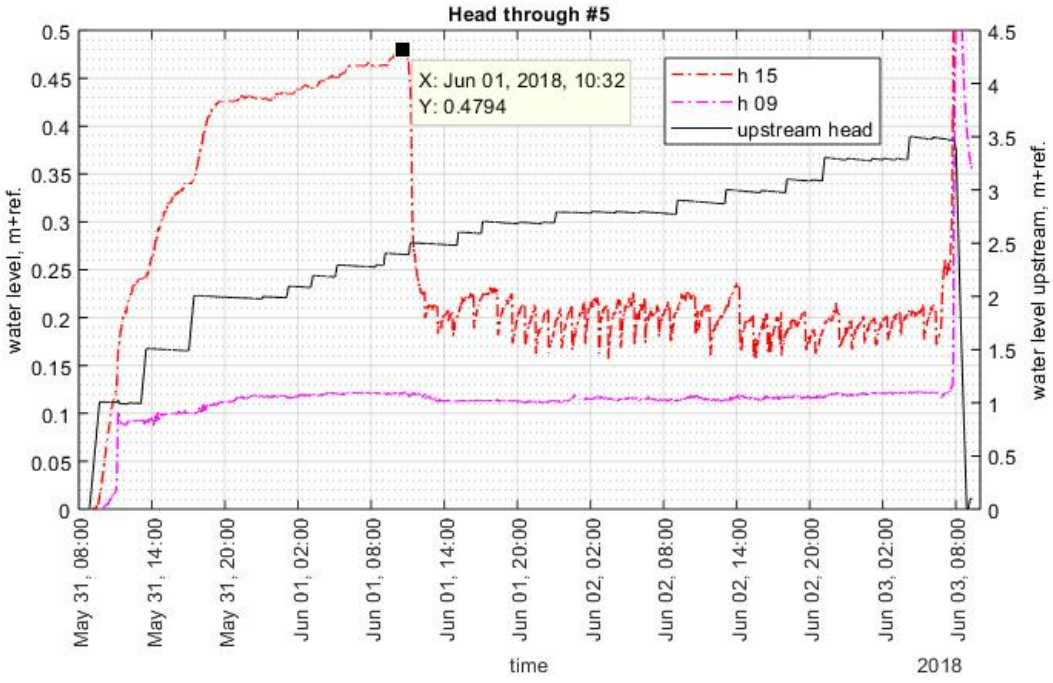

Figure 5.4 Heads measured in the ditch (h09) and in the aquifer just upstream of the ditch (h15), the decline of h15 is due to removal of a layer of clay in the ditch bottom.

Pipe reaches the barrier

The point that the pipe reaches the barrier can be clearly identified from the fall in the heads and from the increase in the gradient in the centre of the barrier. The gradients in the barrier are low initially but the sharp rise at ca 23:30 on June 1st indicates that the pipe reached the barrier close to the centre. The gradient in #3 rises at 11:15 on June 2nd suggesting that the pipe progressed parallel to the barrier. The gradient in h#2 does not rise suggesting that the pipe did not progress all the way to this side.
There are no observations of tracer particles at this time.

The development of the hydraulic conductivity of the entire sample, based on the flow rate and the head drop (between upstream and h09 in the ditch) is shown in Figure 5.5. This does not show a marked increase around the time that the pipe reaches the barrier, similar to the first Delta Flume test.

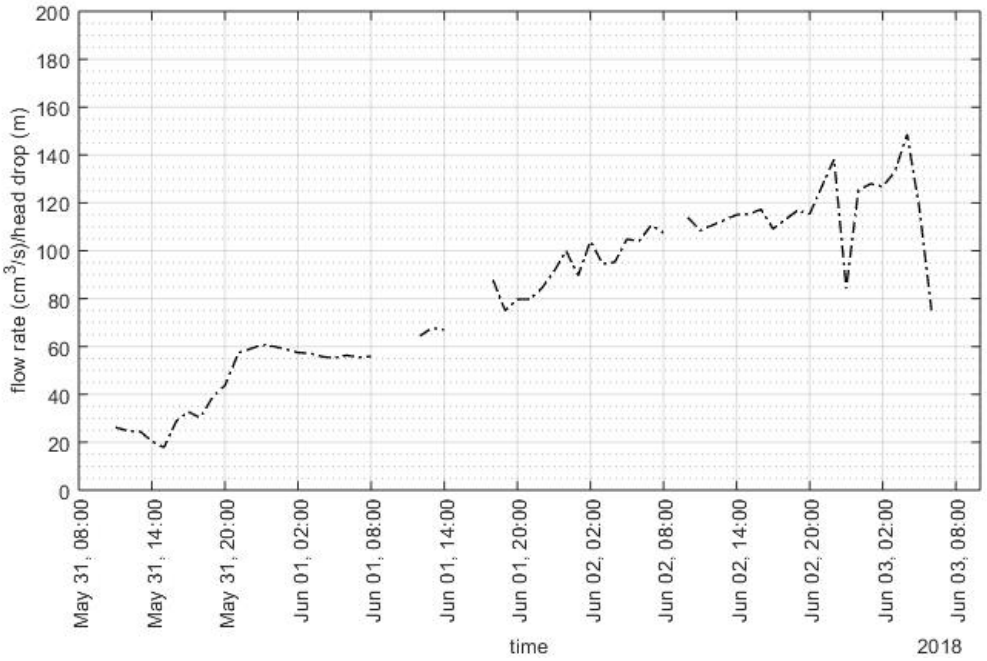

Figure 5.5 Flow rate divided by head drop between upstream water body and h09.

Erosion in the pipe downstream

Head measurements in sections through the model along lines #5 and #3 show that heads at both locations fall when the pipe reaches the barrier in the centre, as also observed in the medium-scale tests. This decline continues when the upstream head is maintained constant, probably due to erosion in the downstream pipe. The heads level off when the next head increment is applied at 09:00 on June 2nd but fall further at constant head drop.

The heads in the row h4# are in the order of 1 m, which indicates that there is significant head drop in the pipe. Observations indicate sand production.

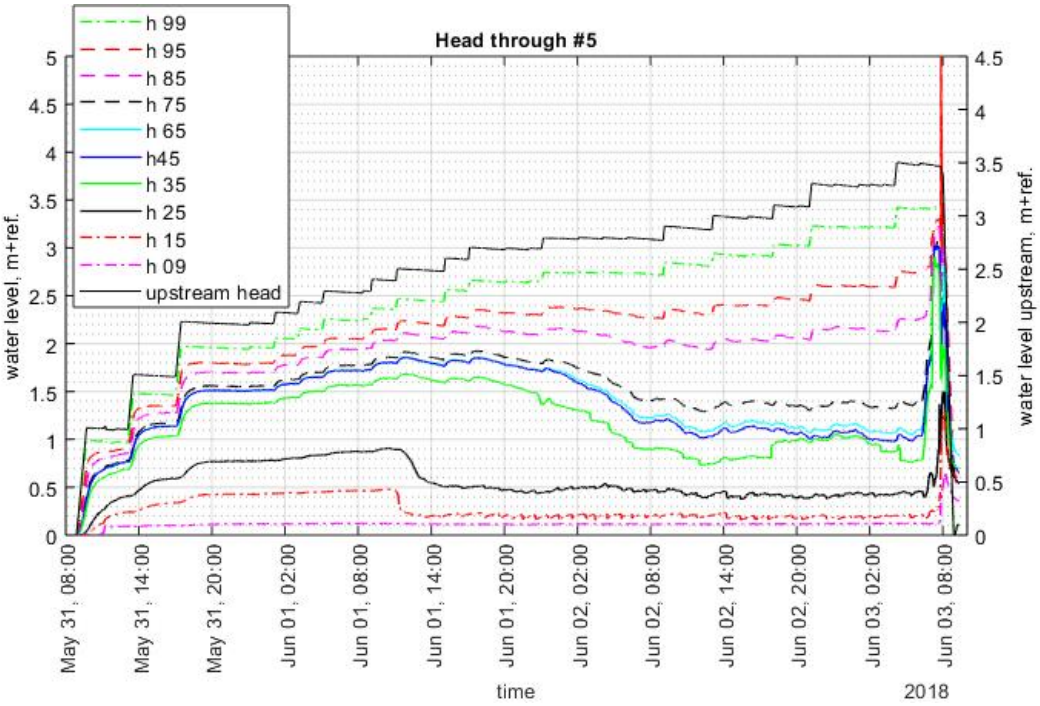

Figure 5.6 Heads along row #5

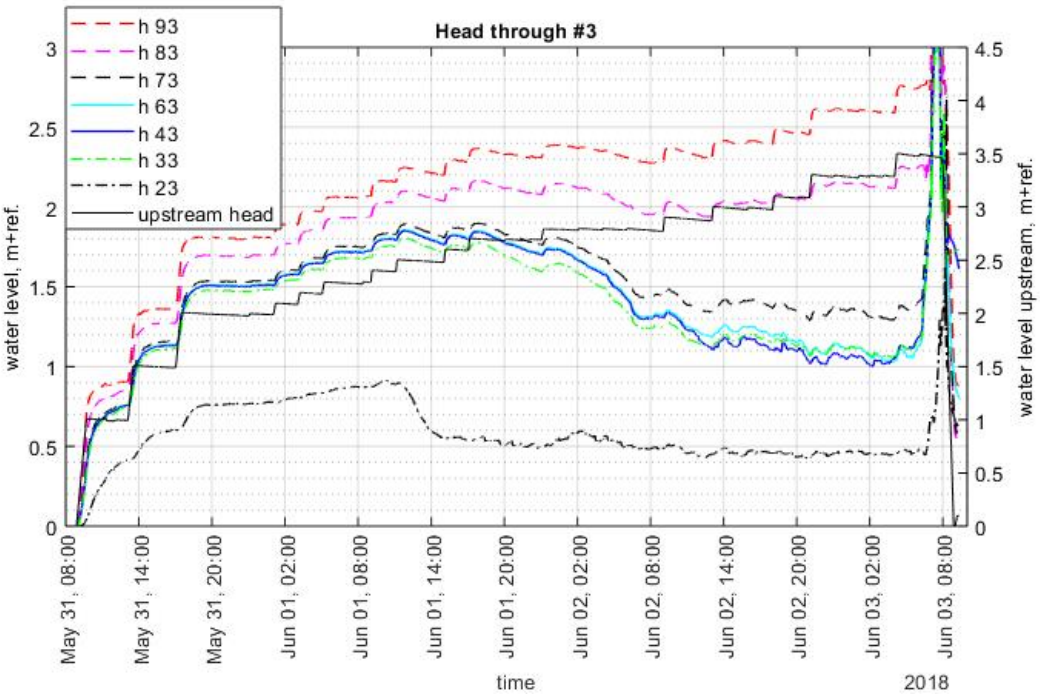

Figure 5.7 Heads along row #3

When the pipe reaches close to or at side #3 this causes a sharp fall in h43, which falls below the head measured downstream of this transducer in h33 which is further downstream. This suggests that there is no pipe directly present below h33, but there is a pipe at h43 (or close to it) and this supports the assumption that the pipe that progressed from the ditch to the barrier in the centre of the model subsequently progresses parallel to the barrier, rather than that a separate pipe progressed from the ditch to h43.

Progression of the pipe into the barrier and subsequent erosion

Between the point that the pipe is considered to have reached the vicinity of h43, June 2nd at 11:15, and 18:35 on the same day the gradient in side #3 fluctuates but remains high.

At 18:35 the gradient at side #3 falls sharply resembling what is seen as a long growth step in the medium-scale tests. At the critical point for progression (the interval from 16:00-17:50) the gradient is 0.41, after progression the gradient is in the order of 0.3. The prior drops are smaller, and after those the gradient increases again to a higher value than previous, and for the long growth step the maximum gradient in the barrier is used. The drop is less steep than was observed in the medium-scale tests, but this might be expected if the pipe progresses at a greater distance away from the transducer pair. Even with the small distances among transducers in the medium-scale tests the difference of the response among transducers is already significant.

There are no observations of tracer particles at this time.

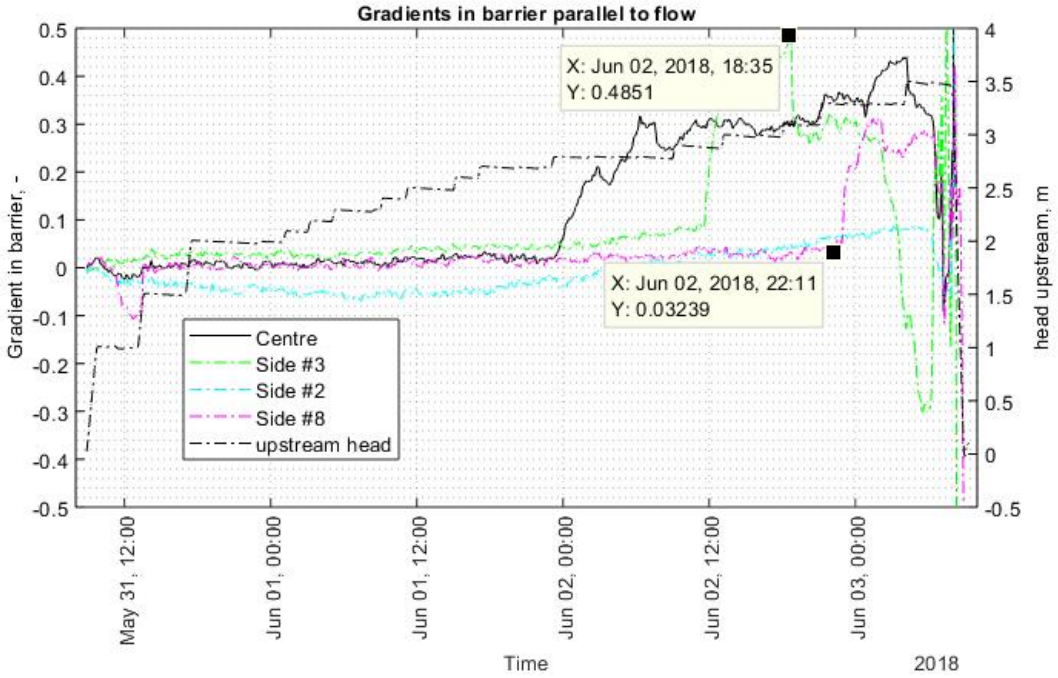

Figure 5.8 Measured gradients in the barrier

Pipe progression in the north side of the model

The gradient at side #8 (north) rises sharply at 22:15 on June 2nd suggesting that the pipe progressed parallel to the barrier to this side, or that a pipe progressed from downstream to this side. The strong reduction in h38 (Figure 5.9) suggests that the latter is the case.

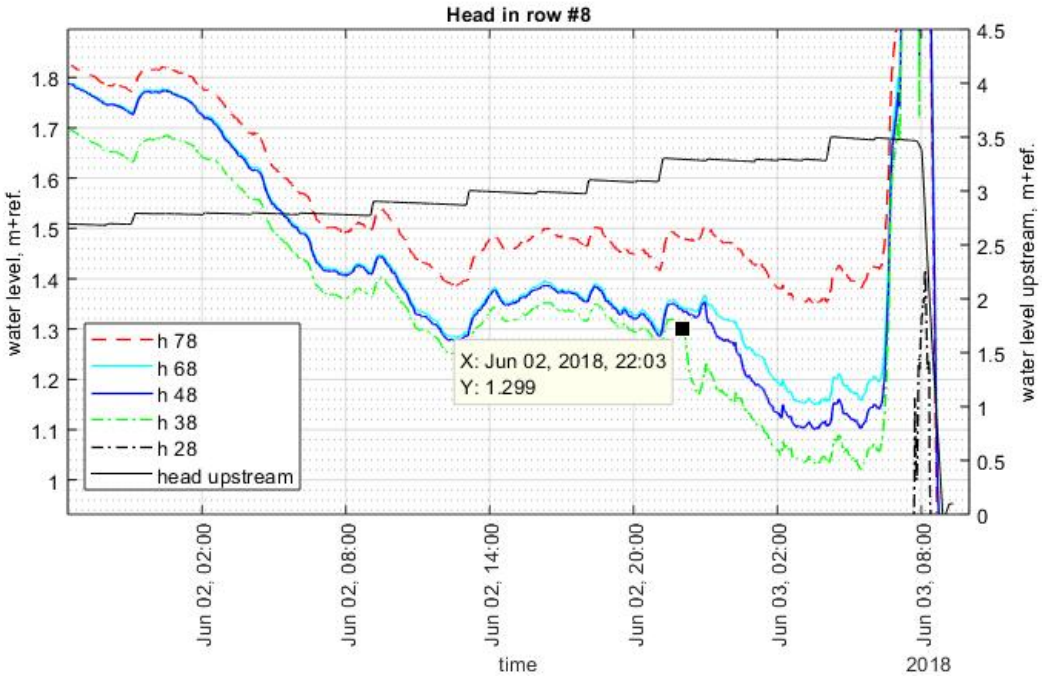

Figure 5.9 Heads along row #8, close-up around time pipe appears to reach the barrier at this side.

Progression of the pipe to the upstream row of transducers inside the barrier and failure
It is difficult to assess what exactly causes the evolution of the heads, and measured gradients, and the following explanation can be considered speculative.

Around 01:20 on June 3rd heads in h63 and h43 start to fall, indicating further erosion at that side (Figure 5.11 and Figure 5.12). The gradient in the barrier remains approximately constant until ca. 02:00 and then falls sharply (Figure 5.10). This fall might indicate progression of the pipe in the vicinity of these transducers, possibly even through the upstream interface.
The fall of the gradient coincides with a jump in the heads in h43 and h63 (Figure 5.14). A jump might indicate a displacement of the transducers, due to settling of the cover layer, which could explain the negative gradient. This jump is also distinguishable in other transducers in row h4#, specifically in h42. That might be because the downstream pipe appears not to have reached h42 yet and therefore a reduction of flow through the area #3 would also reduce flow from the side #2 to the pipe. The transducers upstream of the barrier in row #7 also show a minor jump (Figure 5.13), which might be due to a temporary increase in resistance downstream.
If the pipe had breached the interface around 02:00 on June 3rd, this would have caused an influx of background sand, which might also contribute to clogging if settlement of the cover layer had plugged the pipe.

Observations report that the Vingerling clay, which is present on top of the barrier, is spotted coming from the pipe at 02:00 and at 03:00. This could be produced if there was indeed a settling of the cover layer.

At 04:15 the gradient in the barrier in the centre of the model falls (Figure 5.10), and around 04:30 heads throughout 4# and 6# fall (Figure 5.11 and Figure 5.12), indicating further erosion, probably both in the pipe downstream (reducing all heads) and in the barrier close to the centre (reducing the local gradient). The head transducers on the upstream side of the barrier in 6# start to rise around 05:30 whilst the head is maintained constant, this is also the case in 7#.

This might be expected if the pipe had progressed upstream after breaching the upstream barrier interface and this causes the flow to increase.

The gradients in the centre and at #8 fall sharply at 06:20 suggesting that a pipe also progressed through the barrier at those locations. Those gradients had already increased earlier during the tests, indicating that pipes had already progressed into the barrier at these locations.
The gradient in side #3 on the other hand is negative until ca 06:00 and then starts to rise strongly. This might possibly indicate that the barrier is indeed clogged in the south side of the set-up.

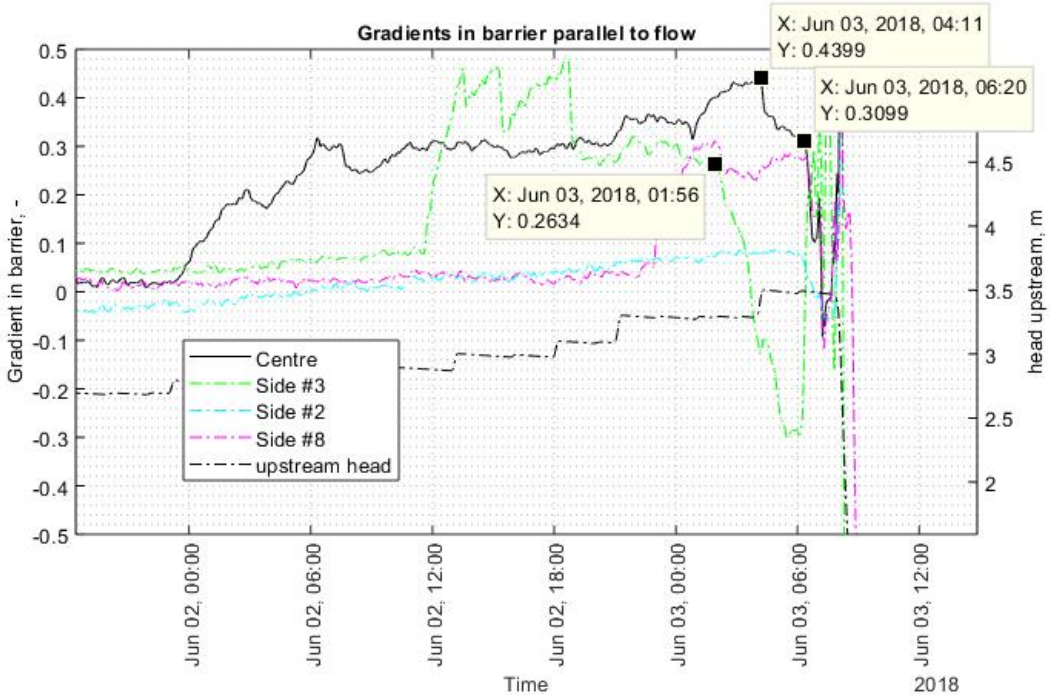

Figure 5.10 Gradients inside the barrier around failure

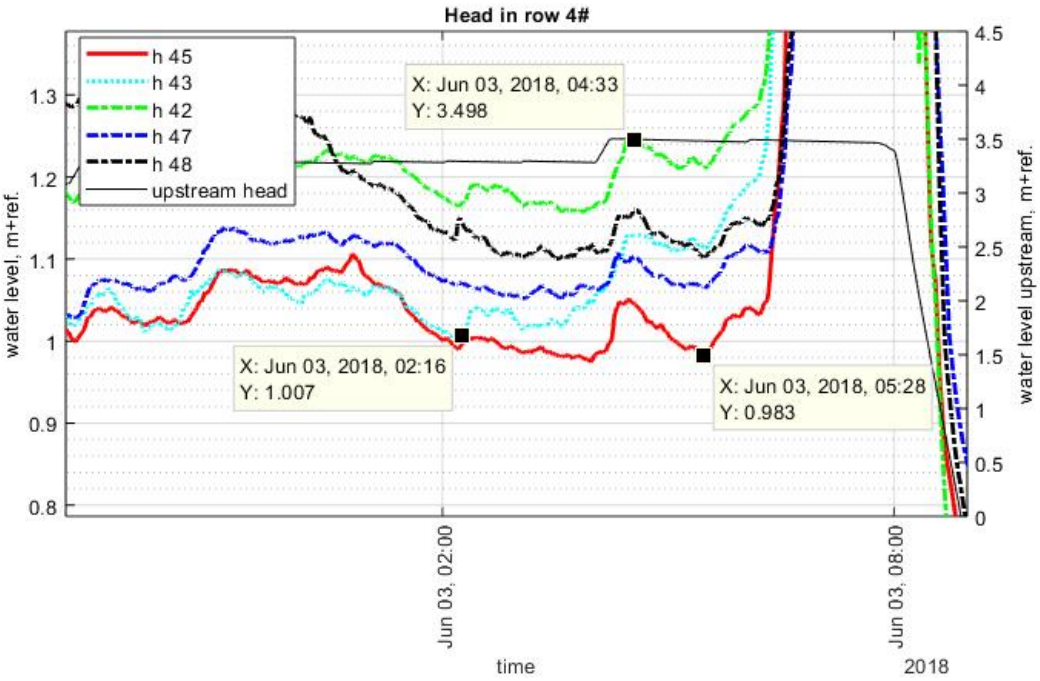

Figure 5.11 Head in row 4# around failure

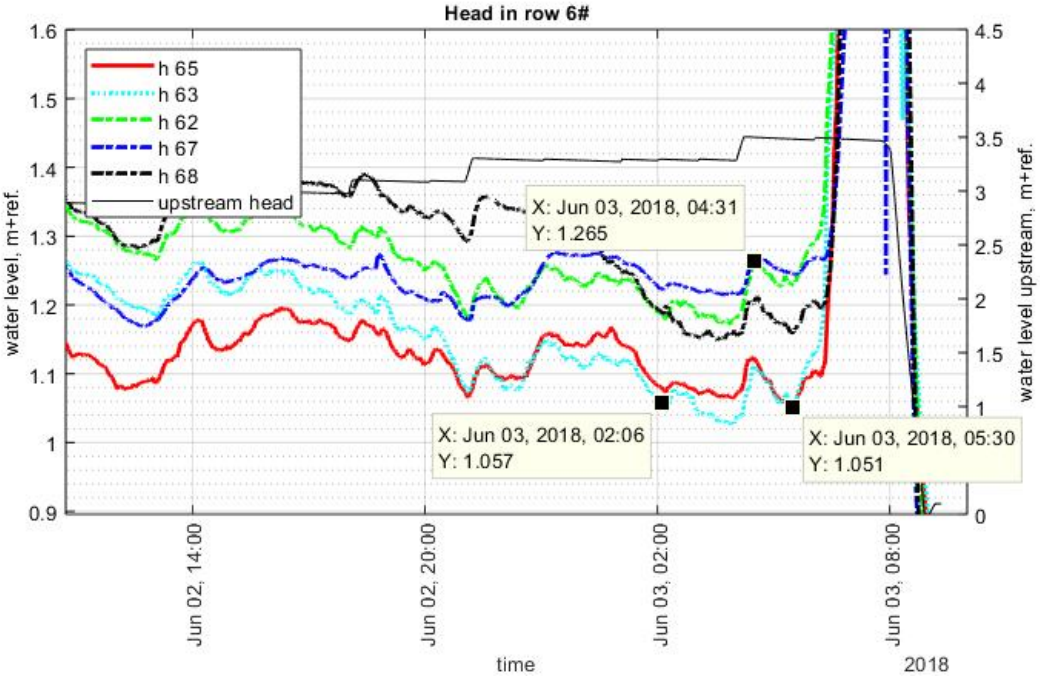

Figure 5.12 Head in row 6# around failure

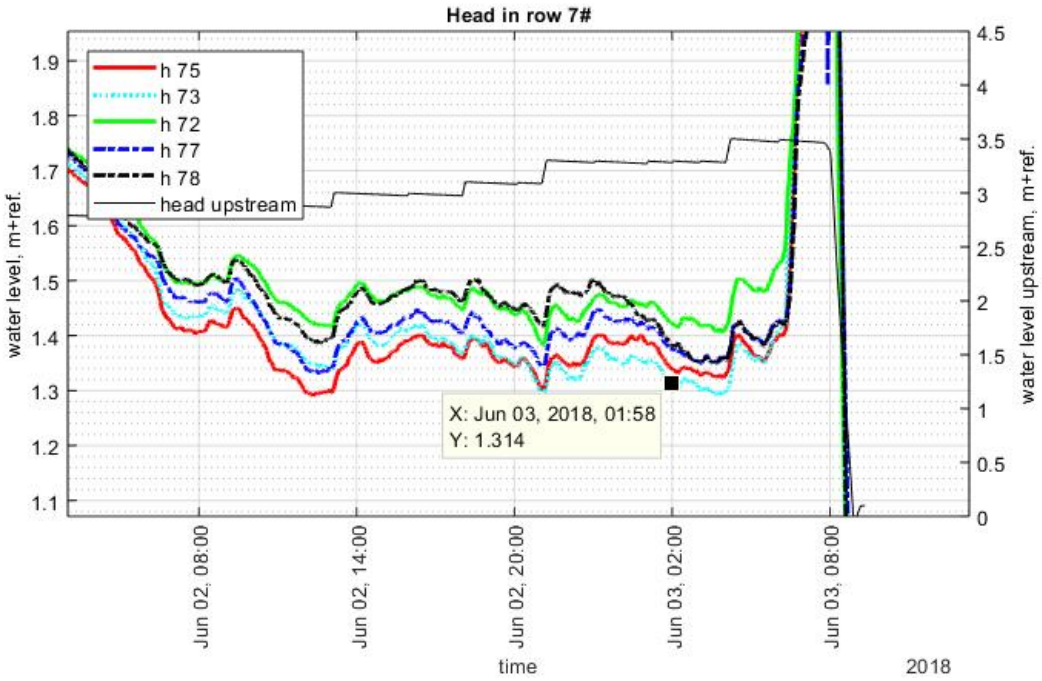

Figure 5.13 Head along 7# around failure

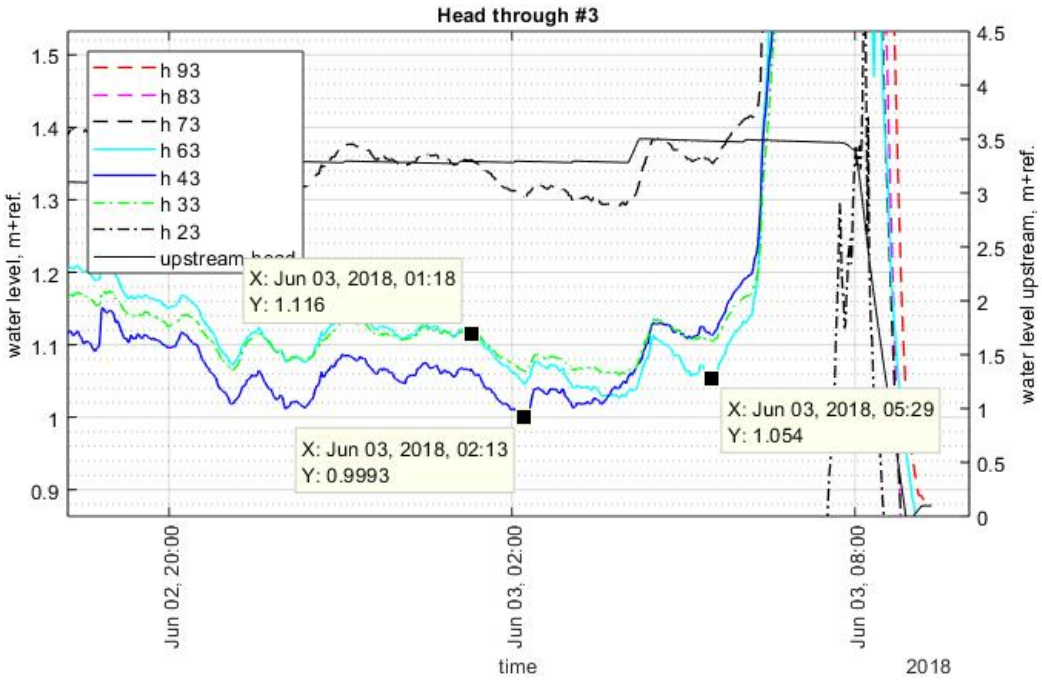

Figure 5.14 Head along #3 around failure

Observations did not indicate anything during the period described above from 1:30 to 06:00, with the exception of the observed Vingerling clay.

Around 07:00 on June 3rd it is observed that measurements in h83 and h93 are ‘remarkable’. Indeed, a small dip followed by a steep rise can be observed in h83 and h93 around 06:22 and 06:40 respectively. At 07:00 these values have increased by almost 1 m. This is probably due to the connection that the pipe makes with the upstream water body around this time.

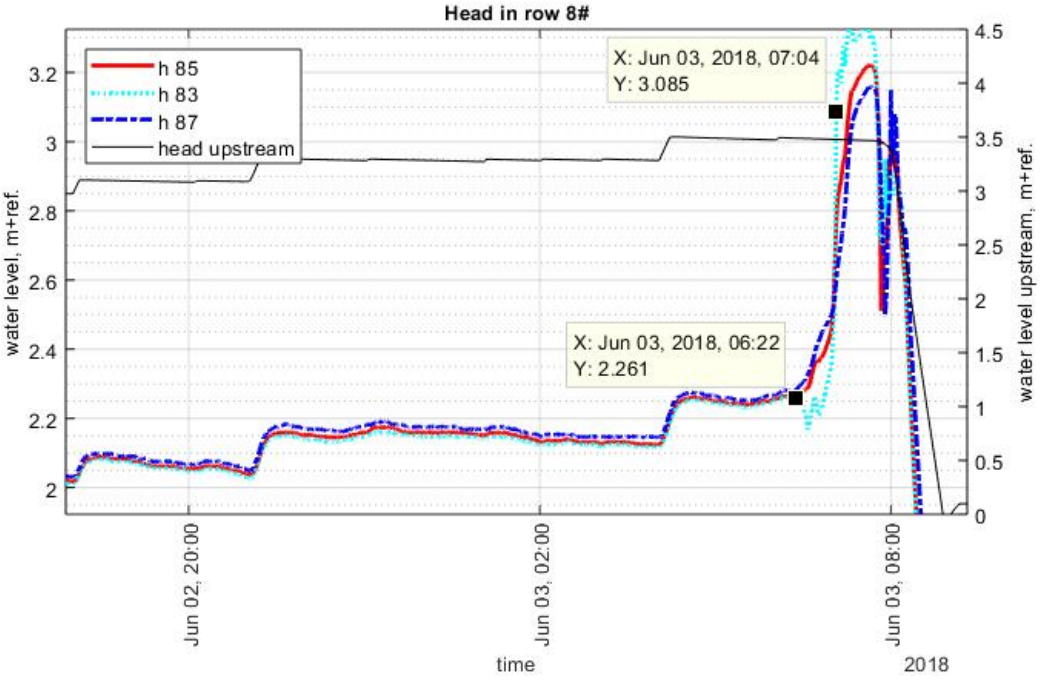

Figure 5.15 Heads in row 8# around failure

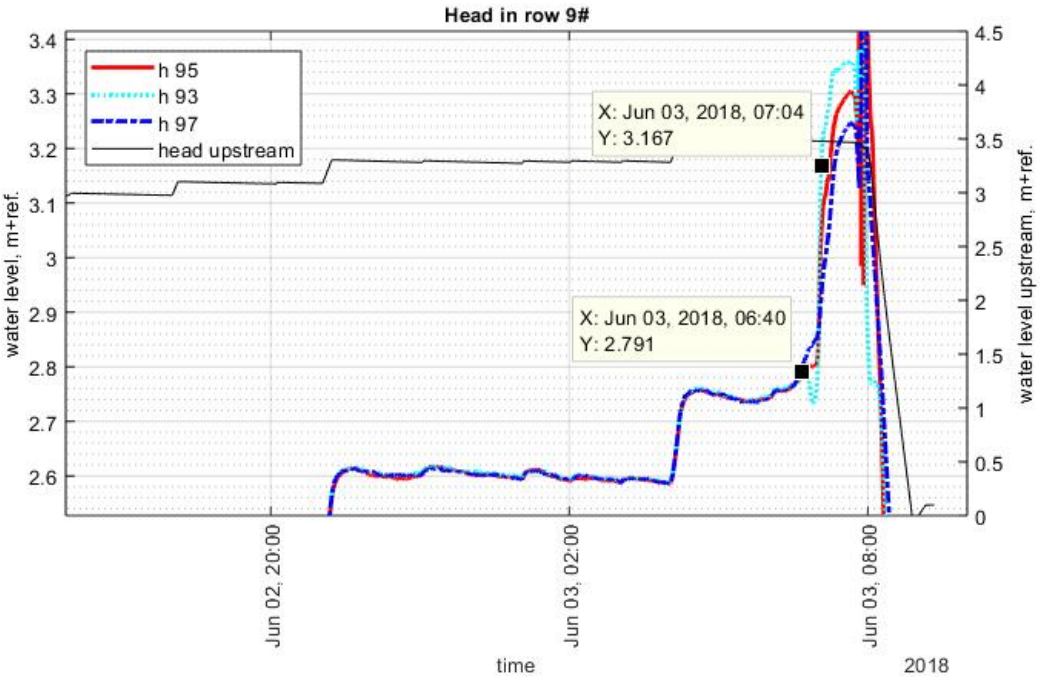

Figure 5.16 Heads in row 9# around failure

At 07:50 air bubbles are observed along the upstream side of the sheet pile wall. It is noted that the sand boil had already turned into a ‘mud fountain’. The time of that transition is unclear. Another observation made around 7 a.m. states ‘during the development of the mud fountain an outblow could be seen in the sand bed at the upstream side.’

5.2 Evidence from excavation

As failure occurred during this test, excavation concentrated on the area near the barrier.

Excavation indicated that the barrier was eroded significantly in the south side of the model, but that a ca. 0.15 m high layer of barrier material was still present. On top of this, fine sand was encountered, and on top of this the Vingerling clay that forms the cover layer above the barrier. This would match the described process whereby the pipe did breach around the south side (side #3) but due to deformation of the cover layer and deposition of sand from the enlarging pipe upstream this location was clogged.

The barrier was missing entirely at the north side of the model, and the remaining barrier material had fluctuating thicknesses along the width of the model. The strong erosion on the north side of the model would support the tentative explanation based on the measurements, of the collapse of the cover layer in the south, in combination with the formation of a separate pipe from the ditch to the barrier at the north side. This would cause the overall resistance to flow on the north side to be less than on the south side and might result in preferential erosion on that side.

It was observed that the cover layer had subsided over large areas downstream. Pockets of sand inside the cover layer are observed. It is not clear whether these formed due to erosion of pipes into the cover layer, as was observed in the excavation of test 1, or whether these are due to deformations along local shear zones in the cover layer.

5.3 Evidence from AH-DTS

During the second experiment of the Delta Flume Experiments Coarse Sand Barrier project [1] AH-DTS (Active Heating Distributed Temperature Sensing) measurements were performed. This technique relies on measuring the rate at which the material heats up and cools down when a heating pulse is applied. The method is detailed in Appendix A, a summary is provided here.
A heating wire connected to a DTS fibre optic cable was installed at the interface of the sand and the blanket layer. The fibre optic cable is used as a sensor by applying the Distributed Temperature Sensing technology. A heat pulse is generated by applying electrical power to the heating wire, increasing the temperature of the cable, the surrounding material and the surrounding water. The rate of heating and subsequent cooling, provides an indication of the heat transfer to the surrounding. As the surrounding material as well as the flow affect the measured temperatures, the temperature can be used as a proxy for piping processes (groundwater flow and sediment transport).

Measurements were made along 4 lines in the Delta Flume.

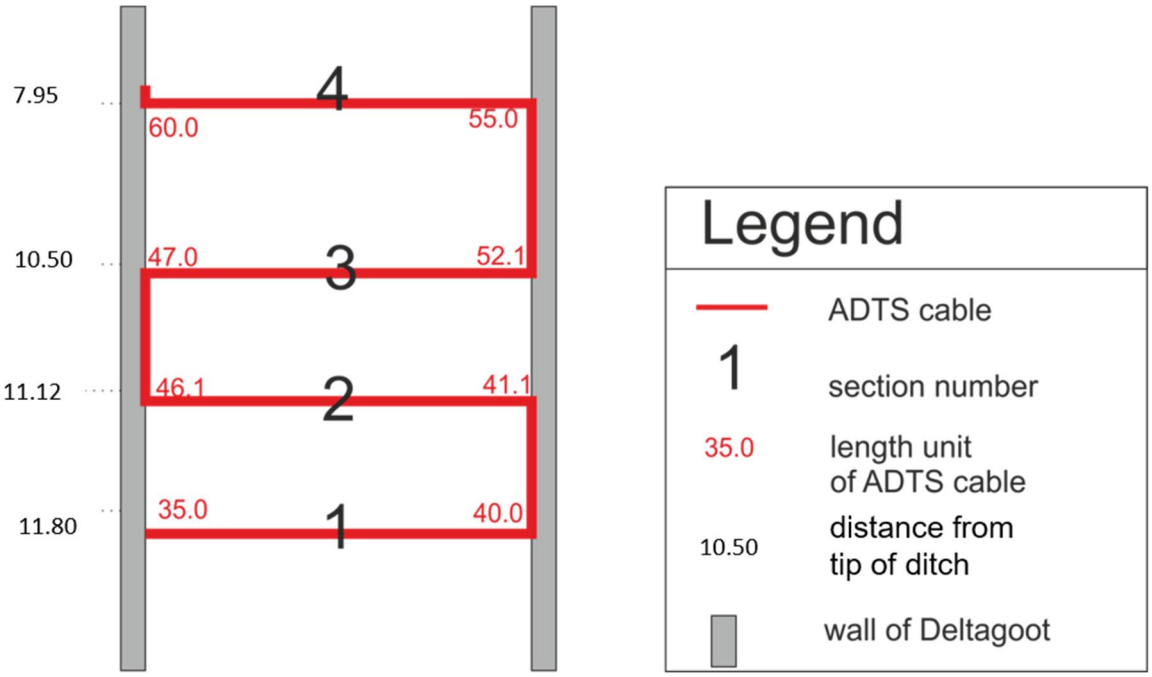

Figure 5.17 Top view of the AH-DTS layout

The measurements and data processing are described in Appendix A. The results can be visualised in plots which show the locations where the thermal properties of the surrounding material changed significantly. Such a significant change in thermal properties could be expected if a pipe formed in a location.

Several locations were identified where changes were significant:

- At 7.95 m from the outlet hole, and -2.29 m from the centreline (south side of the model), at 12:00 on May 31st, peaking at 06:00 on June 1st.
  However, due to the position near the Delta Flume boundary leakage along the wall cannot be excluded. Another explanation may be uncertainty in the cable position; i.e. this particular cable section might not be fully buried but positioned along the Delta Flume wall.
- At 7.95 m from the outlet hole, and 0.99 m from the centreline (north side of the model), changes that could indicate pipe formation may be seen starting at around 04:00 on June 2nd. This coincides with a change in pressure gradient in the head measurements.
- At 10.50 m from the outlet hole, and 2.10 m from the centreline (north side of the model), changes that could indicate pipe formation may be seen at 18:00 on June 1st. The difference becomes more evident on June 2nd at 00:00. Head measurements in row 2# do show that the head in h28 falls below that in h27 during this period.
- At 10.50 m from the outlet hole, and -0.81 m from the centreline (south side of the model), changes that could indicate pipe formation may be seen at 00:00 on June 2nd. This is also seen in pressure sensor P45. Possible widening along the barrier at 11.12 m, or damage to the barrier, may be seen at 02:00 on June 2nd, concentrating at 1.89 m, but ranging from -0.64 m to about 2.0 m from the centreline. Widening is not indicated by the head measurements.
- Activity upstream from the barrier van be seen 11.80 m from the outlet hole, and 2.18 m from the centreline (north side of the model), from about May 31st 12:00. It is unlikely this is caused by piping. Leakage from the sheet pile wall or uncertainty in cable positioning may be more likely explanations.

Overall the AH-DTS measurements do not reflect all the aspects of the piping process that was indicated by the head measurements. Also, there were locations where the AH-DTS data suggest piping occurred where this was not indicated by head measurements.

The active zones in the upstream and downstream lines are close to the flume wall and might represent leakage or possibly the cables were not placed exactly on the interface of the sand body.

It is probable that the head measurements cannot capture all pipe progression, due to their spacing in the model. This could explain activity which is observed in AH-DTS measurements but not in head measurements.
However, the AH-DTS measurements also do not seem to capture the pipe progression which is indicated by the head measurement. This is remarkable as this would be expected. Also, there are observations of activity in the AH-DTS measurements in the three rows further upstream, at times before the piping activity is seen in the row downstream. This might possibly be due to some local heterogeneity in the sample.

As the interpretation of the head measurements is based on the extensive analysis of medium-scale tests, in which visual observations could be directly linked to head measurements, these are considered leading in the interpretation of the piping process for this test. Furthermore, that approach also led to an interpretation that was in accordance with observations during excavation after the test. This means that this test does not clearly show how AH-DTS measurements can be used to monitor the piping process.

5.4 Summary and discussion

Pipe formation in the barrier appears to be similar to medium-scale tests
The results indicate that the piping process was largely similar to what was observed in the medium-scale tests, at least up to the progression of the pipe in the barrier. Gradients in the barrier indicated arrival of the pipe at the barrier, some parallel progression (although not along the entire width of the model as was observed in the medium-scale, which might be related to the rapid increase of head), and progression of the pipe into, and later possibly through the barrier. The local gradient at the transducer pair closest to where the pipe is considered to enter the barrier (in the south at #3 it is 0.41 at what is considered the critical point before the progression step) is in the order of the critical gradient that was determined in the medium-scale tests (ca. 0.4); however this gradient is computed over a shorter distance, over 0.20 m in the Delta Flume and over 0.27 m in the medium-scale. Over a longer distance the gradient would be lower.
A subsequent growth step at the same location in the south appears to have led to failure by breaching the upstream interface, but this also appears to have caused a collapse of the cover layer and plugging of the pipe at the location of the breach. Fine sand is found on top of the remaining barrier material (15 cm deep) in the excavation, suggesting that the pipe first breached the interface, causing background sand to enter the pipe, and that the cover layer subsequently subsided onto the barrier. This plugging appears to have prevented further erosion of the barrier at this location, as some of the barrier (approximately 0.15 m depth) is still present here whereas the barrier is washed away in the other side of the model.
Such subsidence could not occur in medium-scale tests, as the cover layer is a rigid perspex plate.

Limited pipe progression parallel to the interface

The pipe appears to have reached the barrier close to the centre of the model, subsequently it appears to have progressed at least some distance to the south of the model along the barrier, in the direction of h43. The pipe apparently did not progress to h42 at the southern edge of the model. It appears that a separate pipe progressed from the ditch to the north side of the model, to the vicinity of h48. This pipe only reached the barrier after the other pipe appeared to have progressed into the barrier at h43.

Head drop in the pipe downstream

The head in the transducers that are considered to be close to the pipe in the barrier, h43 and h45, is in the order of 1 m during most of the period following the arrival of the pipe at these locations. The head drop between the transducers in the barrier in row 4# and the head measured in h15 just upstream of the ditch is shown in Figure 5.18. This shows a substantial head loss in the pipe.

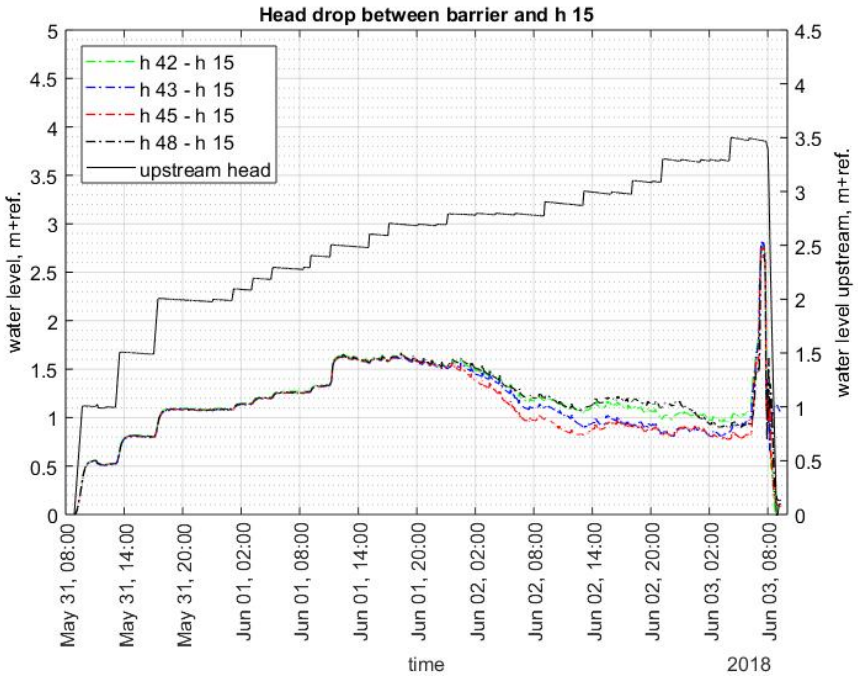

Figure 5.18 Head drop between transducers in the downstream end of the barrier and in the ditch (h09). Measurements and observations indicate that a pipe was present between h45 and h43 and the ditch from June 2nd ca 11:15 onwards, therefore the head drop h45 – h09 and is h43 – h09 considered to characterise the head drop in the pipe

Considering the measurements after the pipe is considered to have reached h43, the head drop from h43 or h45 to h09 is in the order of 1.0 m, corresponding to an average gradient in the order of 0.09. The pipe depth at which the grains on the bottom of the pipe would be in equilibrium is computed using the limit equilibrium by Sellmeijer, using the derivation in van Beek (2015) to compute the bedding angle. This results in pipe depths of ca. 0.8 mm (for the grainsize of the background sand) or 0.4 mm (for the grainsize of the barrier).

There was no excavation of the pipe after the test, as failure was achieved. However, during the tests observations of the sand boil and the pipe leading from the sand boils in the ditch indicate that the pipe was significantly larger than computed based on the limit equilibrium. The pipe would have to be larger to be able to transport the barrier material and tracer particles,

which were found in the ditch. This means that the shear stress on the walls of the pipe would be substantially above the limit equilibrium with a gradient in the pipe of 0.09, so that active erosion would be expected.

There are various factors that can have contributed to the head drop in the pipe. The presence of suspended material, barrier material and background sand, would increase the measured head drop in the pipe. Turbulence can be expected to have contributed to the head drop in the pipe and to erosion. Possibly, also the limited time allowed for erosion, and/or deposition of coarser particles in the pipe, prevented further deepening and widening of the pipe.

Possible erosion of the cover layer
Observations of sand pockets in the in the cover layer might indicate erosion of the cover layer above active pipes, or these could have formed after failure when the cover layer subsided.

Subsidence of the cover layer and fine sand on top of the barrier
In both test 1 and test 2 the excavation of the barrier after the test found background sand on top of the barrier at the location where the pipe appears to have progressed into, or through, the barrier based on the head measurements during the test. For test 2, it is considered plausible that the pipe progressed through the upstream barrier interface, this may have been followed by a subsidence of the cover layer, which prevented excessive erosion at that location.

Strength gain
The strength gain for the situation with the barrier can be compared to a situation without a barrier by assuming that the head drop at which the pipe reaches the barrier is also the critical head drop that would be obtained without a barrier. Using the average head measured over the interval between 23:20 and 23:40 on June 1st in h99 as the upstream water level, and the average head measured in h09 in the ditch as the downstream water level, this gives a head drop of 2.63 m when the pipe reaches the barrier. This compares to a head drop at the critical step of 2.81 between the same transducers at the critical step. That would give a ratio of 1.07. This is very small, but that is because the test was designed in order to have a low critical head drop in order to ensure failure would take place within the applicable range of head drops. If the barrier would have been placed further downstream, as will be the case in a field application, the critical head drop with a barrier will be higher relative to the critical head drop without a barrier.

Monitoring of pipe formation
The gradients over the barrier were used to identify the arrival of the pipe in the barrier and the progression of the pipe in the barrier. Based on these gradients it appears that a very dense network of pore pressure transducers would be required in order to ensure that pipe progression in the barrier is observable. The gradients on the side of the model, h42 and h62 did not respond when the pipe appeared to progress close to h43 and h63. Those transducers are only spaced approximately 1 m apart, which means that such a spacing would be required in order to detect pipe progression in the barrier. That does not appear practical for a field scale situation.

5.5 Critical point for pipe progression

Following the approach in the medium-scale tests to consider the first significant fall in gradient (which corresponded to the point at which the gradient in the barrier is maximum) as the critical (long growth) step, the point at **18:35 at June 02** is considered as the critical step and used for modelling the local critical gradients. As the pipe appears to progress into the barrier on the

h#3 side, the measured head profile on that side can be considered to be most representative for the local heads upstream of the pipe tip.

For modelling the heads that were measured just prior to the growth step are used. The head was raised on June 02 at 18:00, so the point step for pipe progression is the head interval that is prior to this. That corresponds to an upstream head of 2.99 m which was applied from June 02 13:00 until 18:00. The average of the heads measured between 16:00 and 17:50, as shown in Figure 5.19, Figure 5.20 and Table 5.1, are used to fit the model.

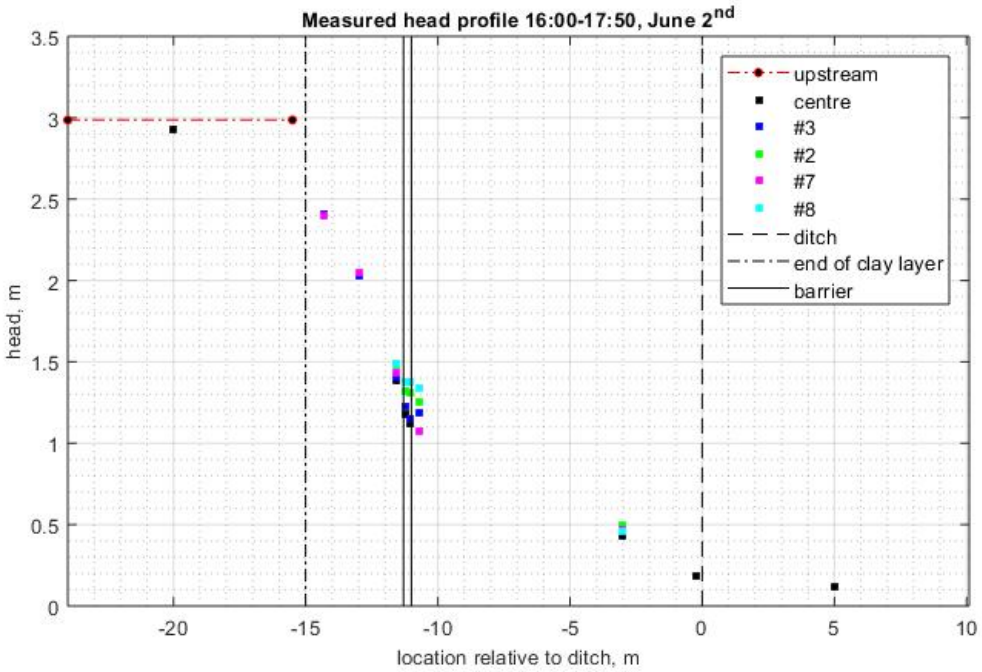

Figure 5.19 Measured head profile at critical point, average between 16:00 and 17:50 on June 2nd in the 2nd Delta Flume test

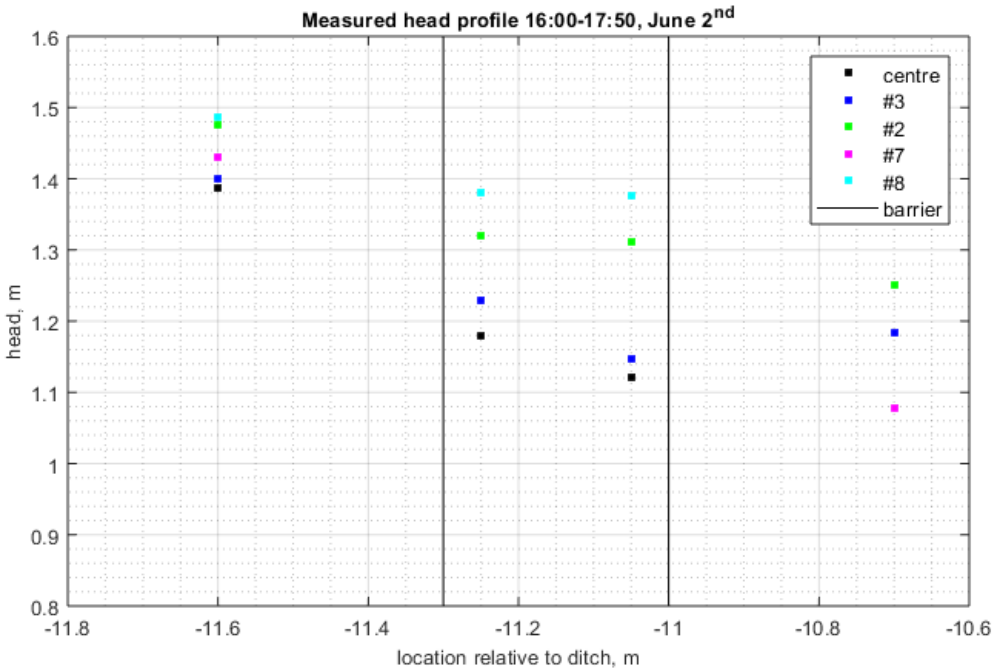

Figure 5.20 Measured head profile at critical point, average between 16:00 and 17:50 on June 2nd in the 2nd Delta Flume test, close-up

Table 5.1 Heads measured during the critical point (16:00-17:50 on June 2nd)

DCTM01	h_09	h_10*	h_15	h_22	h_23	h_246*	h_25	h_27	h_28	h_32	h_33	h_35**
2.99	0.12	0.22	0.19	0.50	0.47	1.16	0.43	0.47	0.46	1.25	1.18	0.82

h_37	h_38	h_42	h_43	h_45	h_47**	h_48	h_62	h_63	h_65	h_67**	h_68	h_72
1.08	1.34	1.31	1.15	1.12	1.16	1.38	1.32	1.23	1.18	1.26	1.38	1.48

h_73	h_75	h_77	h_78	h_83	h_85	h_87	h_90*	h_93	h_95	h_97	h_99
1.40	1.39	1.43	1.49	2.03	2.04	2.05	2.86	2.41	2.40	2.40	2.92

*these transducers were placed at 2 m depth (h_10, h_90) and 0.35 m depth (h_246) below the sand surface however because the sand above them was not densified they are not expected to provide a good indication of the water pressure at depth.

** values measured by these transducers are considered unreliable

As transducers h35, h47 and h67 are considered unreliable, those are not shown in the figures. It can be observed that the head that is measured in h99, which is below the upstream water level and not below a clay layer, is somewhat lower (0.07 m lower) than the upstream head. This suggests that there is some resistance across the top layer of sand, possibly due to the settling of fine grains. This additional resistance should not be included when assessing the overall head drop over the sand body, therefore the head drop at the critical step is computed based on the head in h99, and not based on the upstream flume head.
Therefore, the head drop from h99 to h09 (in the ditch) is considered as the critical head drop for pipe progression in this test, this head drop is 2.81 m.

There is still a significant head loss between the heads measured in the downstream side of the barrier where the pipe appears to be, h43 and h45 and the head in the ditch. The head drop is ca. 1.0 m. In the medium-scale tests, the head loss in the pipe was negligible, but that is not the case here. This high head drop in the pipe might be due to the presence of suspended material, and it could indicate that the limit equilibrium for grains on the bottom of the pipe was not fulfilled, and that grains were still eroded in the downstream pipe. Turbulence may also have contributed to head loss in the pipe downstream.

The head measured in h43 inside the barrier is lower than in h33 (Figure 5.20) suggesting that indeed there is some crumbling or damage of the barrier, resulting in a lower head in the barrier than some distance downstream of the barrier where there is no pipe. The similar heads in h43 and h45 suggest that both of these transducers are in or close to the pipe.
Inside the barrier, the heads measured by h48 and h42 are significantly higher than in h43 and h45, indicating that there is no pipe there. The head measured by h47 and h67 is considered unreliable, as these were consistently lower than the other heads in the early phase of the test prior to piping.

On the upstream side of the barrier, at -11.25 m, the head measured in the centre at h65 is lower than in h63. This results in the lower gradient in the centre of the barrier than on the h#3 side. A lower head in the centre upstream side might be expected if there has been more crumbling in the centre, or if there is a deeper erosion hole in front of the barrier there than on the h#3 side. Such phenomena were also observed in the medium-scale experiments.

A sketch of the possible pipe progression steps is shown in Figure 5.21.

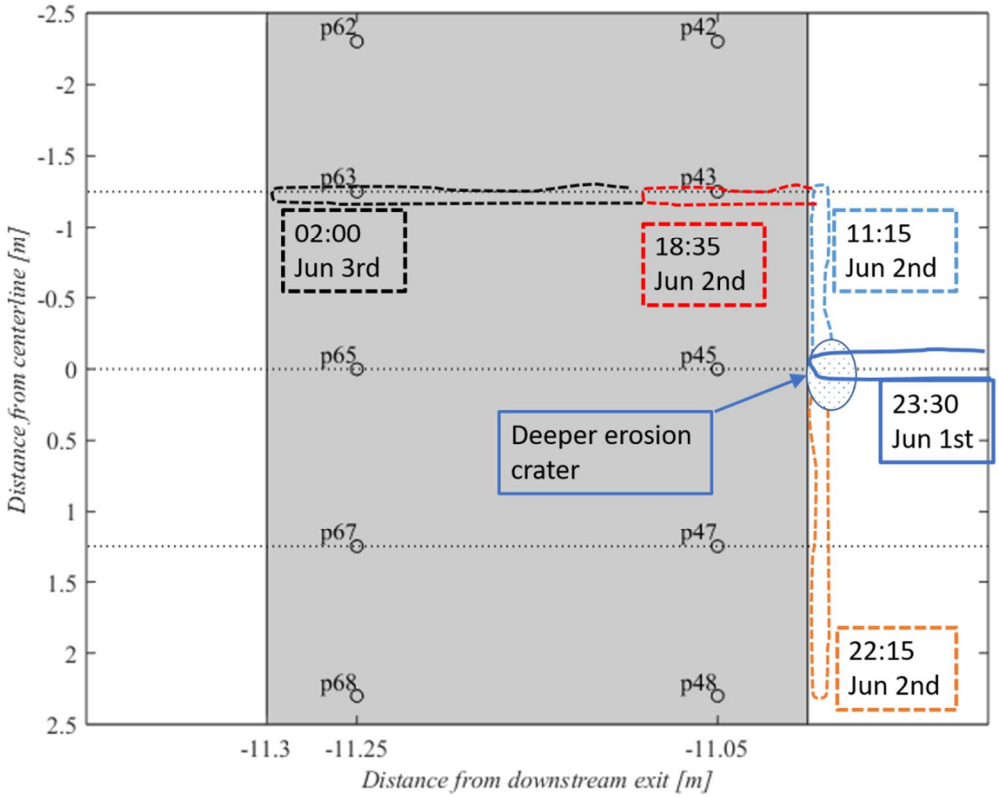

Figure 5.21 Indicative sketch of possible pipe extent during Delta Flume test 2 based on head measurements. The expected minimal extent of the pipe after the progression after *the indicated time steps is shown; it is possible that the pipe progressed further than the locations indicated here.*

6 Modelling the second Delta Flume test

As the barrier was level with the background sand in the second Delta flume test, this test can be used to compare to the medium-scale experiments. This was not the case in the first Delta Flume test. Therefore, the second Delta Flume test is modelled first in this Chapter, and the model for the first test is presented in Chapter 7.

Whereas a 2D model may be applicable to model the medium-scale tests with a barrier that extends the full depth of the model and where the pipe has progressed along the entire width of the barrier interface, the flow field in the Delta Flume is expected to be of a more 3D nature. Because the depth of the barrier is relatively smaller, there is more flow that does not exit to the pipe at the barrier but flows to the ditch, which is not present along the entire width. Furthermore, it appears that the pipe has not progressed along the entire width of the barrier in the Delta Flume tests.
Even in the medium-scale tests, when the long growth step was modelled, the pipe had progressed some distance into the barrier, resulting in a 3D flow field upstream of the pipe. By modelling this in a 2D model to derive a local critical gradient that can be considered as the strength criterion for 2D models, a degree of calibration for 3D flow inside the barrier at the pipe tip is included in the strength criterion. Especially for modelling field situations it is highly desirable to be able to use a 2D flow model. However, a 3D model is also applied to model the critical point in order to assess the influence of 3D effects on the result.

6.1 2D modelling of Delta Flume test 2

The Delta Flume test is modelled in DgFlow using a 2D model where the pipe is modelled with no head drop of physical depth, similar to the models used in the medium-scale phase.

6.1.1 Input for 2D models

In the analysis of the Delta Flume tests the pipe as a boundary condition is only modelled at the barrier over a limited distance instead of all the way to the outlet at the ditch. In the medium-scale analyses, the outflow boundary was modelled from the outflow point to the barrier. This would correspond to a 3D model where the pipe has an infinite width, which contributes to an over estimation of the flow rate. A more appropriate schematisation might be to only model the pipe that has progressed parallel to the barrier as an outflow, which is done in this analysis of the Delta Flume test because the area captured by the pipe is relatively small

- the scale of the model relative to the scale of the pipe is larger than in the medium-scale tests;
- the pipe did not progress parallel to the barrier in the Delta Flume test;

The effect of not modelling a pipe from the outflow point to the barrier, but only over a shorter outflow distance close to the barrier, is analysed in Appendix 9C. The modelled heads in the barrier, and therefore also the computed gradients are higher, with a shorter outflow area, i.e. with only a pipe at the barrier. As the objective of modelling the second Delta Flume test is to fit the measured head profile by changing the hydraulic conductivity of the barrier, this means that a different hydraulic conductivity will be modelled depending on the length of the pipe at the barrier. The modelled critical gradient in the barrier, i.e. the strength criterion, will not be significantly affected, as this is largely constrained by the measured heads.

6.1.1.1 *Schematisation*

As discussed in the previous Section, a 2D model is used to model this test, where the pipe is a boundary condition with zero head drop in the pipe.

6.1.1.2 *Geometry*

Only the sand body and the barrier, not the cohesive cover layer, are modelled. The upstream tip of the ditch is the centre of the axis system and the sand body is present between x = -24 m and x = 10.1 m. The depth of the model is 3 m, and the sides have a 2.67:1 slope, so that the bottom of the model is 18 m long. The barrier is present between x = -11.0 m and x = -11.3 m and has a depth of 0.5 m. The model is shown in Figure 6.1.

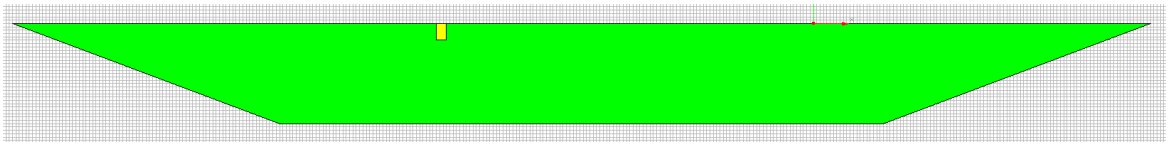

Figure 6.1 Model of the second Delta Flume test, sand body green is background sand yellow is barrier.

6.1.1.3 *Boundary conditions*

The pipe is modelled as a boundary condition with zero head loss in the pipe. The pipe is modelled over a limited distance in front of the barrier, with zero depth but with a certain length inside the barrier that characterises the interface between the barrier and the pipe that has established due to crumbling of the barrier and possible damage of the barrier. As opposed to the medium-scale tests, where the pipe length inside the barrier could be observed, the distance that the pipe progressed into the barrier at the critical step is unknown. Therefore, computations of the head profile are done for different pipe lengths in the barrier.

The length of the pipe in front of the barrier should correspond indicatively with the width of the parallel pipe at the barrier. The head profile at the critical time step shown in Figure 5.20 shows that the heads measured downstream of the barrier in h35 and h33 are higher than the heads inside the barrier at h45 and h43 where the pipe is considered to be present. This indicates that the width of the pipe at the barrier is less than 0.3 m in front of the barrier. During the medium-scale tests significant erosion was observed in front of the barrier, and this was also indicated in excavation at the south side of the barrier in the first Delta Flume test, therefore the width of the pipe in front of the barrier is taken as 0.26 m. It must be noted however, that it appears that the pipe did not progress parallel to the barrier along the entire width of the model in the Delta Flume test, in contrast to the progression in the medium-scale tests. This means that the 2D model with this boundary condition may still tend to over-estimate the flow rate, and under estimate the heads in the model (due to the convergence of flow from the sides). This effect will be to some degree counteracted by the fact that the pipe leading from the ditch to the barrier is also not modelled.

The value of the heads at the boundary conditions is the average over the period of June 2nd from 16:00 to 17:50, the critical point for progression as discussed in Section 5.5. For the downstream boundary, this is the head that is measured inside the barrier at h43 (at -11.05 m), because the pipe appears to progress into the barrier close to this transducer. This head is 1.15 m, which is similar to the head in the centre in h45 (1.12 m), and lower than the other transducers that are at -11.05 m.

The upstream head in the model is the head measured in h99, in the sand body upstream beyond the end of the cover layer. This is used because the head that is applied upstream is

0.07 m higher, which indicates the presence of some entry resistance at the inflow end. The upstream head in the model is therefore 2.92 m.

A boundary condition is also applied at the location of the ditch, this is the head measured in the ditch in h09 of 0.12 m.

The head drop from upstream to the pipe is therefore 1.78 m, from the pipe to the ditch the head drop is 1.03 m and from upstream to the ditch is 2.81 m.

An overview of the model is shown in Figure 6.3.

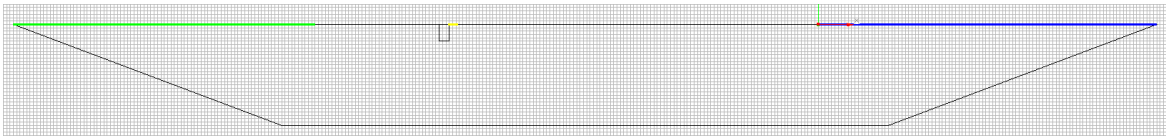

Figure 6.2 Boundary conditions in the Delta Flume model of the second test, green is upstream head, yellow is head in pipe at the barrier, blue is head in ditch downstream.

6.1.1.4 *Fitting hydraulic conductivity and pipe length in the barrier*

The hydraulic conductivity of the background sand is uncertain. Therefore, a 3D model is used in Appendix 9B to model the situation at the start of the test 1 prior to piping to fit the hydraulic conductivity. During test 2, there was a period of heavy rainfall early in the experiment. Furthermore, the ditch was not dug deep enough, therefore there was a clay layer at the outlet, which was only removed on June 1st (ca 1 day after the start of the experiment). At that time sand boils had already formed. These two uncertainties mean that the measured head drop and flux would not be expected to provide a reliable indication of the hydraulic conductivity at the start of that test. As only part of the sand body, the top layer of ca. 1.5 m thick was replaced between the two tests, and preparation and densification were done using the same methods, it will be assumed that the hydraulic conductivity was comparable in the first and second tests.

The modelled intrinsic permeability of the background sand is 9.95e-12 m^2, based on fitting the data from the first test in Appendix 9B. As the average air temperature during the first Delta Flume test (11^{o}C) was lower than during the second Delta Flume (15^{o}C) test the hydraulic conductivity during the second test is 8.57e-5 m/s, which is slightly higher than during the first test.

The water is modelled as an incompressible fluid, assuming full saturation of the soil.

For modelling the head profile, the hydraulic conductivity contrast, rather than the absolute hydraulic conductivity of the materials is of importance. The absolute value of the hydraulic conductivity of the barrier is only relevant for estimating the achieved RD of the barrier.

The hydraulic conductivity contrast in combination with the length of the pipe inside the barrier determines the head profile in the model. This could theoretically mean that an infinite number of combinations of pipe length and hydraulic conductivity can be found, therefore knowledge from the medium-scale experiments regarding the minimum pipe length at the critical step is used to constrain the minimum pipe length to 0.04 m into the barrier.
Furthermore, there is a minimum to the values that the hydraulic conductivity of the barrier can have; at a relative density of 1, which is not likely to be achieved in this experimental situation.

6.1.1.5 *Mesh*

The model uses an unstructured mesh with triangular elements of 2.5 cm for the background sand, due to the geometry of the Delta flume tests. The barrier is modelled with a structured mesh with square 1 cm elements. A close-up is shown in Figure 6.3.

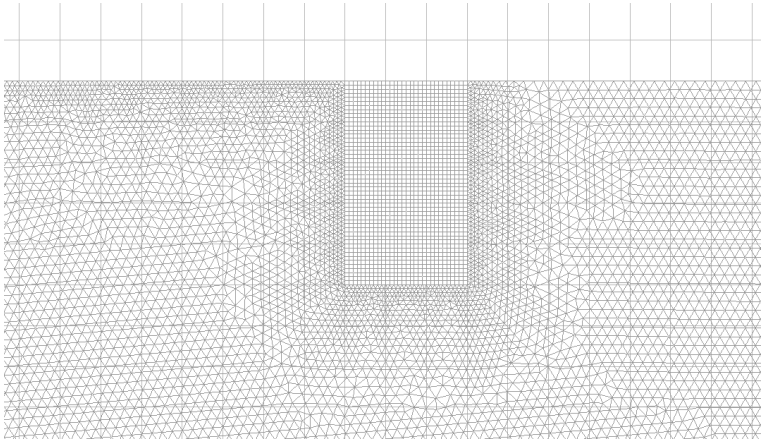

Figure 6.3 Close-up of the barrier and the mesh in the 2D Delta Flume model

6.1.1.6 *Overview of computations*

A summary of the 2D computations is shown in Table 6.1.

Table 6.1 Overview of models

Model name	Hydraulic conductivity background m/s	Hydraulic conductivity barrier m/s	Contrast	Pipe length in barrier cm	RD barrier corresponding to this contrast
DG_test2_pip4_Con_110	8.58E-05	9.39E-04	11.0	0.04	0.75
DG_test2_pip4_Con_085	8.58E-05	7.30E-04	8.5	0.04	0.95
DG_test2_pip6_Con_085	8.58E-05	7.30E-04	8.5	0.06	0.95
DG_test2_pip6_Con_080	8.58E-05	6.85E-04	8.0	0.06	1.0
DG_test2_pip5_Con_085	8.58E-05	7.30E-04	8.5	0.05	0.95
DG_test2_pip5_Con_080	8.58E-05	6.85E-04	8.0	0.05	1.0

6.1.2 Results and analysis of 2D models

6.1.2.1 *Fitting pipe length and hydraulic conductivity*

As the pipe length and the hydraulic conductivity are unknown, the model is used to simultaneously fit these two parameters so that the modelled head profile matches the measured head profile.

The best match is obtained in model DG_test2_pip5_Con_080 with a 0.05 m long pipe and a hydraulic conductivity contrast of 8.0. The hydraulic conductivity of the barrier is 6.85e-4 m/s (intrinsic permeability 7.95e-11 m^2). This would correspond to a relative density of 1.0 for the barrier material, which is very high. The question is whether this is really likely to have been achieved. The relative density of the barrier was not determined at the start of the test. Measurements of the first Delta flume test indicate a relative density of 0.74. As a 2D model

underestimates flow to the pipe for a 3D configuration, the RD may have been lower, in the experiment, which is investigated in the 3D models in Section 6.2.

Reducing the pipe length in the model, would allow for a fit with a lower relative density of the barrier. Because the head measured in h42 is used as the boundary condition for the pipe, and this is 0.05 m into the model, using models with a pipe shorter than 0.05 m results in an overestimation of the head in h42 in the model, and thereby in a lower computed gradient in the barrier. With a 0.04 m long pipe in the barrier, the lower limit of pipe lengths in the barrier at the critical step in the medium-scale tests, the best match is obtained in model DG_test2_pip4_Con085, with a contrast of 8.5 corresponding to a relative density of 0.95 of the barrier material.
As the accuracy cannot be expected to be in the order of percentage points on RD or single centimetres for pipe length, these results indicate that the barrier had a high relative density, and that the strength, critical gradient upstream of the pipe tip, would therefore be expected to be in the range of the values found in the medium-scale experiments with a high RD.

The measured and modelled head profiles for pipe length 0.05 m together with contrast 8.0 and pipe length 0.04 m with contrast 8.5 are shown in Figure 6.4 and Figure 6.5.

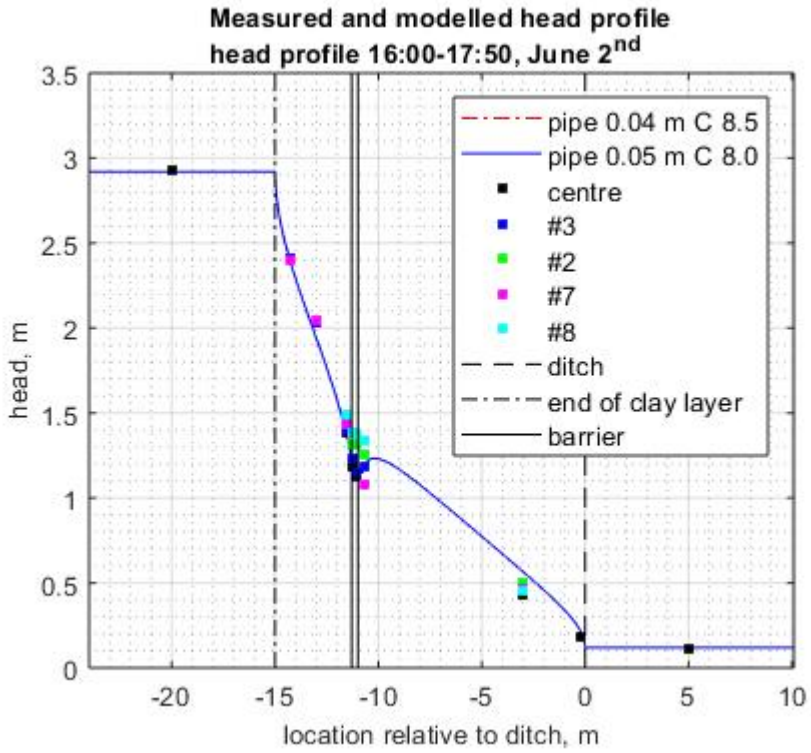

Figure 6.4 Modelled head profile along the top line of the model for test 2 profiles for pipe length 0.05 and 0.04 overlie in this figure.

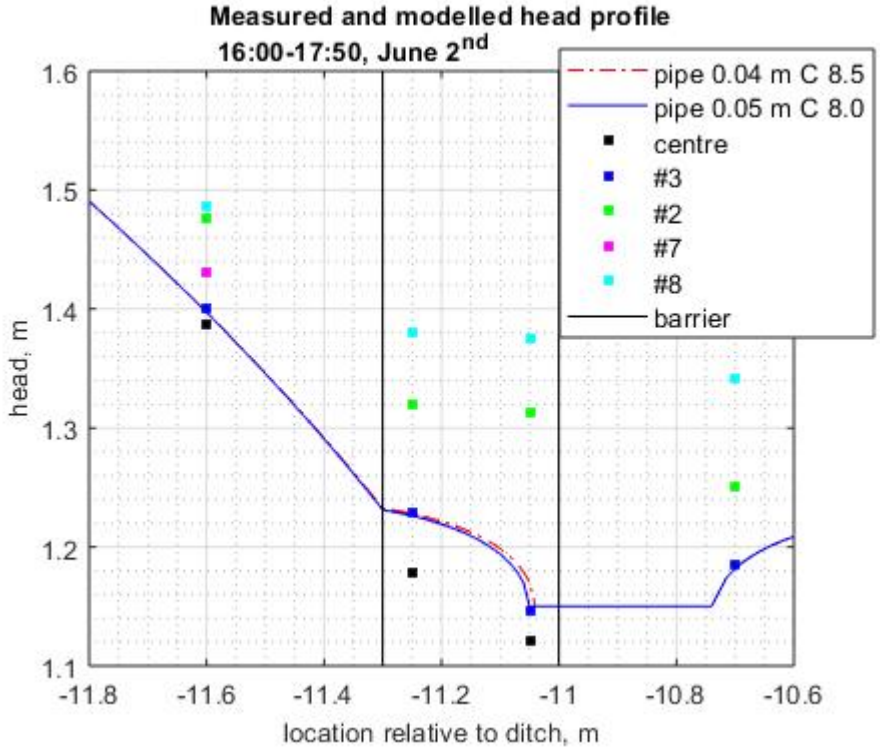

Figure 6.5 Modelled and measured head profiles along the top line of the model for test 2, close-up near the barrier. Data from h47 and h67 is considered unreliable and is not shown.

6.1.2.1. *Measured and modelled head profiles*

The measured head profile in the barrier at the location of side #3 is considered to be the critical profile, as this is the location where the pipe progression appears to have occurred. Measured heads in the centre of the model are lower, possibly because the pipe arrived at the barrier closer to the centre of the model. This would suggest that the pipe from the ditch to the barrier is closer to the centre, and this may have an additional draining effect in the centre. The heads inside the barrier at sides #2 and #8 are significantly higher than in the centre and at side #3 which indicates that the pipe has not progressed parallel to the barrier to those locations (Figure 6.5).

The head in h33 downstream of the barrier (head h35 is unreliable and not shown) is higher than inside the barrier (Figure 6.5). This indicates that there is no pipe present at that location, constraining the possible width of the pipe parallel to the barrier to less than 0.30 m (excluding its length inside the barrier). The modelled head profile, with a 0.26 m wide pipe in front of the barrier matches this head quite well, suggesting this is a reasonable approximation of the dimensions of that pipe.

Considering the overall head profile, Figure 6.4, the head in line 9# is modelled well (at x = -14.3 m), but the head in line 8# at x = -13.0 m is underestimated by ca 0.06 m. The head at line 7# is modelled well again for the transducers h73 and h75 close to the location of the pipe inside the barrier, but the head is higher in transducers h72, h77 and h78. This probably represents the 3D convergence of flow which is not captured by a 2D model. The heads close to the barrier, in h73 and h75 can be modelled quite well if flow is relatively 2D as these are close to the barrier and these transducers are in the zone where the pipe enters the barrier. Heads in h72 and h77 and h78 are further away and therefore higher. Further upstream at row 8# the convergence of flow towards the centre and side #3 would give higher heads in reality than in the model. The head in row #9 on the other hand would mainly be affected by the upstream boundary condition, and is therefore modelled well.

Downstream of the barrier in row 2# the head is overestimated by the model. This could be because the pipes that progress from the ditch to the barrier are not modelled. These would be present in reality and have a draining effect lowering the heads in the test.

6.1.2.1. *Modelled head and flow distribution*

The head and flow distribution for the model with a 0.05 m long pipe in the barrier and a contrast of 8.0 is shown in Figure 6.6 and Figure 6.7. These figures suggest that a large part of the flow passes through the background sand to the ditch downstream, rather than into the barrier. Therefore, an estimate of the flow to the ditch and to the pipe at the barrier is made. This is only an estimate, as the real situation is 3D with limited pipe development parallel to the barrier and the presence of the ditch over a width of only 0.5 m.

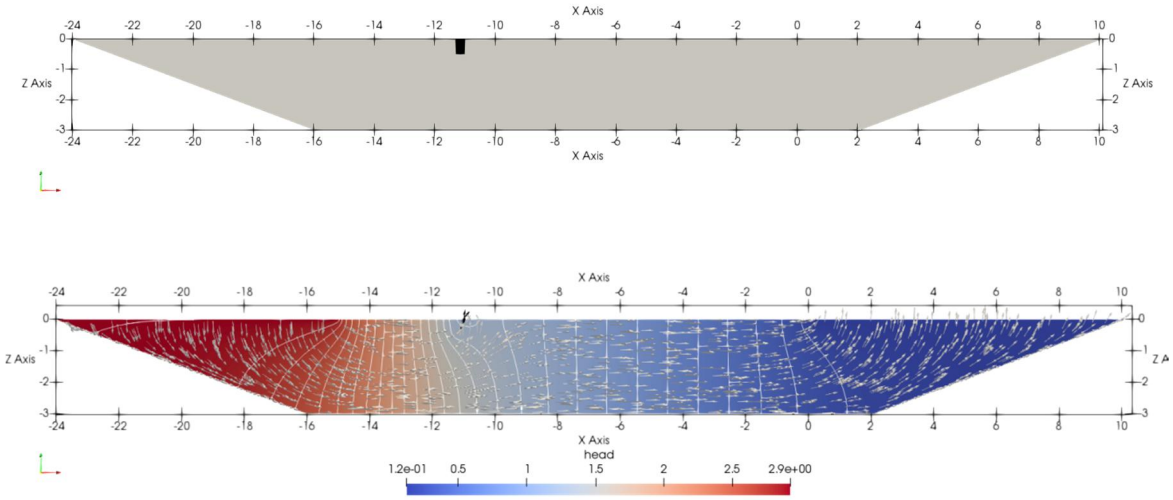

Figure 6.6 Top: figure indicates background sand (grey) and barrier (black). Bottom modelled head (red to blue scale 2.92 m to 0.12 m), head contours (white lines) are spaced 0.10 m), arrows are scaled to represent flow velocity magnitude and direction. Grey arrows are in background sand, black arrows are in barrier.

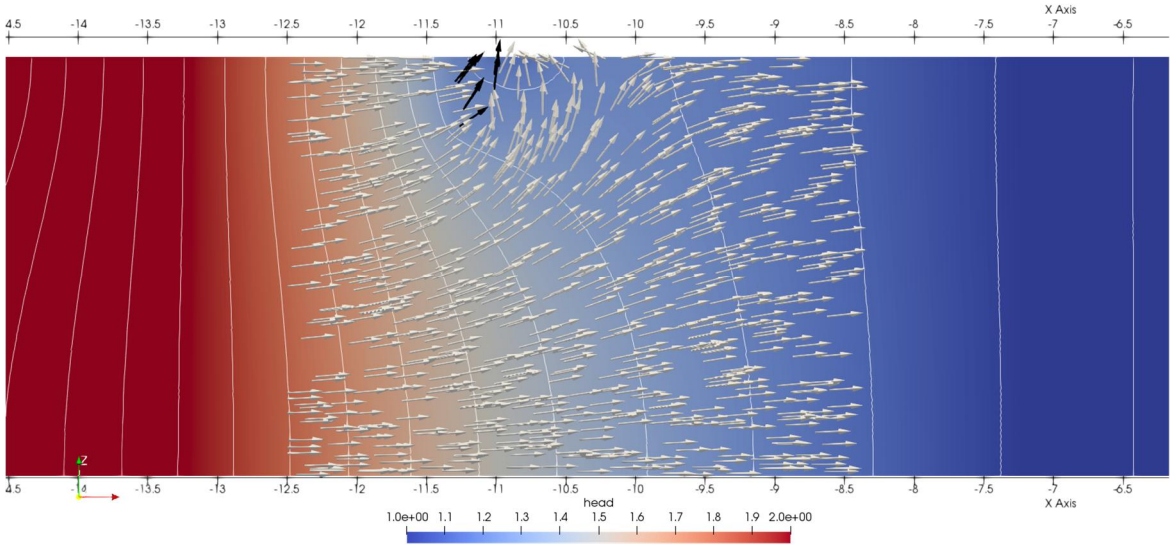

Figure 6.7 Close-up of barrier, head (red to blue scale 2.0 m to 1.0 m)head contours (white lines) are spaced 0.10 m), arrows are scaled to represent flow velocity magnitude and direction. Grey arrows are in background sand, black arrows are in barrier.

Computing the flux into the pipe from the velocity in the model, multiplied by 5 m, i.e. assuming the pipe is along the entire width of the model gives a flux of 14.45 l/min. For the ditch the value is approximately half of this: 7.97 l/min (again assuming the ditch is along the entire width of the model). These two values, add up to the inflow that is computed along the upstream area, as should be the case. This suggests that approximately 2/3rd of the flow is into the pipe at the barrier. This distinction could not be verified based on observations during the test, as flow into the pipe at the barrier was transported to the ditch in the pipe perpendicular to the barrier.

The modelled flow rate is ca 15% higher than the measured flow rate, 19.5 l/min. This can be the result of using a 2D model. In reality, both the ditch and the pipe at the barrier have a limited extent. Neglecting the flow towards the pipe in between the barrier and outflow area does not compensate for this.

6.1.2.2 *Effect of contrast with constant pipe length*

The effect of contrast, for a given pipe length inside the barrier is shown using two models with a pipe length of 0.04 m and contrasts of 11.0 and 8.5 respectively. The effect on the head profile in the entire model is negligible but inside the barrier a higher contrast results in a lower head profile, and therefore lower computed gradients as shown in Figure 6.9.

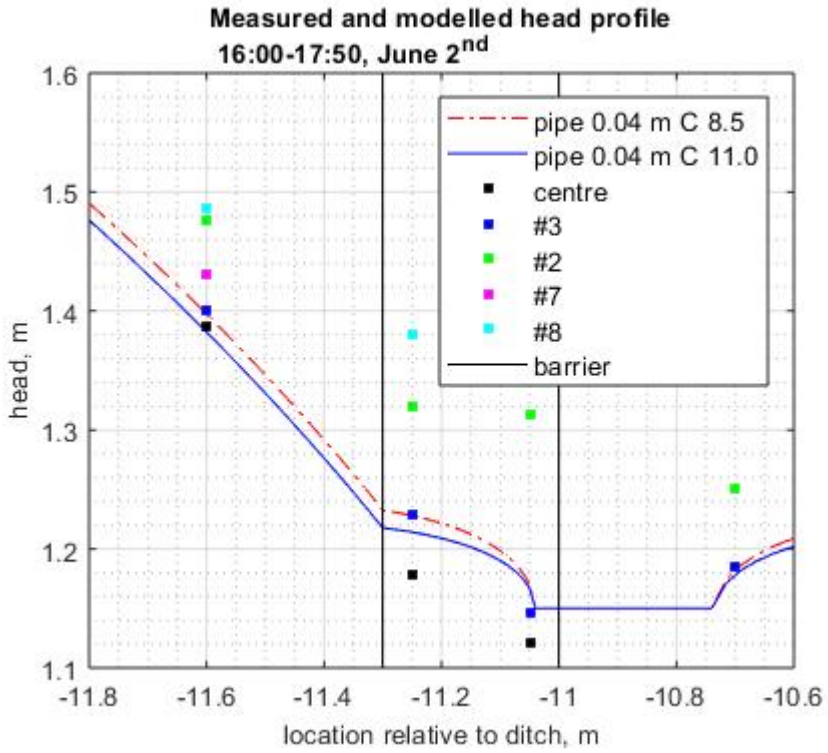

Figure 6.8 Modelled and measured head profiles along the top line of the model for test 2, close-up near the barrier. Data from h47 and h67 is considered unreliable and is not shown.

6.1.2.3 *Comparison to medium-scale head profiles*

Figure 6.9 shows the head profiles that were modelled upstream of the pipe tip for the medium-scale tests with GZB 2, tests MSP 24 (Baskarp 25) and MSP 28 (Metselzand) and for the Delta flume test with the best fit (the model with 5 cm pipe and a contrast of 8.0).

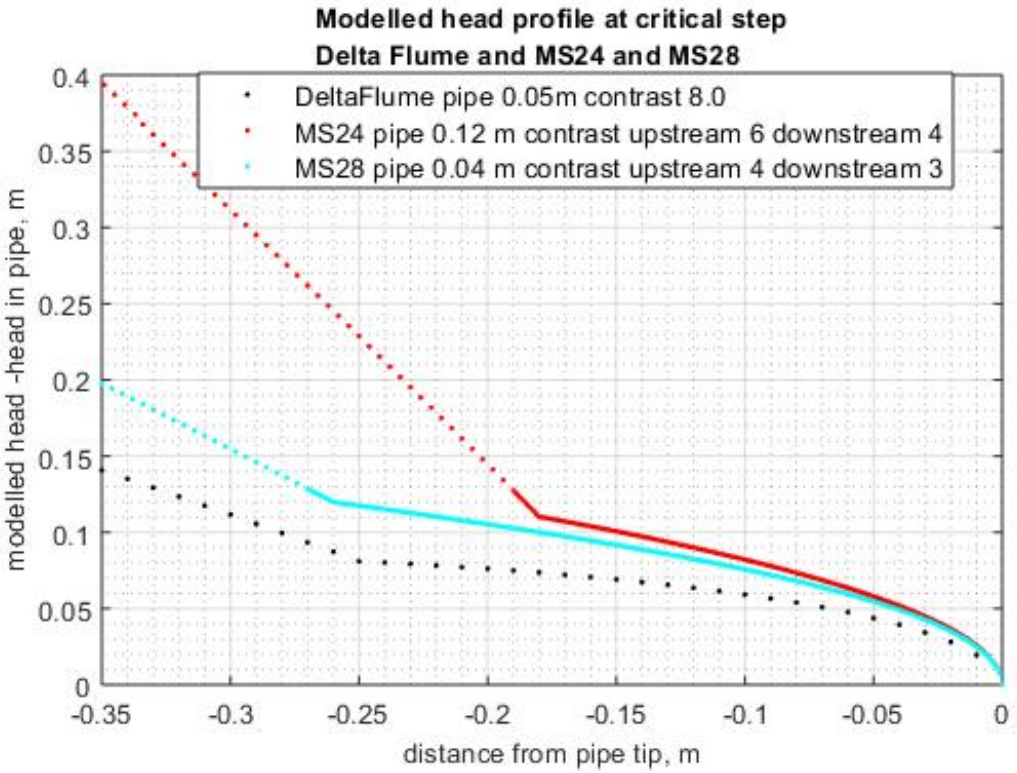

Figure 6.9 Modelled head profiles for medium-scale tests MSP 24 and MSP 28 and for the Delta Flume test. Distances are normalised to the distance from the pipe tip and heads are normalised to the head in the pipe.

The modelled gradients start to diverge already a short distance from the tip. The gradient modelled in the Delta Flume test is lower than for the two medium-scale tests, and the difference increases with increasing distance from the pipe tip.

One possible reason for a shallower profile would be that the pipe progressed at a greater distance from the transducers which were used to fit the model in the Delta Flume test than in the medium-scale tests. This would mean that the downstream transducer, h43 which is assumed to be in the pipe in the model, was not actually in the pipe. This would lead to a lower computed gradient. However, considering that the measured heads in h43 and in h45 are very similar, more similar than between h43 and h42 which are closer together, it appears plausible that both h45 and 43 are in the pipe or very close to the pipe.

Another reason for a shallower profile would be if the hydraulic conductivity contrast and pipe length that were considered most probable are too low. Increasing the length of the pipe in the Delta Flume model, in combination with reducing the contrast (a lower hydraulic conductivity of the barrier) would give a steeper modelled head profile in the barrier. The length of the pipe in the barrier remains unknown and this might have been greater than 0.05 m. However, this would require hydraulic conductivity values of the barrier material that are greater than 1.0, which was used as the upper realistic limit in the current analysis.

6.1.2.3. Modelled critical gradient

The modelled critical gradient over 0.10 m from the pipe tip is 0.59. This is lower than for tests MS 24 (0.82) and MS 28 (0.76). Although the 2D model indicates that the RD of the barrier had to have been very high this result would be affected by 3D convergence of flow to the pipe.

This means that the barrier might in reality have a higher hydraulic conductivity, and thus lower RD than modelled in 2D. A 3D model can give more clarity on this matter. As the head profile is fit to the measurements, the influence of the 2D calculation on the strength criterion is expected to be small.

6.1.2.4 Discussion and Conclusions

A 2D model was made for Delta Flume test 2 in order to model the critical gradient for pipe progression. The modelled gradient over 0.10 m from the pipe tip is 0.59 which is significantly less than the values found for the two tests on the medium scale with this barrier material (0.82 and 0.76 respectively).

The model uses the hydraulic conductivity that was modelled using a 3D model of Delta Flume test 1 for the background sand. The pipe length and hydraulic conductivity of the barrier were fit to the data. The combination of a pipe of 0.05 m length inside the barrier, with a hydraulic conductivity contrast of 8, which corresponds to a barrier material with a relative density of approximately 1.0 fits the measured head profile at the location where the pipe appears to have progressed best (side #3). This is higher than the expected value of around 0.73-0.74 based on the measurements in experiment 1. In this model the pipe was modelled as a boundary condition at the barrier, with a length of 0.26 m in front of the barrier.

There are a number of factors which contribute to uncertainty regarding the model results:

- a 2D model is used, whereas the pipe has not progressed parallel to the barrier. Concentration of flow in the barrier in 3D would have led to higher gradients close to the pipe tip than are modelled in 2D if the same hydraulic conductivity of the barrier is used. In the current model the estimate of the hydraulic conductivity in the model may be somewhat lower than it was in 3D reality i.e., the actual relative density could have been somewhat lower, which could explain the relatively low critical gradient;
- The downstream transducer h43 is assumed to be in or very close to the pipe, and this value is used as boundary condition for the pipe
- The length of the pipe inside the barrier is unknown, and had to be fit in combination with the hydraulic conductivity contrast. In order to fit two unknowns, additional limitations were imposed:
  - the maximum RD of the barrier was set at 1.0, limiting the range of possible hydraulic conductivity contrasts
  - the minimum pipe length in the barrier was set at 0.04 m based on medium-scale experiments;
- The dimension of the pipe in front of the barrier is unknown, a pipe of 0.26 m is modelled downstream of the barrier. As a 2D model is used, this pipe represents a pipe that would have progressed along the entire width of the model whereas in reality the pipe did not progress along the width of the model. The 3D flow profile might have affected results.
- The pipe from the ditch to the barrier (perpendicular to the barrier) is not modelled this may have some effect on the head profile
- The relative density of the barrier material and the background sand were not measured for the second Delta Flume test and are fitting parameters.
  - the hydraulic conductivity of the background sand is based on a 3D model of the first Delta Flume test, and assumed to be comparable in the second test as the second test could not be used to determine this. The RD of the background sand based on the model (87%) is significantly higher than the RD that was expected based on samples taken after preparation of the test (35-65%), but it is not clear whether this could also be due to the difficulty of sampling the material (which

contains shell fragments) and/or partial saturation during the test. The relative density of the background sand does not affect the strength criterion though.

6.1.2.4. Elaboration

The objective of the models is to reproduce the head profile inside the barrier and compute the critical gradient that caused piping. This does not depend on the absolute value of the hydraulic conductivity of the barrier or the background sand but on the contrast between the barrier and the background sand. Therefore, the estimated hydraulic conductivity based on the flow rate is primarily of importance to relate the contrast to a hydraulic conductivity of the barrier, and thereby estimate the relative density of the barrier. In that sense the hydraulic conductivity of the background is important, as the limit to the hydraulic conductivity contrast in the current models is set to be a relative density of the barrier material of 1.0. If the hydraulic conductivity of the background sand were higher, the contrast could be reduced further without raising the RD of the barrier over 1.0. This would mean that models with a longer pipe in the barrier, and a steeper gradient profile would be possible.

In the numerical analysis in the phase of the small-scale tests, it was shown that the 2D model can represent the local gradient in the barrier for situations where the pipe has widened along the width of the barrier and the barrier has the depth of the model. If the pipe has not widened along the entire width of the barrier, the 2D model will underestimate the head profile in the barrier. This effect can be compensated by modelling a lower hydraulic conductivity which also gives a steeper profile. That means that the hydraulic conductivity which is fit in a 2D model would always be somewhat lower than in a 3D situation if there is convergence of flow. As there is clearly a 3D flow configuration in the Delta Flume test, this might be a reason to consider models with a lower hydraulic conductivity of the barrier. However, it is uncertain how strong this effect would have been. Rather than modelling with a higher RD in the 2D model, a 3D model is presented in the next Section to analyse the effect of modelling this situation in 3D.

In the medium-scale models, after the pipe has entered the barrier at discrete points the 2D model will also underestimate the head profile as compared to the 3D situation. This implies that in all 2D models there is also some degree of underestimation of the local gradient. This effect could therefore be considered as a calibration effect. However, the magnitude of this effect may be dependent on geometry, and more importantly, in the medium-scale tests the pipe had progressed along the entire width of the model. The data strongly indicates that this was not the case in the Delta Flume test, and therefore, for this geometry it is important to assess local gradients by using a 3D model, which is done in the next Section. This is not expected to strongly affect the computed strength criterion, as the head profile in the barrier is fit to the measurements, but it will affect the estimate of the RD of the barrier. If the barrier were to have a lower RD, such as the 0.74 which is indicated by the samples taken in the first Delta Flume test, a lower strength would also be expected.

6.2 3D modelling of Delta flume test 2

In the Delta Flume experiment, due to the apparently limited progression of the pipe parallel to the barrier and the barrier's shallow depth in combination with a ditch that does not extend to the entire width of the flow, the flow field is expected to be affected by 3D effects. These would lead to a stronger concentration of flow to the pipe inside the barrier. This effect is analysed by making a model of the expected situation at the critical step, using the pipe length in the barrier and hydraulic conductivity contrast that provided the best match in the 2D model. Subsequently, the effect of a higher contrast (i.e. a lower relative density of the barrier) on the head profile is analysed.

6.2.1 Key aspects of the schematisation

The model is presented in Appendix 9D. Key aspects of the model which also affect interpretation are:

- The extent of the pipes in front of the barrier: measurements indicate that the pipe has reached to the vicinity of side #3 and enters the barrier in this area. Furthermore, it does not appear to have reached to side #2 or side #8. Therefore, the pipe is modelled from the centre to the location of side #3, in reality the pipe may have stopped prior to this point or progressed further.
  - If the pipe had progressed further, this will reduce the steepness of the head profile in the barrier, and vice-a-versa.
- The extent of the pipe in front of the barrier is unknown, therefore the same dimension (0.26 m) is used as in the 2D model.
  - A wider pipe would give a lower gradient in the barrier and vice versa.
- The pipe from the ditch to the barrier is only modelled in the centre of the model and has a width of 0.25 m, and the same head as the pipe at the barrier. In reality there may be more pipes downstream (which appear to have not yet reached the barrier) and the head in the pipe downstream will decline from the barrier to the ditch.
  - This schematisation may lead to a steeper profile in the barrier as more flow converges to the pipe in the barrier.
- The extent of the pipe in the barrier is unknown, the 0.05 m from the 2D model is used;
  - A larger outflow area in the barrier would give a lower gradient in the barrier.

- An overview of the models is given in Table 6.1.

Table 6.2 Overview of 3D models for Delta Flume test 2

Name	Hydraulic conductivity barrier, m/s	Hydraulic conductivity background sand, m/s	Contrast	Pipe length in barrier, m	Head upstream, m	Head in pipe, m
Test2_3D_M2	6.85e-4 (RD 1.0)	8.57e-5	8	0.05	2.92	1.15
Test2_3D_M2_Con20	1.69e-3 (RD 0.25)	8.57e-5	20	0.05	2.92	1.15

6.2.2 Results and Discussion

The head profile along the top of the model differs along the width of the Delta flume. As it is not known exactly where the pipe entered the barrier, the head profile is shown at x = 1.25 m (i.e. at the very end of the pipe that progressed parallel to the barrier), and at x = 0.6 m (i.e. half way along the pipe that progressed parallel to the barrier), and at the centre of the model. The modelled head distribution in the model, and the locations used to extract the head profile are shown in Figure 6.10.

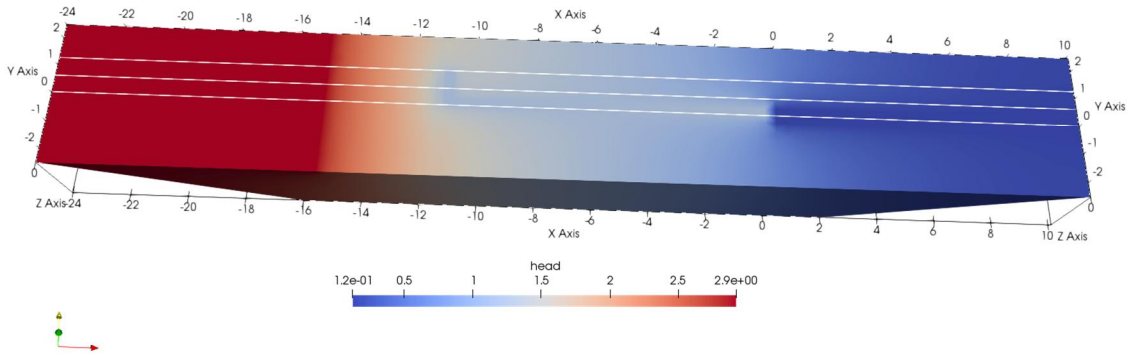

Figure 6.10 head distribution in model

6.2.2.1 *Head profile 3D vs 2D model*

The modelled head profiles for the 3D model (Test2_3D_M2) and the 2D model (DG_test2_pip05_Con080) with the best fit are shown in Figure 6.11. The 3D head profiles are much steeper than in the 2D model. Especially the head profiles at the ends of the pipe which is parallel to the barrier (at side #3 and in the centre) are significantly steeper. This means that in order to match the measured heads with a 3D model, the higher hydraulic conductivity of the barrier in the model must be increased.

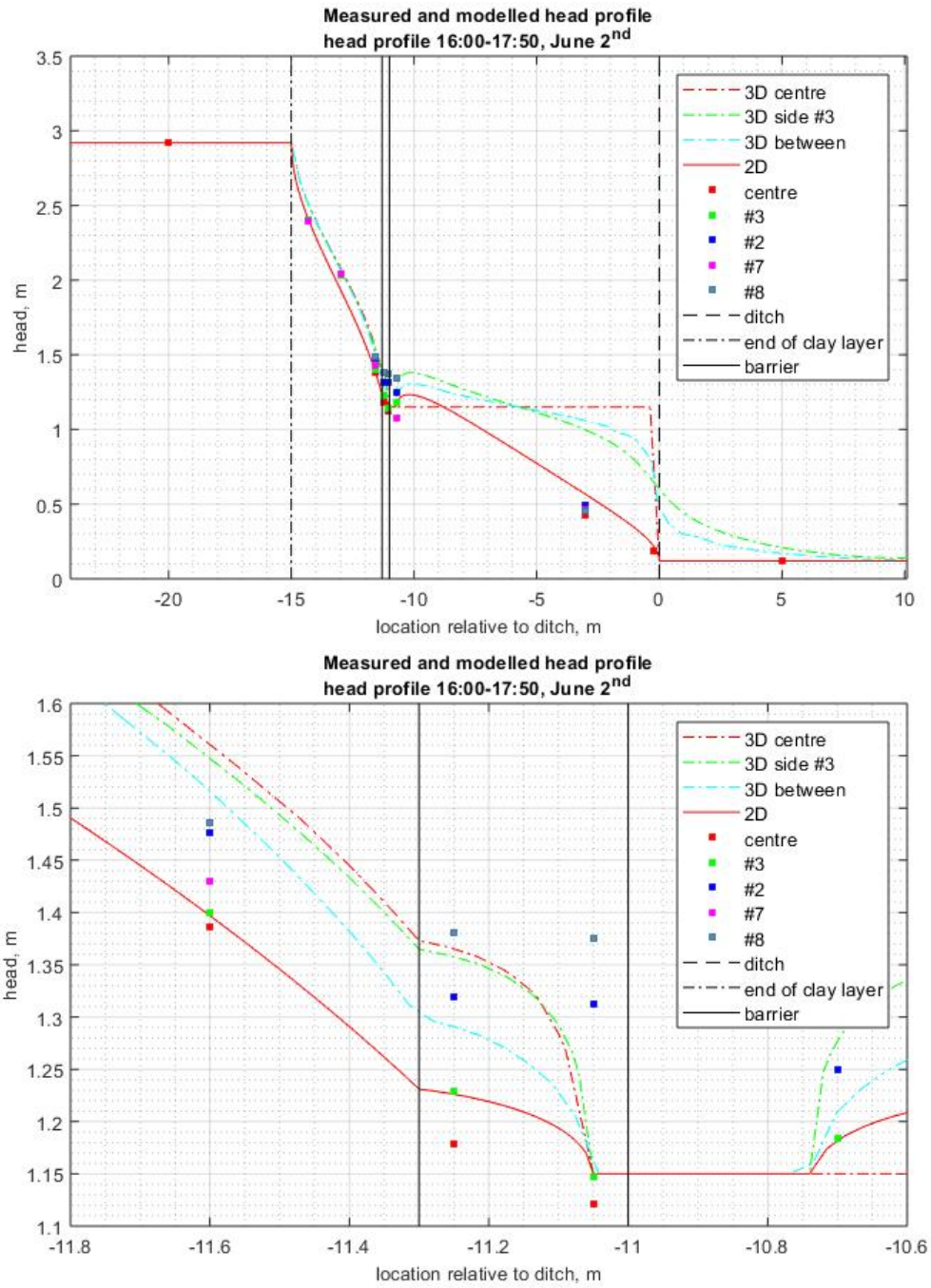

Figure 6.11 Head profiles in 2D and 3D models of the second Delta Flume test. The profile of the 3D model in the centre (top figure, red line) has a straight head line which is due to the boundary condition of a constant head in the pipe.

6.2.2.2 *Modelled flow rates*

The modelled flow rate with a contrast of 8 (Test2_3D_M2) is 19.64 l/min, which approximates the measured 19.50 l/min well. With a higher contrast, the flow rate increases to 20.96, which is still a good approximation of the measured flow rate.

This suggests that the background hydraulic conductivity which was fit based on test 1 is indeed similar in test 2.

6.2.2.3 *Head profile 3D model with higher contrast*

With a contrast of 20, corresponding to a RD of the barrier of 0.25 the modelled head profile for the line half way between the ends of the pipe parallel to the barrier approximates the head that is measured at h63-h43. The other profiles remain too high.

It is considered to be highly unlikely that the contrast is higher, as this would give an extremely low RD of the barrier. Even 0.25 is considered improbable. One possible explanation for the overestimation of the measured heads would be that the pipe progressed further along the width of the model, or if the pipe had progressed further into the barrier. Both options are considered plausible. The presence of pipes close to the barrier on the other side of the model, closer to sides # 7 and #8, would also lower the heads in the barrier at the locations that are shown.

Due to the large number of unknowns in the 3D model, it is not possible to assess which combination of pipe width along the barrier, length inside the barrier, hydraulic conductivity contrast, and extent of pipes in the downstream end of the model, was actually present in the experiment. The 3D model does clearly show that it is probable that the RD of the barrier was lower than the 1.0, which indicates that the 2D model overestimates the RD of the barrier due to 3D flow effects.

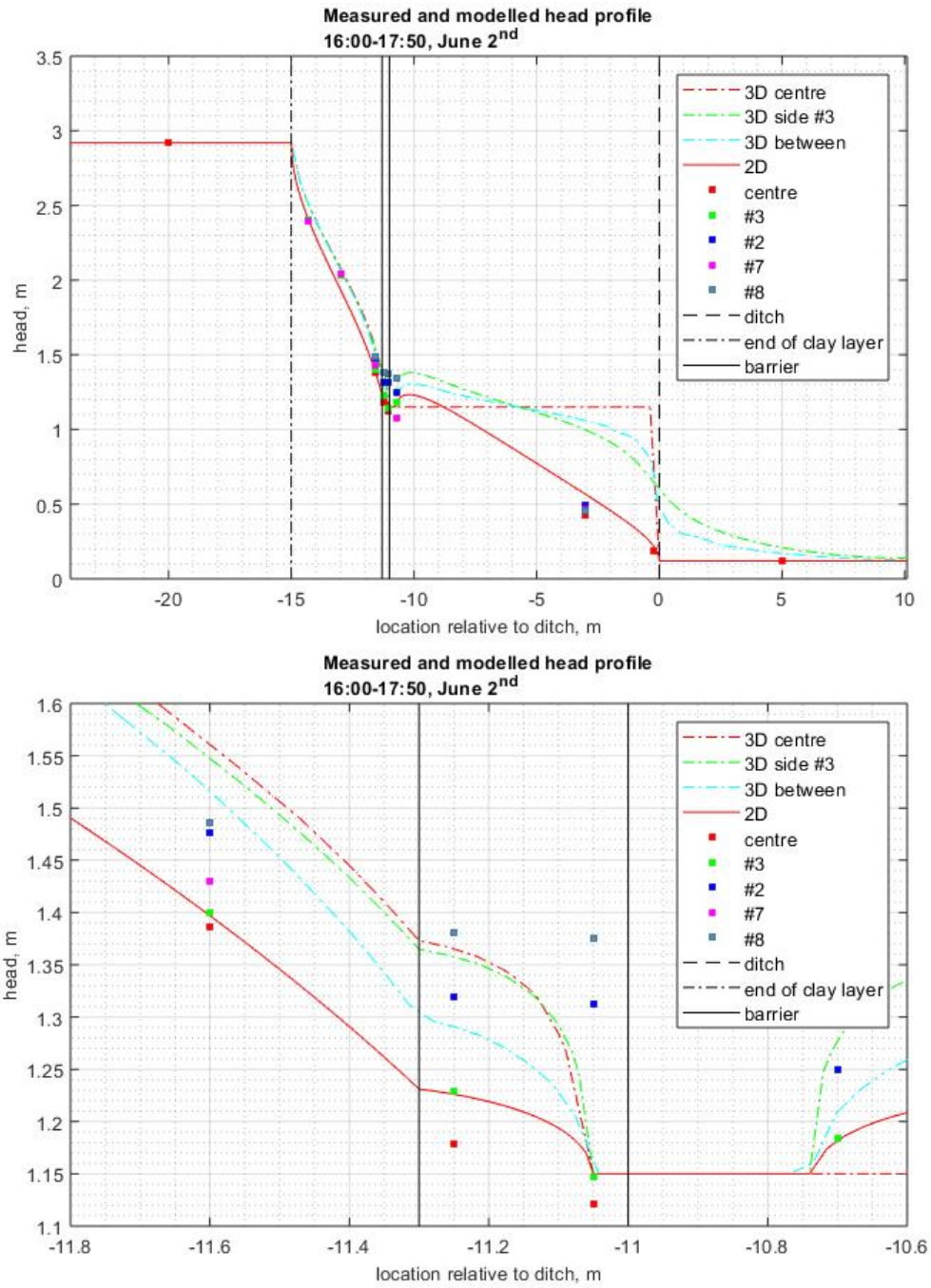

Figure 6.12 Head profiles in 3D models of the second Delta Flume test.

6.2.2.3. *Modelled strength criteria*

The modelled strength criteria for the 3D models will depend on the location that is considered. The only line which fits the data is for a contrast of 20, the profile that is half way between the end of the pipe in the centre and at side #3. This results in a gradient of 0.61 over 0.10 m, which is very comparable to the 0.59 which was found for the 2D model with a contrast of 8. This illustrates that the modelling exercise is mainly important to assess the RD of the barrier in the

test. Unfortunately, also that 2D models used for prediction require a correction when the pipe has not progressed along the entire width of the barrier. Due to the large number of unknowns for a 3D model, 3D models are also unsuitable to determine the RD of the barrier, although the models do indicate that it is plausible that the RD was lower than 1.
Therefore, it appears that the RD that was measured for test 1 is the best indication of the RD of the barrier in test 2 as well. This RD of 0.74 is lower than the 1.05 (test MS 24) and 0.83 (test MS28) in the medium-scale tests, which might be a reason for the lower modelled gradient as well.
In the medium-scale tests, tests were done with high RD samples for GZB2, but for GZB1 there was also one test with a low RD of 0.55. Figure 6.13 shows the relative density (based on preparation for the medium-scale tests and based on the sample of Delta Flume test 1 for the Delta Flume test) and the modelled strength criterion (in the 2D models) for the tests.
Overall it appears that the modelled strength criterion for the second Delta Flume test does not disprove the hypothesis that the critical gradient for pipe progression is the same at different scales. However, the limited data set is also insufficient to prove this hypothesis.

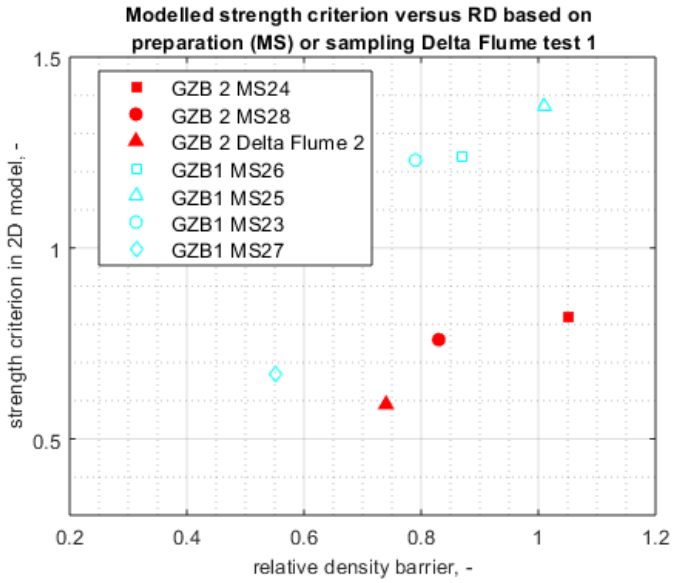

Figure 6.13 Modelled strength criteria for GZB 2

7 Modelling the first Delta Flume test

In the first Delta Flume test, the failure mechanism was different from the small- and medium-scale tests and from the second Delta Flume test, because the barrier penetrated into the cover layer above the sand aquifer. Therefore, there is no strength criterion in terms of a horizontal gradient. However, there was clear erosion of the barrier, and the presence of background sand on top of the barrier even suggests that failure might have occurred. Therefore, the experiment was modelled in order to better understand what the gradients in the barrier were at the time that the barrier was damaged.

Due to the geometry of the barrier penetrating above the cover layer, the erosion of the barrier is expected to cause the formation of a slope inside the barrier. The dimensions of this slope would depend on the space available for the barrier material to crumble into the pipe downstream. The critical pipe progression is expected to have led to a slope that has progressed all the way through the barrier, creating a void of at least ca. 0.05 m depth below transducer h62 (as this appears to be the depth by which the transducer was displaced). This would be a slope of ca. 30 degrees. Depending on the hydraulic gradients in the barrier, which are directed out of the slope, a shallower slope might be established due to the forces on the grains on the slope.

For failure to occur, background sand must be transported into the barrier zone. This can occur either when the slope becomes so shallow that background sand washes over it, or when the vertical gradient at the upstream interface of the slope is high enough to cause fluidisation of the barrier material, and transport of the background sand over the barrier.

A numerical model of the situation with a slope inside the barrier is therefore used to compute the gradients inside the barrier, both the gradients perpendicular to the slope which might be expected to cause erosion of the slope, and the vertical gradients at the upstream interface of the barrier.

The heads used for modelling are the heads at the critical point for pipe progression as described in Section 4.5. As this point is just prior to pipe progression inside the barrier this model will not be able to reproduce the exact head profile in the downstream end of the barrier (the geometry of the model corresponds to the point after progression, the measured heads are before progression). Nonetheless this gives an indication of the gradients that may have been present in the barrier at that time, and a correction can be made for the overall head drop to account for a reduction of the head downstream due to erosion as shown in Section 7.2.3.

7.1 Input

7.1.1 Schematisation

If the first assumption is that failure occurs due to high vertical gradients at the upstream side of the slope, a model with a shallower slope would result in the most critical situation, as the vertical gradients are computed over a shorter distance than in the case of a steeper slope. Therefore, a model is made with a 20-degree slope. Above the slope is a void. The slope effectively increases the outflow area of the barrier, flow can exit through the entire slope as opposed to only through the pipe that forms inside the barrier for the configuration when the barrier is level with the aquifer.

The depth of the pipe in front of the barrier is unknown, as is the depth of the toe of the slope. Preliminary computations showed that modelling the toe of the slope to a depth that is still above the top of the background sand results in a high head in the void above the slope and a strong concentration of flow at the tip of the pipe. This is considered less realistic, as barrier material will have eroded from the downstream end of the barrier into the pipe downstream. This is expected to form a zone of looser material on the downstream end of the barrier, at the tip of the slope, where the finer fraction may have been washed out, resulting in a high hydraulic conductivity. That would allow flow to leave the void above the barrier more easily. Furthermore, excavations indicate that the erosion pipe cuts into the cover layer, which also facilitates a connection between the void above the slope in the barrier and the pipe downstream. It is this connection, which is important for modelling the head in the barrier. This connection is also obtained by modelling the slope in the barrier to a depth of 0.02 m (i.e. to the bottom of a 0.02 m deep pipe at the barrier), flow can exit through the slope in the barrier and then through the pipe at the barrier.
This schematisation (with a connection between the void above the barrier and the pipe) results in a more critical situation, in the sense that it leads to higher computed gradients in the model than the option of a slope that ends above the top of the background sand.

The model with the slope in the barrier is shown in Figure 7.1.

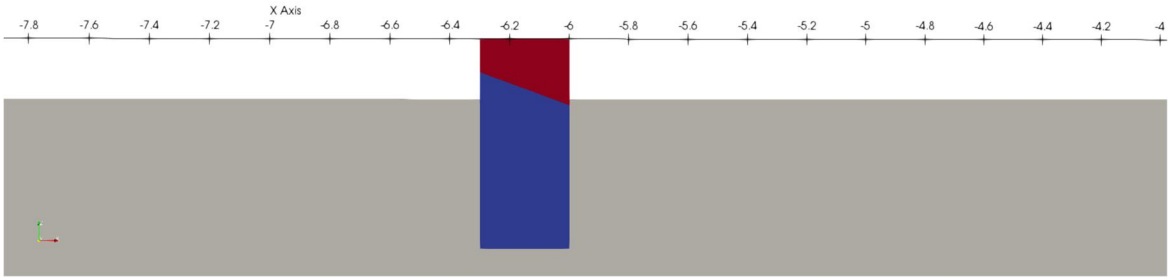

Figure 7.1 Schematisation of the slope in the barrier, grey is background sand, dark red is void above the slope, blue is barrier.

A 2D DgFlow model is used to model the situation, which is 3D in reality. Due to convergence of flow, the hydraulic gradients in a 3D situation will be higher than in the 2D model, however, a 2D model is expected to give a good first indication of how close to a critical situation the gradients are. If the situation is indeed critical, a 3D analysis could be a second step in order to obtain a more precise estimate of the conditions during the test.

7.1.2 Geometry

Only the sand body and the barrier, not the cohesive cover layer, are modelled. The end of the ditch is the centre of the axis system and the sand body is present between x = -24 m and x = 10.1 m. The maximum depth of the model is 3 m and the sides slope with a 2.67:1 slope, so that the bottom of the model is 18 m long. The barrier is present between x = -6.0 m and x = -6.3 m and has a depth of 0.5 m and a height of 0.2 m above the surface of the background sand. The slope in the barrier runs from x = -6.0 m, y = -0.02 m to x = -6.3 m, y=0.09 m, below the slope is barrier material above the slope is void (Figure 7.1). The model is shown in Figure 7.2.

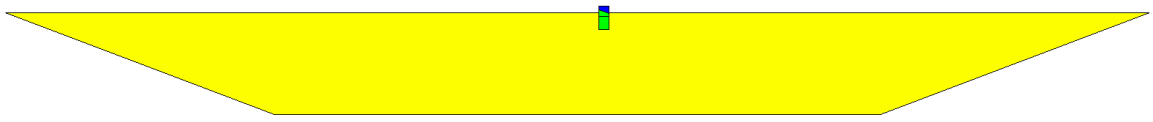

Figure 7.2 Model of the Delta Flume test, sand body yellow is background sand green is barrier, blue is void (see Figure 7.1for close-up of the barrier).

7.1.3 Boundary conditions

The upstream boundary condition is from x = - 24.0 m to x = -15.5 m and has the upstream head of 3.85 m. The downstream boundary condition for the ditch is the head that was measured in h15, which was just upstream of the ditch, this is 0.03 m. The ditch is modelled from x = 0 m to x = -10.1 m.

The pipe is modelled as a 0.02 m long vertical line at the downstream interface of the barrier and the background sand, i.e., at x = -6.0 m from y = 0.00 m to y = - 0.02 m (representing a 2 cm deep pipe in front of the barrier) and as a horizontal line below the cover layer from x = -6.0 m to x = -5.74 m (representing the pipe leading up to the barrier). The head in the pipe is based on the head measured in h42 which is 0.67 m.

All boundary conditions are the average values of the various hydraulic heads measured from 10:00 to 11:00 on April 20th.

The boundary conditions are shown in Figure 7.3.

Figure 7.3 Boundary conditions in the Delta Flume model of the first test, green is upstream head, yellow is head in pipe at the barrier, blue is head in ditch downstream. Top overview of entire model, bottom close-up of the barrier.

7.1.4 Hydraulic conductivity

The intrinsic permeability of the background sand and of the barrier in this model are assumed to be the same as for the second Delta Flume test due to the similar method of preparation. As the temperature is slightly lower during the first Delta Flume test, the hydraulic conductivities are somewhat lower. The hydraulic conductivity contrast, however, is the same for both tests. The values are shown in Table 7.1.

Table 7.1 Overview of hydraulic conductivity and intrinsic permeability in the model of the first Delta Flume test.

Intrinsic permeability background sand, m^2	Intrinsic permeability barrier, m^2	Hydraulic conductivity background sand, m/s	Hydraulic conductivity barrier, m/s	Hydraulic conductivity void, m/s
9.95e-12	7.95e-11	7.69e-5	6.14e-4	6.14e2

7.1.5 Mesh

The barrier is divided into two segments, as it is important to have a fine mesh in the upper part of the barrier. Due to the geometry of the slope, an unstructured mesh is used. In the upper part of the barrier the elements are 0.01 m, in the void above the barrier and in the lower part of the barrier the elements are 0.02 m and the rest of the model has elements of 0.04 m. A close-up of the mesh is shown in Figure 7.4.

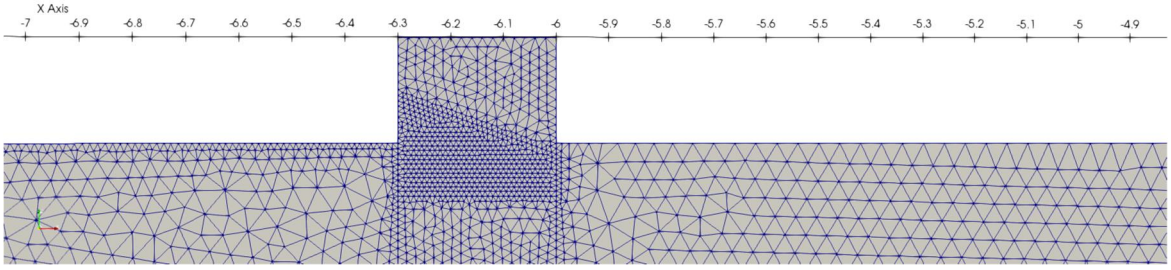

Figure 7.4 Close-up of the mesh at the barrier in the model of the first Delta Flume test

7.2 Results and analysis

7.2.1 Head profile and flow distribution

The modelled head profile is shown in Figure 7.5. This shows that most of the head drop occurs in the upstream part of the model over the background sand. There is only a very small head drop in the barrier.

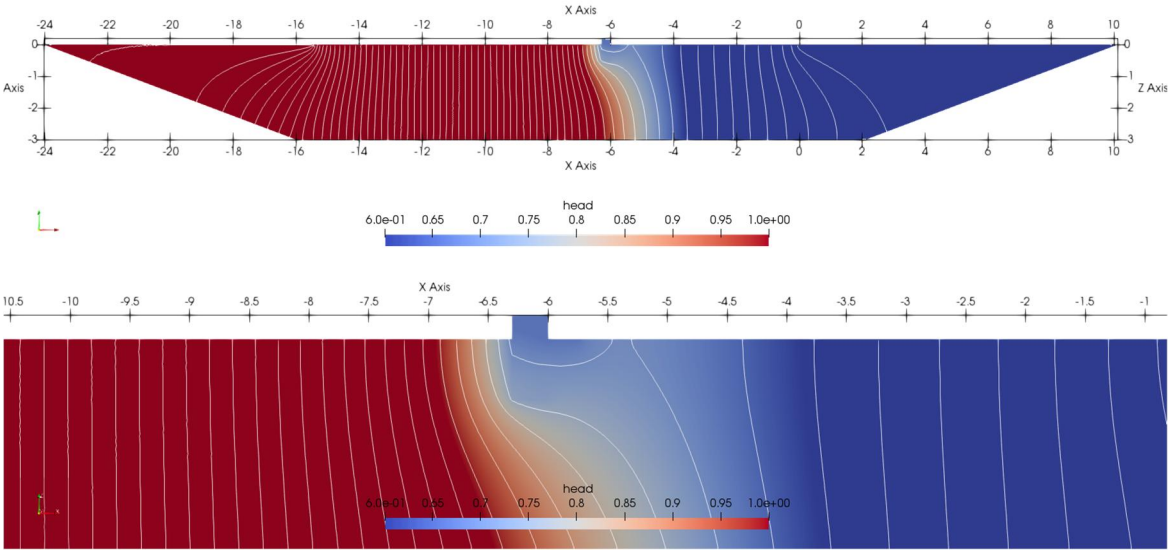

Figure 7.5 Modelled head profile for the first Delta Flume test. Head contours are spaced 0.056 m.

7.2.2 Computed gradients

The gradient perpendicular to the slope (out of the slope) is computed in two ways. By dividing the flow velocity on the slope by the hydraulic conductivity of the barrier, giving a point estimate of exit gradient and by computing the gradient between the slope and the head modelled 0.05 m inside the barrier of the slope. Both methods give comparable results: gradients that are in the order of 0.1 to 0.2 for the largest part of the slope. The computed gradients only start to rise sharply close to the downstream slope tip.

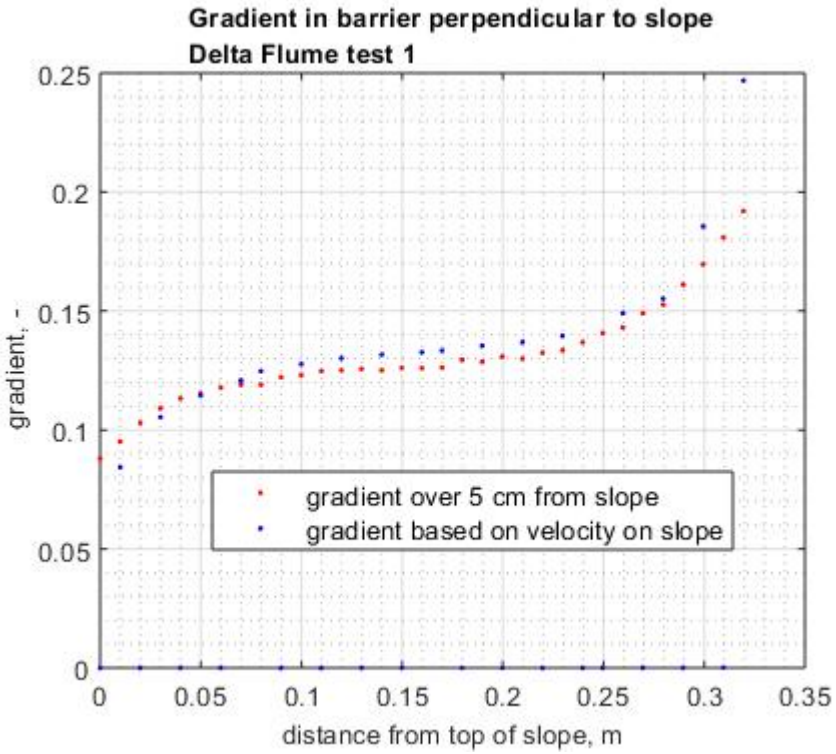

Figure 7.6 Computed gradient perpendicular to slope for Delta Flume test 1

The vertical gradient is computed along the line x = - 6.28 m i.e. 2 cm from the upstream interface of the slope, over the distance from the top of the aquifer, y = 0.08 m, to the surface of the slope at that point, y = 0.08 m. The obtained gradient is 0.15, a value similar to that of the gradient perpendicular to the slope.

This low vertical gradient would not be enough to cause fluidisation of the slope or vertical transport of the background sand.

7.2.3 Sensitivity to head in downstream end of barrier

The model geometry represents the situation after progression of the slope in the barrier, the heads that are used as boundary conditions are the critical heads prior to progression. If the progression caused formation of the slope this could have reduced the head in the downstream side of the barrier increasing the gradient over the barrier. In order to investigate the effect of this, a model is made where the head in the pipe downstream of the barrier is equal to the head in h15 at the ditch. This can be considered to be an extremely unfavourable schematisation, which would result in higher gradients inside the barrier. This does result in somewhat higher computed gradients along the slope, and at the upstream interface. However, the computed vertical gradient of 0.23 remains significantly lower than one which would be required for fluidisation.

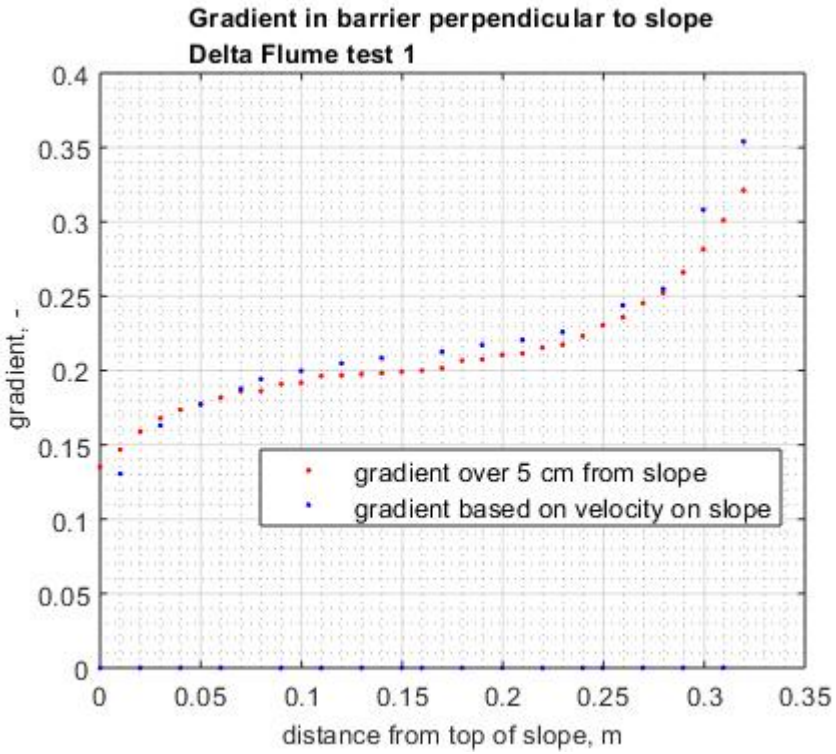

Figure 7.7 Computed gradient perpendicular to slope for Delta Flume test 1 using a head of 0.03 m in the pipe on the downstream side of the slope.

7.2.4 Discussion and Conclusions

The modelled head drop over the barrier is very small at the critical point, as the majority of the head drop was dissipated over the background sand upstream. The computed gradients perpendicular to the slope in the barrier and the vertical gradient on the upstream side of the slope are relatively low. This indicates that it is unlikely that fluidization of the barrier material occurred. This suggests that there was no failure of the barrier around this time, and that the background sand which was observed on top of the barrier was not transported into the barrier from upstream during a failure.

The current model only provides a simplistic schematisation, and contains various uncertainties:

- The model is 2D, whereas due to the presence of only one pipe that did not progress parallel to the barrier a 3D situation occurred in reality. This would lead to a higher convergence of flow in the barrier and possibly gradients were higher than modelled. However, given the low modelled vertical gradient of 0.15 (or 0.23 with the maximum plausible head drop to the barrier), it is unlikely that gradients were high enough to cause fluidisation;
- The slope dimensions were not known:
  - the slope might have been steeper due to a higher top of the slope, this would have resulted in a lower computed vertical gradient, and not affected the conclusion that fluidisation and failure was unlikely.
  - the slope might have been less steep, however, with a gradient of 0.2 perpendicular to the slope (based on the current model) and an internal friction angle of 30 for the barrier material, the equilibrium slope based on van Rhee and Bezuijen (1992), would be 26 degrees. This indicates that the 20-degree slope which was used here is already a safe estimate. There is a possibility that the convergence of flow in 3D, which is not captured by the 2D model might have led to a higher gradient on the slope and a shallower slope.
  - the toe of the slope might have been higher above the top of the sand aquifer, this means a lower head in the pipe downstream would be required in order to have the head that was measured in h42 in the model. With the current boundary conditions, a slope that ends higher above the top of the sand body would give lower gradients in the barrier;
- The hydraulic conductivity contrast was based on models of the second Delta Flume test, which contains significant uncertainty. However, this results in a relatively low contrast, and a higher contrast would result in even lower gradients inside the barrier and therefore not affect the conclusion.

8 Conclusions and recommendations

8.1 Conclusions

Two large scale experiments were conducted in order to test the feasibility of the CSB on a larger scale. In the first test, the barrier protruded above the top of the sand body by ca. 0.2 m, in the second test the barrier was level with the top of the sand body. During the first test, leakage caused the test to be abandoned before a clear failure was observed, failure was achieved in the second test. The set-up was instrumented with PPTs, buoyant tracer particles, active distributed temperature sensors, and observations were made during the test as well as flow rate measurements. After the tests there was an excavation.
This chapter summarises the main findings.

8.1.1 Analysis of observations and measurements

The exact piping process that occurred is unknown, however based on the analysis of available data a speculative process is suggested in this section.

- During test 1:
  - Initially one pipe progressed to the barrier at the south side of the flume.
  - This pipe cut into the cover layer.
  - The pipe did not progress far in lateral direction, parallel to the barrier (probably less than 1 m)
  - The barrier crumbled into the pipe and a slope established into the barrier, probably reaching all the way to the upstream end of the barrier. This occurred at an upstream water level of 4 m, however, due to a gap in the data collection during this period there is uncertainty regarding the exact timing and head development at this point. During this gap in the data, the test also had to be interrupted and the upstream head was lowered for repairs against leakage.
  - This slope through the barrier, and the resulting void between the slope and the blanket layer, probably did not yet allow for transport of the background material from upstream through the barrier, as background sand would have to be washed up over the slope. This means there was a different failure mechanism from the medium-scale tests and from test 2. Vertical gradients at the upstream end of the slope may govern failure for this configuration, as these are required in order to fluidize the barrier in the slope and transport background sand over the barrier. However, this mechanism is speculative.
  - During excavation, background material was observed on top of the barrier, the origin of which is uncertain. It cannot be ruled out that this is from upstream, however, modelled gradients in the barrier suggest that this is unlikely.
  - During the repair activity the cover layer subsided into the barrier plugging the void between the slope in the barrier and the cover layer.
  - After the head was raised again, pipes on the north side of the flume also progressed to the barrier but did not appear to damage the barrier significantly.
  - These pipes were smaller than the original pipe, probably due to a redistribution of flow.
  - The test was ended due to leakage, not due to failure of the barrier.
- During test 2:
  - A pipe progressed to the barrier (close to the centre of the flume) and some distance along the barrier (towards the south side of the flume) but not along the entire width of the model

- o A step similar to the long growth step in the medium-scale tests was observed.
- o After this step another pipe appeared to have reached the barrier at the north side of the flume.
- o The pipe appears to have breached the barrier in a new growth step at the same location where the long growth step occurred, at a higher head drop starting the failure process.
- o The cover layer may have subsided onto the barrier at this location preventing the complete erosion of the barrier at that location.
- o Excavation indicated that failure eroded all of the barrier on the north side of the model.

An overview of critical steps and the associated head drops is shown in Table 8.1.

Table 8.1 Overview of heads and important steps.

Test	Time of progression in barrier*	Time of failure of barrier*	Critical head drop for progression*, m / *time interval used to compute critical head drop for progression*	Critical head drop for failure*, m / *time interval used to compute critical head drop for failure*	Maximum applied head drop, m / *time interval used to compute maximum applied head drop*	Data used to compute critical head drops
Delta Flume test 1	Between 10:00 and 16:30 on April 20th	No failure	3.81 m / *09:00 to 10:00 on April 20th*	No failure	5.93/*20:00-21:00 on April 23rd*	Upstream: DCTM01 or manual (for maximum head drop) Downstream h15 at tip of ditch
Delta flume test 2	18:35 on June 2nd	02:00 on June 3rd	2.81 / *16:00 to 17:50 on June 2nd*	2.97 / *19:00 to 21:00 on June 2nd*	3.29 / *06:15 to 06:55 on June 3rd*	Upstream: h99 in top of sand bed, Downstream: h09 in ditch

* the progression of the pipe in the barrier (test 2) or of the erosion front in the barrier (test 1) and the possible failure of the barrier (test 2) are interpretations of the test data.

Both tests indicate that eroded tracer particles were retained in the pipe, rather than washed out of the model, these could not be used to indicate the location of the pipe progression.

AH-DTS measurements do indicate zones where at different points during the second test there may have been more flow, however, these generally do not correspond to the locations where erosion is expected based on the head measurements. It is possible that head measurements do not capture all pipe progression, as these are point data, however, the temperature measurements also do not appear to capture all aspects of the pipe progression that are inferred based on head measurements. For interpretation of this test, the head measurements were given priority, as these were based on extensive analysis in the medium-scale experiments. The applicability of AH-DTS measurements for monitoring of the piping process in the presence of a CSB was limited in the current experiment.

In both tests the head drop between transducers that are close to or inside the pipe in the barrier and the ditch is relatively high, indicating significant head loss in the pipe which was not measurable in the medium-scale tests. A higher head drop in the pipe downstream could result in a higher head drop that can be retained in the field. There are various factors that can have contributed to the head drop in the pipe, and some of these may apply in the field, but others

not. The presence of suspended material, barrier material and background sand, would increase the measured head drop in the pipe, this may not be the case in a field situation. Turbulent flow in the pipe can be expected to have contributed to the head drop in the pipe this might be the case in the field. Possibly, also the limited time allowed for erosion, and/or deposition of coarser particles in the pipe, prevented further deepening and widening of the pipe, this cannot be counted on for a field situation.

Both tests indicate that the pipe does not progress along the entire width of the model, which is an important factor affecting the concentration of flow inside the barrier. Less progression parallel to the barrier is unfavourable for the critical head drop.

The erosion of the pipe into the cover layer which was observed for the first Delta Flume test is remarkable. This might be due to limited compaction of the clay layer on preparation, but this may also be the effect of high flow rates in the pipe. Since no head loss is assumed in the pipe in models, the shape of the pipe is not very relevant for practice.

8.1.2 Numerical modelling

- A 3D model was made to estimate the hydraulic conductivity of the background sand based on data from the first Delta Flume test. This resulted in an estimated RD of 87%, which is used as the hydraulic conductivity for both Delta Flume tests.

Test 2 with barrier level to the clay layer

- A 2D DgFlow model was made for the test 2 to estimate the hydraulic conductivity of the barrier and the length pipe of the pipe in barrier at the long growth step, this resulted in a high relative density barrier and a short pipe (RD 1, pipe length 0.05 m).
- A 3D model of the same test was made, which showed that with a pipe length of 0.05 m, the hydraulic conductivity of the barrier would need to be higher (i.e. the RD lower, less than 0.25) in order to fit the head profile at the location at which pipe progression occurred. Due to the number of uncertain parameters in the 3D model, it was not possible to establish which combination of barrier RD, with pipe length and extent in front of the model was the most probable during the test. The model does show that the RD of the barrier was probably overestimated by the 2D model. It also shows that the modelled gradient is effectively the same for the 2D and 3D model provided that the pipe length inside the barrier is the same, as would be expected because the heads inside the barrier are used to achieve the fit.
  - This means that for practice a correction will be required for possible limited lateral development.
- The modelled strength criterion, the horizontal gradient over 10 cm upstream of the pipe tip was 0.59 in the 2D model, which is lower than the values from medium-scale tests (0.76 and 0.82). This may be due to a lower RD of the barrier in the Delta Flume tests. Samples of Delta Flume test 1 indicate that the RD was 0.74, which is lower than 0.83 and 1.05 in the medium-scale tests. It may also be the case that the pipe did not develop directly below the transducers used to fit the model.

Test 1 with barrier protruding in the clay layer

- A 2D DgFlow model was made for the test 1 to estimate vertical gradients at the point that a slope formed through the barrier. Computed vertical gradients at the upstream end of the slope are low (0.15) indicating that it is unlikely that failure occurred.

There are a number of assumptions and uncertainties involved in modelling these tests. Mainly:

- The use of the 2D models for the Delta Flume tests, 3D effects can be more significant than in the medium-scale tests due to the lack of development of the pipe parallel to the

barrier, the greater dimensions of the model, and the relatively smaller depth of the barrier. The comparison of a 3D model for the critical point for test 2 shows that a 3D model does result in a different RD for the barrier material if the head profile is to be fit with similar assumptions as in the 2D model. The 3D model has too many parameters to be able to fit a unique solution. However, the computed strength criterion does not change significantly, as this is largely constrained by the measured heads.
  - This means that the assumption that the pipe progresses relatively close to the transducers is important for the modelled strength criterion, if the distance between the pipe and the transducers is larger, the models will underestimate the strength criterion.
- The unknown hydraulic conductivity of the background sand, this had to be fit using a 3D model, which gave a lower estimate that would be expected based on samples taken during preparation of the first Delta Flume test. However, the 3D model for the second Delta Flume test reproduces the measured flow rate well, suggesting the fit was applicable for the test. Considering also that sampling of the background sand to determine RD was difficult, it appears the hydraulic conductivity of the barrier from the model for the first test is appropriate. This uncertainty does not have a significant effect on the modelled head profile, or the computed strength criterion of the barrier.
- The unknown extent of the pipe in the model for test 2, and the unknown dimensions of the slope for test 1. It is assumed that the transducers h42 in test 1 and h43 in test 2 represent the head in the pipe at the barrier
  - For test 2 if the pipe were further developed into the barrier, this could lead to a higher strength criterion. A longer pipe would have to be combined with a lower contrast, i.e., a lower hydraulic conductivity of the barrier to fit the measured heads. In the 2D model, this would give a RD > 1.0 which was considered unlikely. In the 3D model, the modelled RD is much lower, and this would be possible. The problem however is that in the 3D model the extent of the pipe along the barrier is also unknown. Thus, the three parameters, pipe length inside the barrier, pipe extent along the barrier and hydraulic conductivity of the barrier, would provide a large number of possible solutions.

8.2 Recommendations

- As the failure mechanism with a barrier that extends above the top of the background sand is different from what was investigated in earlier tests, it is recommended to analyse this failure mechanism in more detail. The progression of a slope through the barrier, in combination with a vertical failure mechanism at the upstream end of the barrier which has been postulated here requires further analysis in terms of medium-scale experiments and consideration of the effect of barrier dimensions on the erosion process. It is expected that this type of configuration could be favourable, as the slope inside the barrier provides a much larger outflow area out of the barrier as compared to the 0.04 m pipe which is modelled inside the barrier for the horizontal failure mechanism when the barrier is level with the background sand. This would reduce local gradients in the barrier, and increase the head drop that can be retained. However, the angle of the slope would play a large role in determining the distance over which a vertical gradient has to be exceed for fluidisation to occur. More importantly, this mechanism has now been speculated upon but needs to be observed in medium-scale tests with a transparent cover to verify whether indeed this mechanism occurs.
- The large-scale models show a larger head drop in the pipe, which might be applicable in the field too. This depends on the cause of this high head drop, it is recommended to assess the plausible head drop that can be expected for field situations.

- The lack of progression parallel to the barrier means that the gradients inside the barrier will be strongly underestimated in 2D models. It is recommended to investigate the magnitude of this effect for field scale application by using 3D modelling.
- Tracer particles with a lower buoyancy are recommended for characterising pipe progression.

9 References

Deltares (2017a). Feasibility study on the effectiveness of a coarse sand barrier as a piping measure. Report 1220240-004-GEO-0003.

Deltares (2017b). Literatuurstudie Filtercriteria ten behoeve van grofzandbarriére. Deltares memo 11200952-003-GEO-0001.

Deltares (2017c). Sand selection coarse sand barrier experiments. Deltares memo 11200952-004-GEO-0001-m.

Deltares (2017d). Factual Report Small-scale experiments coarse sand barrier. Deltares report 11200952-004-GEO-0003.

Deltares (2017e). Analysis report coarse sand barrier. Analysis of small-scale configuration (phase 2a). Deltares Report 11200952-006-GEO-0006.

Deltares (2018a). Factual report Medium-Scale Experiments Coarse Sand Barrier (Phase 2b). Deltares Report 11200952-007-GEO-0004

Deltares (2018b). Primary Erosion Tests for the Coarse Sand Barrier. Deltares Report 11200952-035-GEO-0001.

Deltares (2018c). Analysis Report Coarse Sand Barrier. Analysis of medium-scale configuration (phase 2b). Deltares report 11200952-007-GEO-0005.

Deltares (2018d). Numerical Simulation Coarse Sand Barrier Experiments using USACE Preliminary Model. Deltares Report 11200952-036-GEO-0001.

Deltares (2019a). Factual Report Delta Flume Experiments Coarse Sand Barrier (Phase 2c). Deltares Report 11200952-010-GEO-0008.

Van Rhee, C., Bezuijen, A., Influence of Seepage on Stability of Sandy Slope. 1992. J. Geotech. Engrg. 118:1236-1240. 92929292929292

A Analysis of AH-DTS measurements

Memo

Deltares
Enabling Delta Life

To
dr. E. Rosenbrand

Date
June 3, 2019

Number of pages
19

Contact person
Jarno Terwindt
Pieter Doornenbal

Direct number
+31(0)88 335 7238
+31(0)88 335 7799

E-mail
Jarno.Terwindt@deltares.nl
Pieter.Doornenbal@deltares.nl

Subject
Delta Flume AH-DTS Measurements

Summary
During the second experiment of the Delta Flume Experiments Coarse Sand Barrier project [1] AH-DTS (Active Heating Distributed Temperature Sensing) measurements were performed. During each heating and cooling phase an exponential function was fitted. The derived exponential coefficient was used to assess any change in thermal properties, which could indicate either increased flow, removal of material (i.e., pipe growth) or a combination of the two. With the derived coefficients the key spatial-temporal points were identified. These are outlined in Table 1.

Table 1 – Spatial Key Points

Position	Co-ordinate		Time of Increased Activity	Comments
	x [m]	y [m]	[mm/dd HH:MM]	
Upstream of Outflow	68.25	-2.29	05/31 12:00	Possible Error
Upstream of Outflow	68.25	0.99	06/02 04:00	
Downstream of barrier	66.00	2.10	06/01 12:00 (or 06/02 00:00)	
Downstream of barrier	66.00	-0.81	06/02 02:00	
Barrier	65.35	-0.26	06/02 04:00	
Barrier	65.35	-1.89	06/02 04:00	
Upstream of barrier	64.70	2.18	05/31 12:00	Possible Error

Introduction
This memorandum presents interpreted results from AH-DTS (Active Heating -Distributed Temperature Sensing) measurements (also referred to as ADTS). The data were collected during the 2nd experiment of the Delta Flume Experiments Coarse Sand Barrier [1], dated 31st of May to 3rd of June 2018.

Active Heating- Distributed Temperature Sensing (AH-DTS) has potential to measure piping processes. We placed a heating wire connected to a DTS fibre optic cable in a model experiment simulating piping processes. In this case, the AH-DTS cable was installed in between the sand-clay interface of the sand and the blanket layer. The fibre optic cable is used as a sensor by applying the Distributed Temperature Sensing technology. The temperatures are measured with a sampling interval of 0.125 m and a spatial resolution of 0.29 m (Selker et al., 2014), as shown in Figure 1. In other words, the data is averaged over intervals of 0.29 m, with the centres of each averaging interval spaced at 0.125 m.

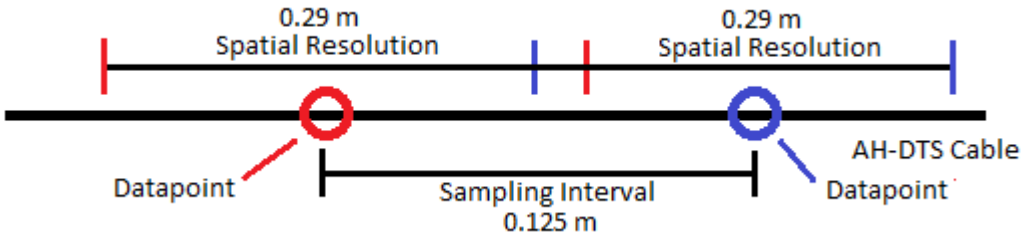

Figure 1 – Difference between sampling interval and spatial resolution.

A heat pulse is generated by applying electrical power to the heating wire, increasing the temperature of the cable, the surrounding material and the surrounding water. The rate of heating and subsequent cooling, provides an indication of the heat transfer to the surrounding. As the surrounding material as well as the flow affect the measured temperatures, the temperature can be used as a proxy for piping processes (groundwater flow and sediment transport).

The goal of this memorandum is to present the AH-DTS data collected, the theory applied to the data to analyse piping processes and the processed AH-DTS data. It is assumed that the reader is familiar with the Delta Flume Piping Experiments. Please refer to [1] for further information.

Test Setup

In this experiment, temperature monitoring is executed using Distributed Temperature Sensing (DTS) in glass fibre optic cables. The DTS monitoring is performed with the Silixa Ultima (https://silixa.com/products/ultima-dts) unit monitoring temperatures at a temporal sampling frequency of 6 measurements per minute per channel (this excludes the active heating, but refers to the sampling frequency of the measurement system). It is decided to use the data of channel 1, while the moment to pick the starting of the heating curve could better be determined using data of 1 channel only. The fibre optic cable used in this experiment is the multimode duplex cable produced by LEONI (www.leoni-fiber-optics.com). Attached to the fibre optic cable are heating wires, making it possible to create heat pulses along the fibre

The fibre optic cable has a total length of 61 meters. From 5.8 – 11.1 meters and 12.1 – 14.1 the fibre optic cable runs through two calibrations baths. From 14.1 – 35.0 meters the fibre optic cable is used as a lead in. From ~35 to 60 meters the fibre optic cable can be heated and is described as an ADTS fibre optic cable. This section is installed under the dike, with four sections perpendicular to the Delta Flume wall (see Figure 2 for overview and Figure 3 for an impression.

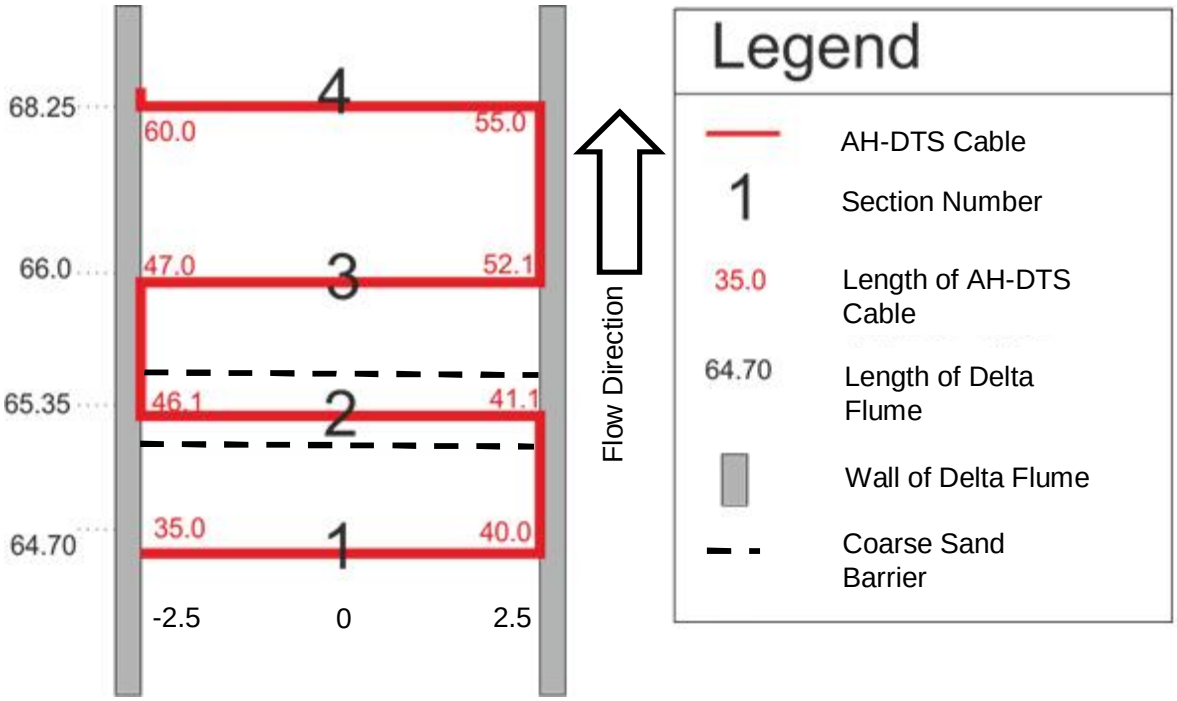

Figure 2 – Top-view of the AH-DTS layout, the upstream water body is present at 61.5 m, the tip of the ditch is at 76.5 m

Figure 3 - Photo of the fibre optic cable on the sand bed.

The start and stop of the heat generation is done manually. The period of heat generation is typically around between 20 and 40 minutes, followed by a cooling period of comparable length. The cooling period allows for the temperature to return to equilibrium. The data collection started on 31st May 00:00 and ended at 5th of June 11:55. The first heating period is around 31st of May 09:20, and the last one at 3rd of June 2018. A final, longer, heating pulse, after the end of the experiment, was also generated from 10:38 to 12:03, June 4th 2018.

Data Processing

Piping processes are the development of small flow channels that begin on the downstream side of the structure. When the piping process continues the internal erosion, taking away sediment and works its way to the upstream side of the structure which may even cause the structure to collapse (e.g. van Beek et al., 2011, van Esch et al., 2013). During the piping process it is expected that flow rates increase and sediment is eroded. When heat pulses are applied, it is expected that at sections where flow rates are low temperatures will become higher than at points where flow rates are higher. Heat transfer from a heating wire to the surrounding sediment and waterflow is influenced by conduction and convection. The relation between the measured temperatures and the groundwater flow velocity is currently under research [5], so future improvements may certainly be possible.

To get a first assessment of the heat transfer in this experiment the data are analysed using the solution of Newton's Cooling Law:

$$T(t) = T_{ENV} + (T_0 - T_{ENV})e^{-r \cdot t}$$

Where T is the temperature at a given time t, T_{ENV} is the temperature of the environment, T_0 the temperature at t=0 (start of heating or cooling cycle) and r is characteristic for the surrounding sediment and the groundwater flow. E.g., clay has a low thermal conductivity and thus it may be expected that the temperature rises more quickly when compared to sand. Flow rate also has an influence; in porous materials where the flow rate is high the temperature increase is expected to be less in comparison to the same material when the flow rate is low. In order characterize the material surrounding the AH-DTS, r is fitted for each interval. Figures 4 and 5 show examples.

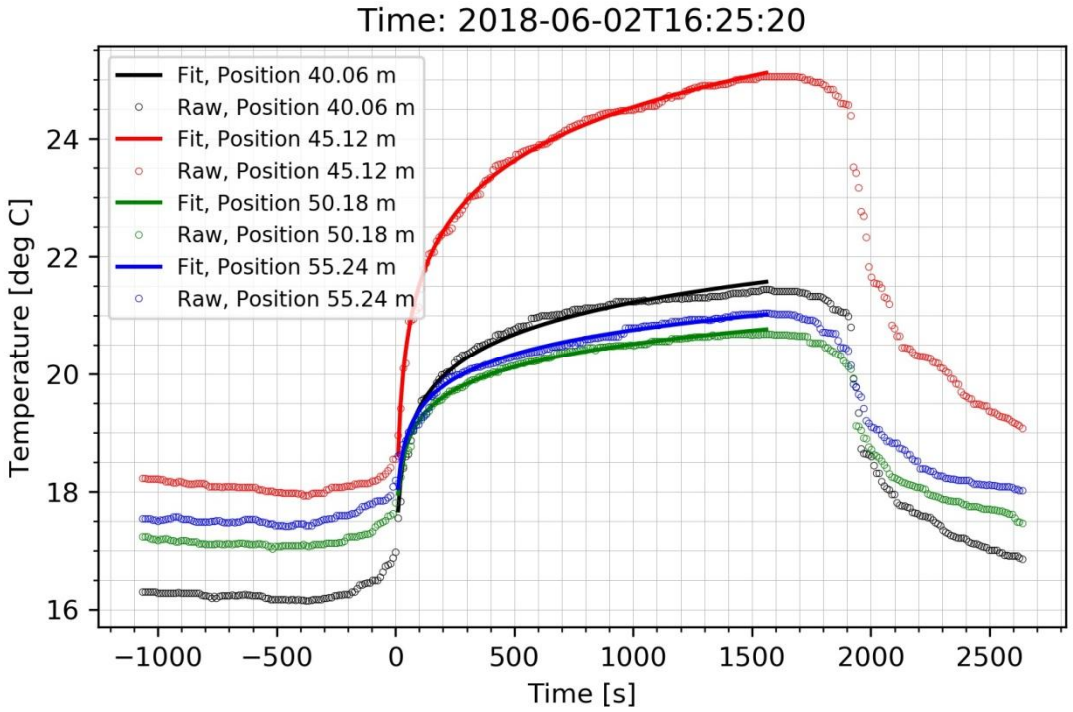

Figure 4 – Heating phase for four different spatial points around 16:25 at 2 June 2018.

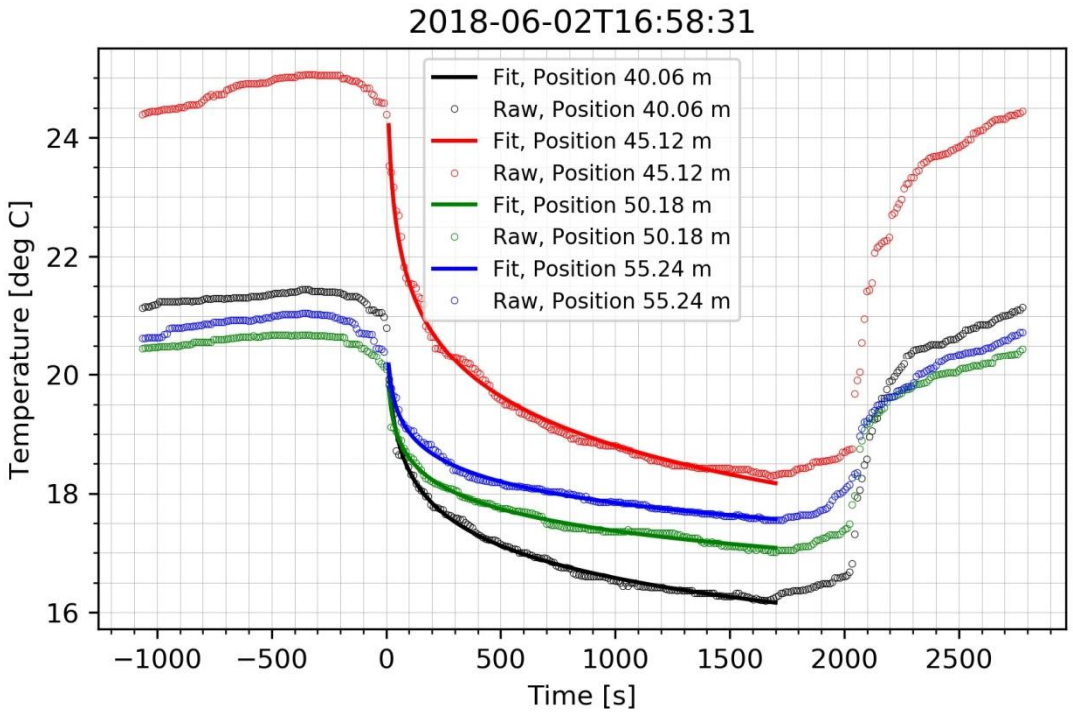

Figure 5 – Cooling phase for four different spatial points around 16:58 at 2 June 2018.

After calculating the *r* values for all spatial and temporal points for both the heating and cooling phases these are offset by the average of the first five points in time for each spatial point (the period of five points was found to provide most representative offsets, after trialling various offset periods). The offsetting is done in order to remove any bias of the initial surrounding

material and variance due to difference in heating time. This removes any physical meaning for the derived *r* values but accentuates any change relative to the initial state of the model. Finally, the absolute values have been taken of the *r* values to allow better comparison between cooling and heating phases and thus increasing the temporal resolution. The final result is a number between 0 and approximately 1, where 1 signifies the greatest change relative to the initial state and 0 the least.

Measurement Results

In order to optimize data visualization, the data has been split between spatial plot, for different points in time (Figure 6 to 13) and temporal plots for different selected spatial points (Figure 14 to 20). Notable is the deviation from the general initial state at position xy=(68.25, -2.30). Possibly the cable has not been fully covered here, or there is uncertainty in the cable position, or leakage along the wall.

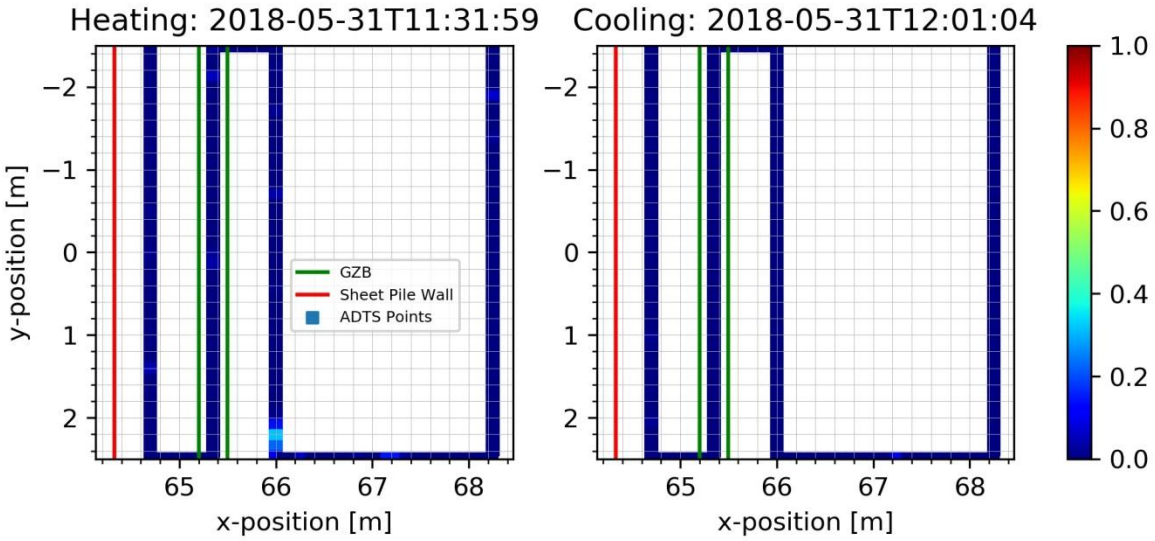

Figure 6 – Spatial plot

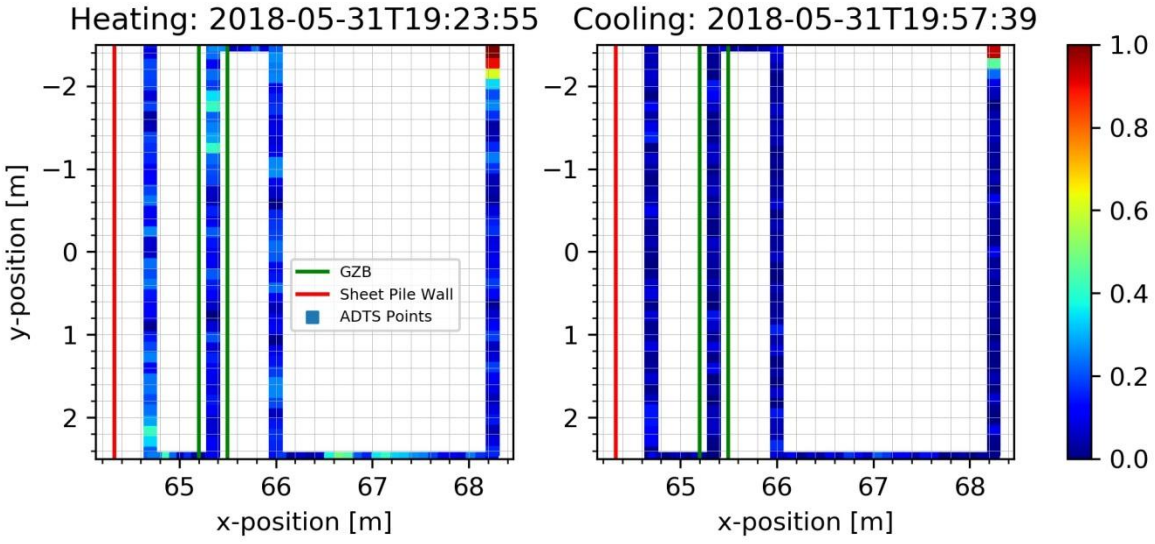

Figure 7 – Spatial plot

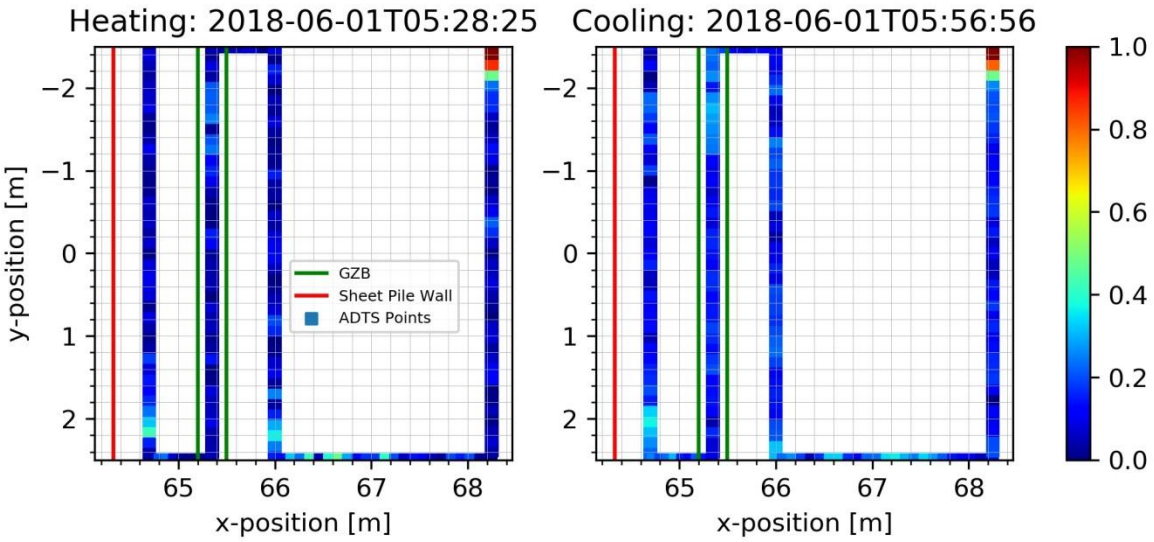

Figure 8 – Spatial plot

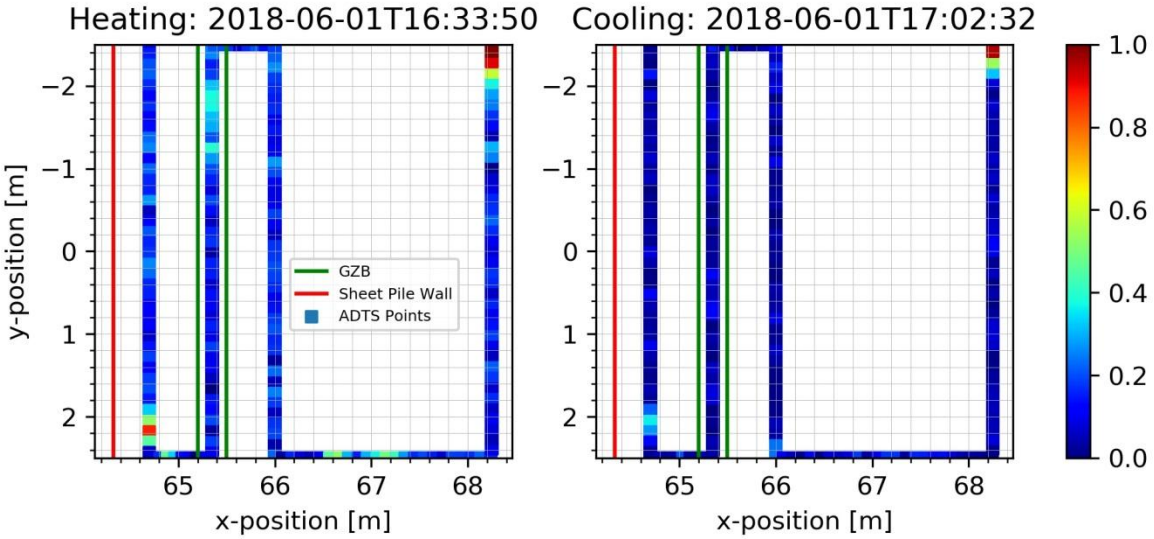

Figure 9 – Spatial plot

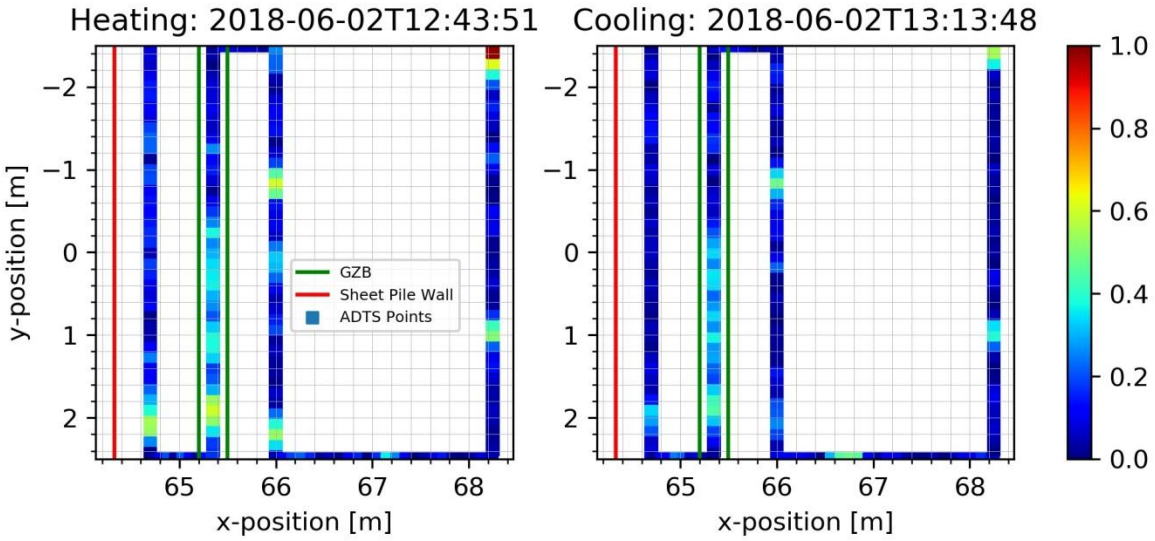

Figure 10 – Spatial plot

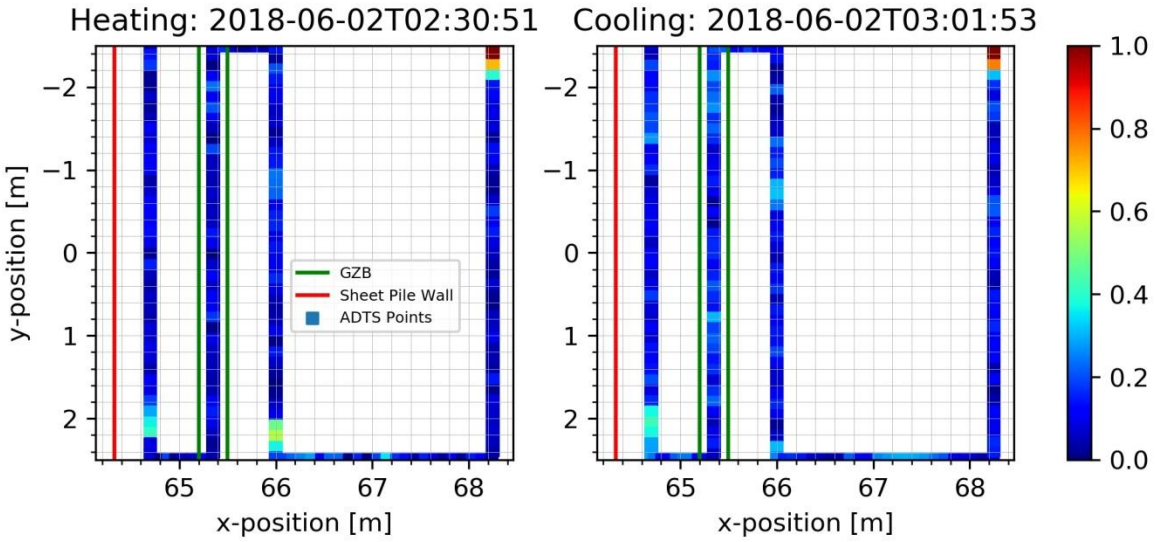

Figure 11 – Spatial plot

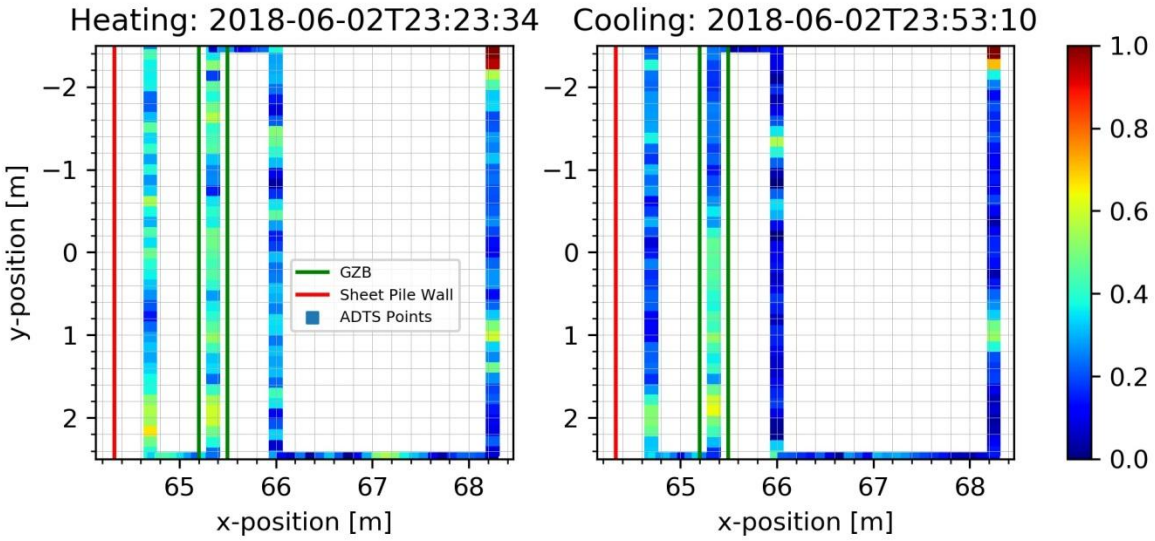

Figure 12 – Spatial plot

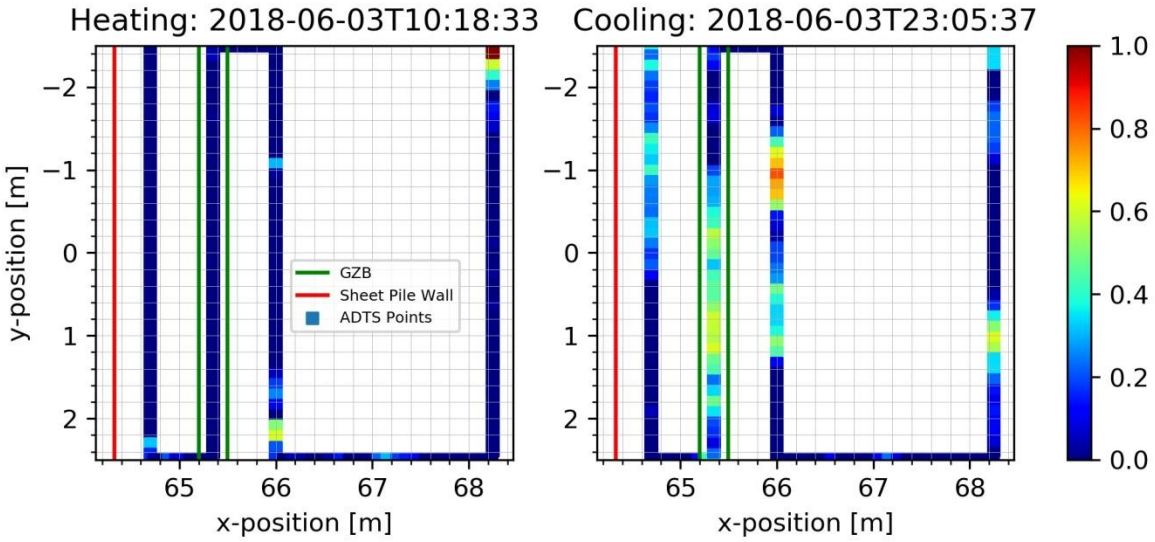

Figure 13 – Spatial plot of final post-test heating and cooling pulse. Note that the time period differs from the intervals during testing.

From Figures 6 to 13 certain spatial positions can be identified where the activity is the highest. These points are detailed in Table 2. Temporal plots have been made for these specific points and are shown in Figure 14 to 20. The gradients of the pressure sensors are also shown in these figures. Please note that the limits on the vertical axis differ in order to allow for maximum detail. The bottom graph of Figures 14 to 20 shows the maximum activity in each spatial measurement point. This has been done in order to illustrate why this specific point has been selected.

Table 2 – Spatial Key Points

Position	Section	Co-ordinate		Time of Increased Activity	Figure
		x [m]	y [m]	[mm/dd HH:MM]	
Upstream of Outflow	4	68.25	-2.29	05/31 12:00	14
Upstream of Outflow	4	68.25	0.99	06/02 04:00	15
Downstream of Barrier	3	66.00	2.10	06/01 12:00 (or possibly 06/02 00:00)	16
Downstream of Barrier	3	66.00	-0.81	06/02 02:00	17
Barrier	2	65.35	-0.26	06/02 04:00	18
Barrier	2	65.35	-1.89	06/02 04:00	19
Upstream of Barrier	1	64.70	2.18	05/31 12:00	20

Please note that the pressure sensors are referred to as e.g. h62, h47 etc. in [1]. But in this document the convention of P62, P47 is used. Furthermore h35, h47 and h67 are not presented in [1] because they were assessed to be unreliable. To make sure that no correlation between the anomalies in the pressure sensors and the AH-DTS sensors is missed, the data of h35, h47 and h67 is presented in the memorandum.

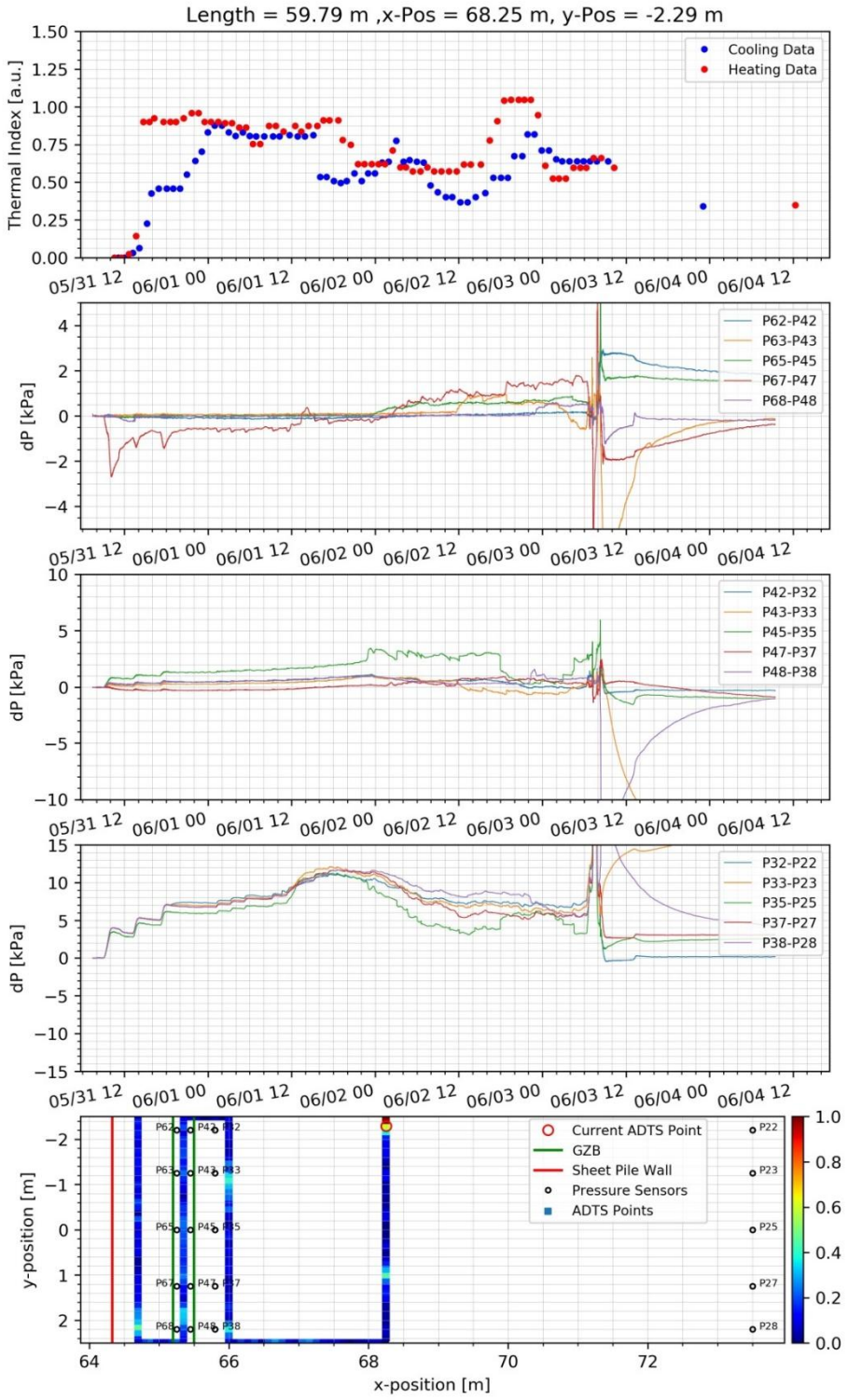

Figure 14 – Top to bottom: temporal plot of thermal index; temporal plot of gradients in pressure sensors in the barrier; temporal plot of gradients in pressure sensors between barrier and downstream; temporal plot of gradients in pressure sensors downstream of the barrier; spatial plot of the maximum activity in each spatial measurement point

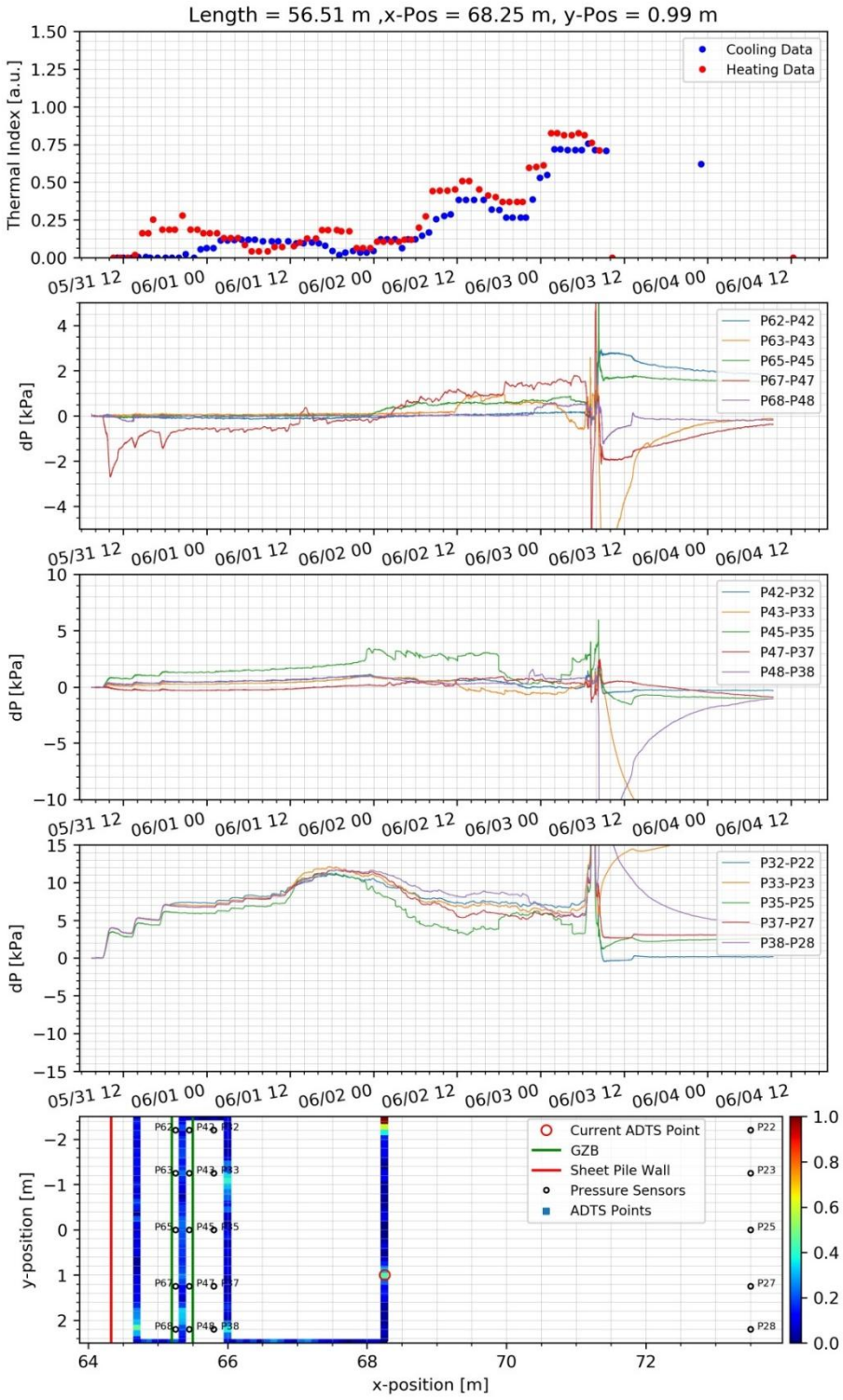

Figure 15 – Top to bottom: temporal plot of thermal index; temporal plot of gradients in pressure sensors in the barrier; temporal plot of gradients in pressure sensors between barrier and downstream; temporal plot of gradients in pressure sensors downstream of the barrier; spatial plot of the maximum activity in each spatial measurement point

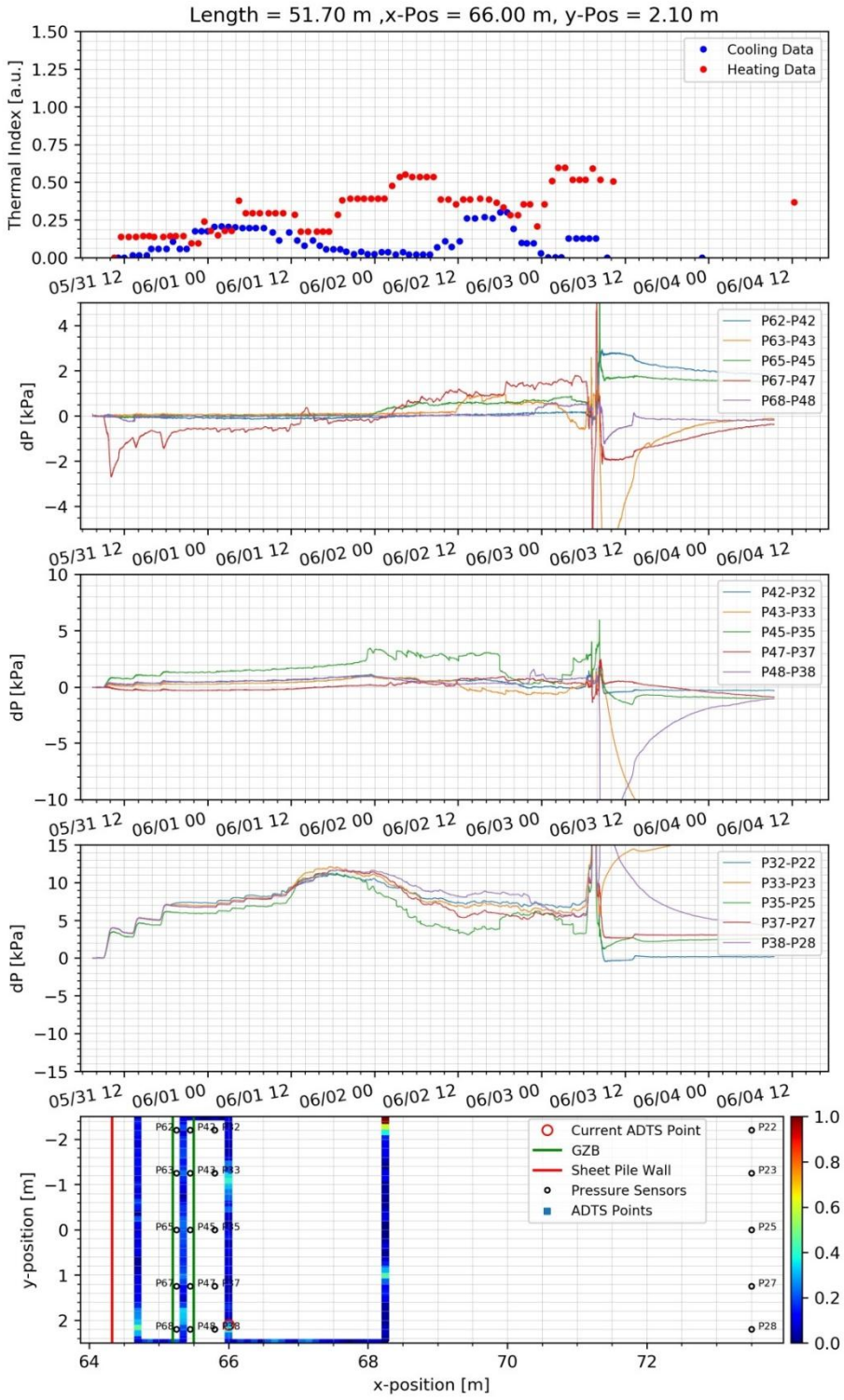

Figure 16 – Top to bottom: temporal plot of thermal index; temporal plot of gradients in pressure sensors in the barrier; temporal plot of gradients in pressure sensors between barrier and downstream; temporal plot of gradients in pressure sensors downstream of the barrier; spatial plot of the maximum activity in each spatial measurement point

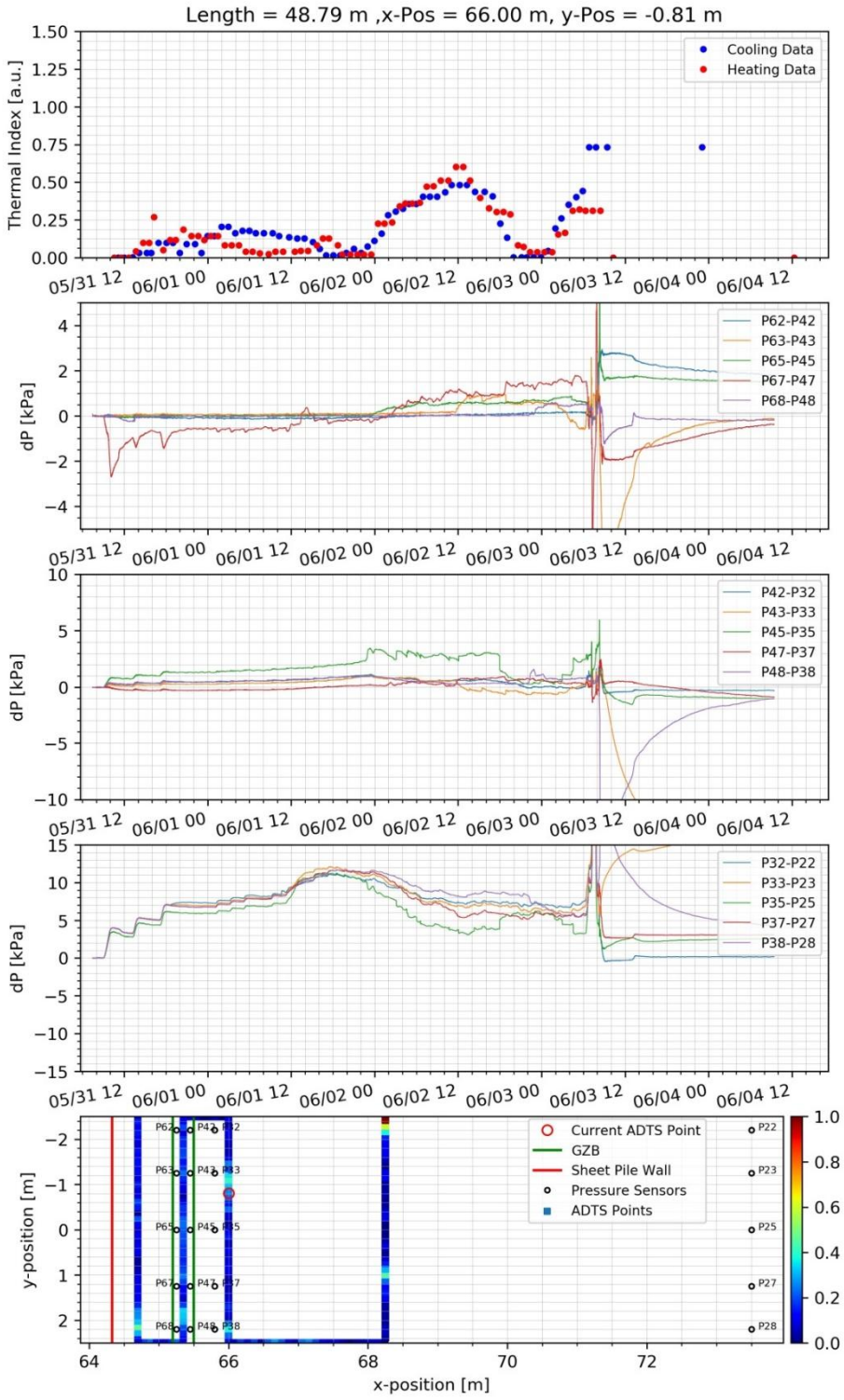

Figure 17 – Top to bottom: temporal plot of thermal index; temporal plot of gradients in pressure sensors in the barrier; temporal plot of gradients in pressure sensors between barrier and downstream; temporal plot of gradients in pressure sensors downstream of the barrier; spatial plot of the maximum activity in each spatial measurement point

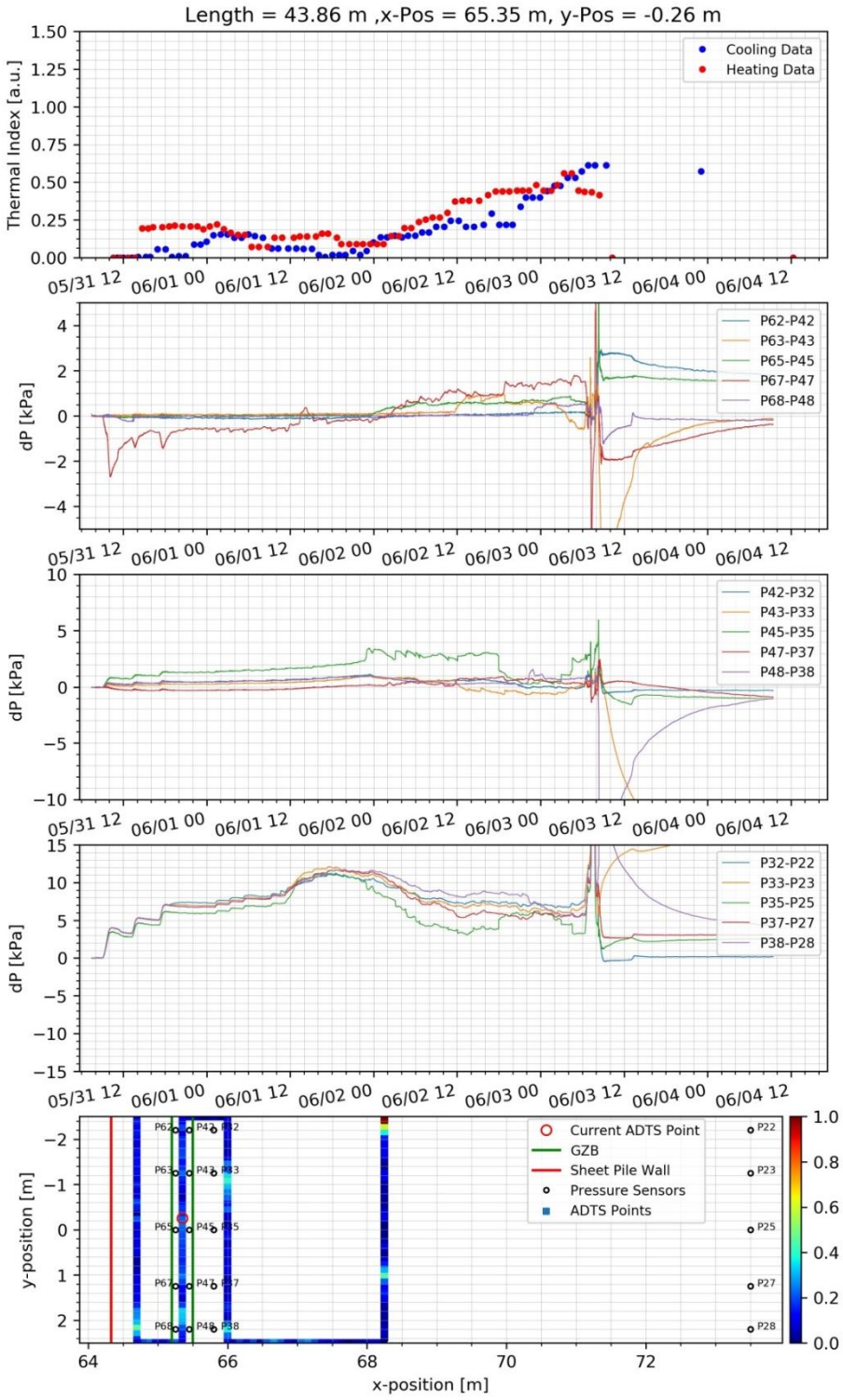

Figure 18 – Top to bottom: temporal plot of thermal index; temporal plot of gradients in pressure sensors in the barrier; temporal plot of gradients in pressure sensors between barrier and downstream; temporal plot of gradients in pressure sensors downstream of the barrier; spatial plot of the maximum activity in each spatial measurement point

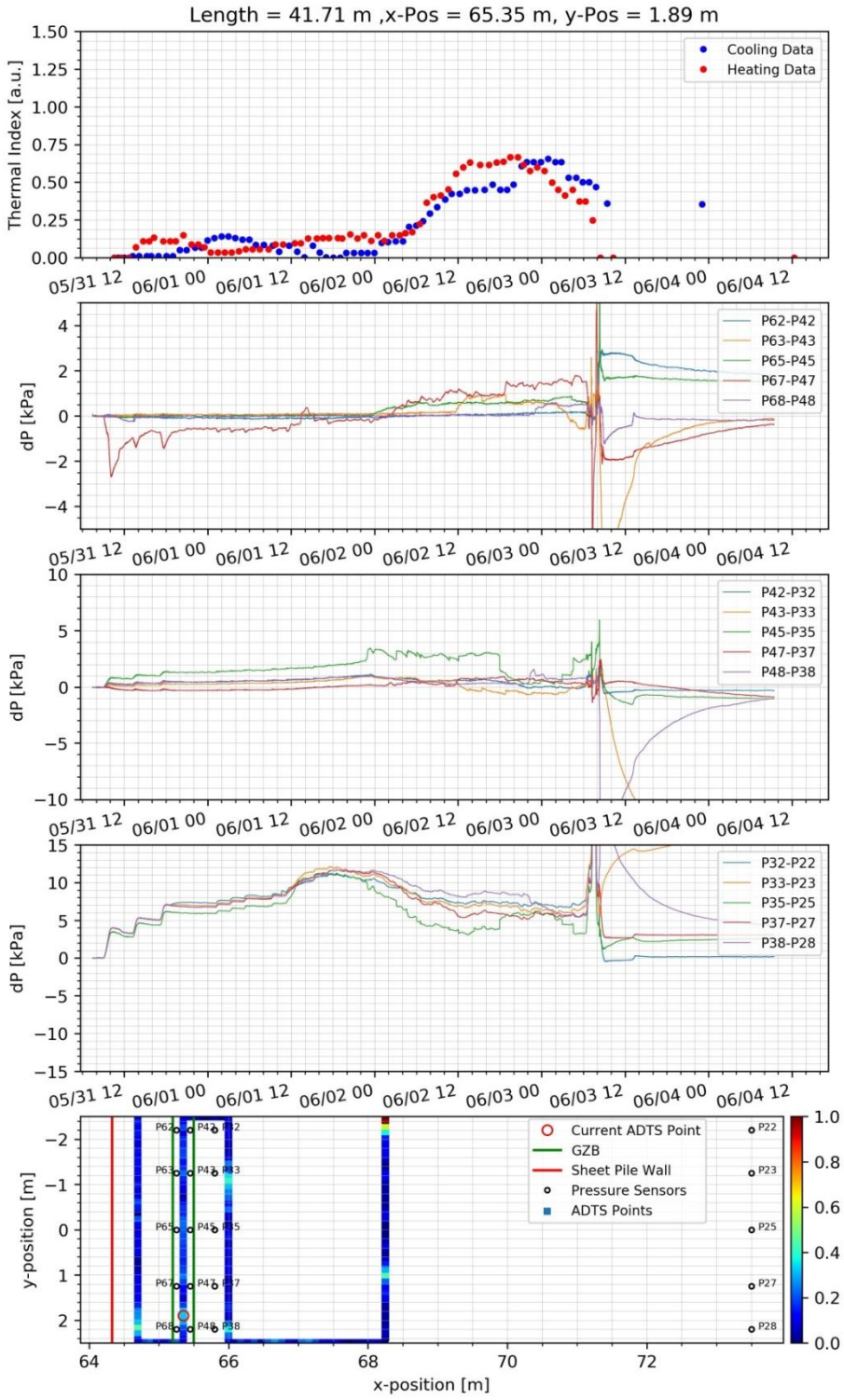

Figure 19 – Top to bottom: temporal plot of thermal index; temporal plot of gradients in pressure sensors in the barrier; temporal plot of gradients in pressure sensors between barrier and downstream; temporal plot of gradients in pressure sensors downstream of the barrier; spatial plot of the maximum activity in each spatial measurement point

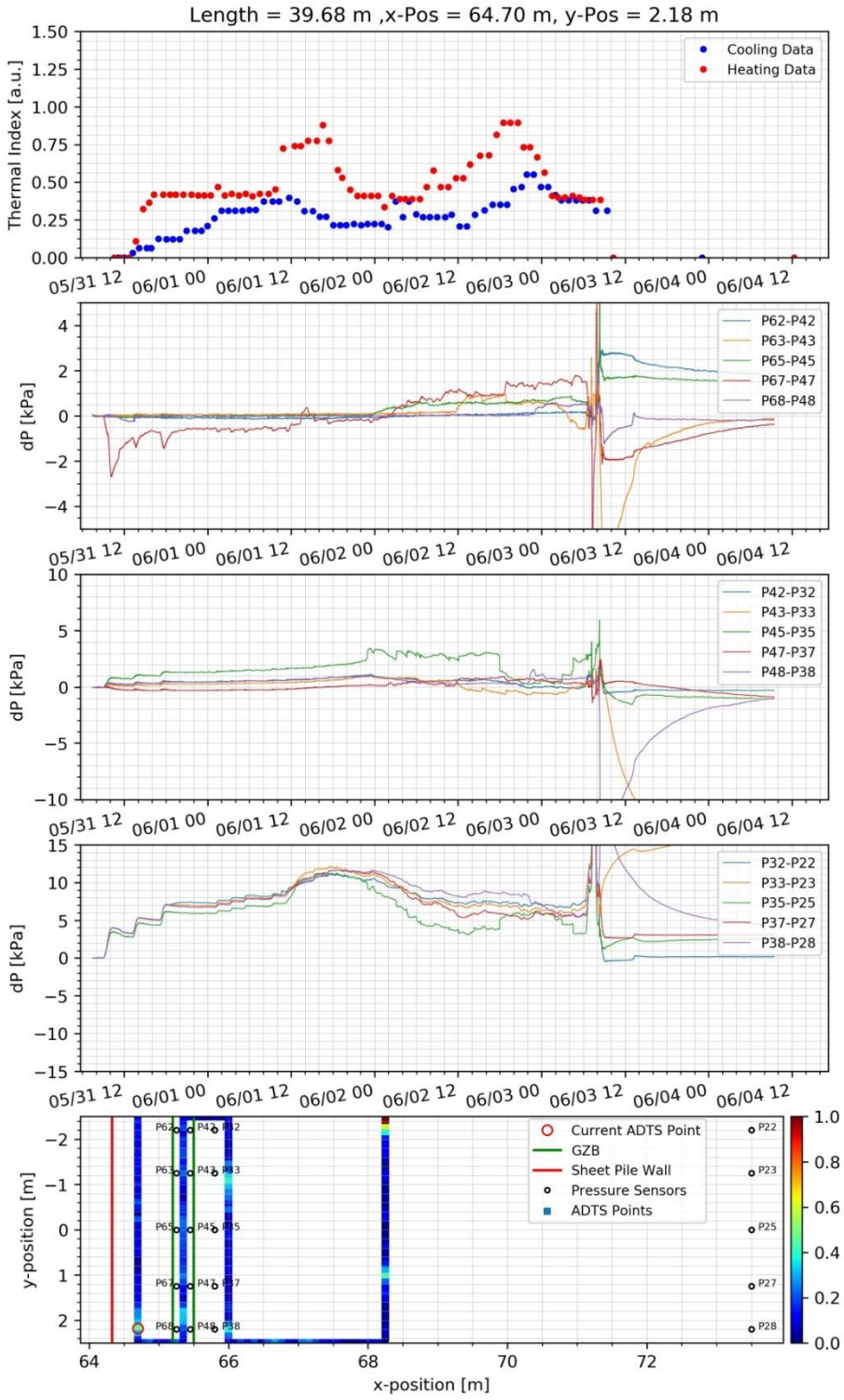

Figure 20 – Top to bottom: temporal plot of thermal index; temporal plot of gradients in pressure sensors in the barrier; temporal plot of gradients in pressure sensors between barrier and downstream; temporal plot of gradients in pressure sensors downstream of the barrier; spatial plot of the maximum activity in each spatial measurement point

Comments on Results

The temperature changes in both the heating and cooling phase consistently follow an exponential trend, allowing for a confident determination of the temperature increase with the logarithm of time. Both the cooling and heating phases could be consistently identified. The temperature data is relatively noisy, but median filtering resulted in interpretable data. The resulting exponential factors *r* still show a fair degree of variance. This may be attributed to too long heating times, or too short cooling times. This creates a situation where the temperature at the start of next heating phase is not yet in equilibrium, possibly creating additional variance in the exponential constants. Therefore, it is difficult to pinpoint the exact time of any change in thermal properties.

Additionally, one cannot distinguish between increase in groundwater flow and an increase in sediment erosion by evaluation of the heating and cooling rate alone. However, Bakx et al. [5] are currently working on a method to distinguish between the two processes.

Furthermore, to the authors knowledge, AH-DTS has not been applied to detect piping processes in earlier work. This lack of prior experience with linking AH-DTS data with erosion makes interpretation difficult, particularly where AH-DTS and pressure sensor data contradict each other. Further laboratory controlled experiments, where AH-DTS response may be linked directly to piping processes may improve interpretation.

The interpretation as determined from the AH-DTS data is as follow:

- Initial pipe growth may occur at position xy=(68.25,-2.29), already at 12:00 05/31/2018, peaking at 06:00 06/01/18 (Figure 14). However, due to the position near the Delta Flume boundary leakage along the wall cannot be excluded. Another explanation may be uncertainty in the cable position; i.e. this particular cable section met not be fully buried but positioned along the Delta Flume wall.
- Another pipe may be interpreted at position xy=(68.25,0.99) starting at around 04:00 06/02 (Figure 15). This coincides with a change in pressure gradient
- At position xy=(66.00, 2.10), pipe initiation may be seen at 18:00 06/01. The difference becomes more evident at 06/02 00:00 (Figure 16). At position xy=(66.00,-0.81), pipe initiation may be seen at 00:00 06/02 (Figure 17). This is also seen in pressure sensors P45-P35, widening along the barrier at 65.35 m, or damage to the barrier, may be seen 02:00 06/02, concentrating at 1.89 m, but ranging from -0.64 m to about 2.0 m.
- Activity upstream from the barrier van be seen at position xy=(39.56,2.06) from about 05/31 12:00 (Figure 7). It is unlikely this is caused by piping. Leakage from the sheet pile wall may be a more likely explanation.

References

[1] Deltares, January 25, 2019, 11200952-010-GEO-0008-r-Factual report Delta Flume Experiments Coarse Sand Barrier.

[2] Selker, J. S., Tyler, S. and van de Giesen, N.: Comment on “capabilities and limitations of tracing spatial temperature patterns by fiber-optic distributed temperature sensing” by Liliana Rose et al., Water Resour. Res., 50(12), 9777–9779, doi:10.1002/2013WR014979, 2014.

[3] J.M. van Esch, J.B. Sellmeijer, D. Stolle. (2013) Modelling transient groundwater flow and piping under dikes and dams. Conference paper, Researchgate .

[4] Van Beek V.M., Knoeff H., Sellmeijer H. 2011. Observations on the process of backward erosion piping in small-, medium- and full- scale experiments. European Journal of Environmental and Civil Engineering 15(8): 1115-1137

[5] W. Bakx, P.J. Doornenbal, R.J. van Weesep, V.F. Bense, G.H.P. Oude Essink, M.F.P. Bierkens, “Determining relation groundwater flow velocities and temperature differences using Active Heating - Distributed Temperature Sensing: a laboratory experiment”, under review.

B Modelling hydraulic conductivity of background sand of Delta Flume test 1

The hydraulic conductivity of the background sand is uncertain. Therefore, a 3D model is used to model the situation at the start of the test 1 prior to piping to fit the hydraulic conductivity. During test 2, there was a period of heavy rainfall early in the experiment. Furthermore, the ditch was not dug deep enough, therefore there was a clay layer at the outlet, which was only removed on June 1st (ca 1 day after the start of the experiment). At that time sand boils had already formed. These two uncertainties mean that the measured head drop and flux would not be expected to provide a reliable indication of the hydraulic conductivity at the start of that test. As only part of the sand body, the top ca. 1.5 m was replaced between the two tests, and preparation and densification was done using the same methods, it will be assumed that the hydraulic conductivity was comparable in the first and second tests.

During the first test, the flux measured on 18-04 at 15:45 is used. This is 1.45 hours after the target upstream water level was raised to 0.8 m, and 15 minutes before the target level is increased again. Therefore, this time is considered the best approximation of an equilibrium situation that is possible with the data set, prior to pipe formation.

B.1 Geometry schematisation

Only the sand body, not the cohesive cover layer, is modelled. As the barrier has a minor impact on the flow, the Delta Flume is modelled using only the background sand. As in the 2D models, the end of the ditch is the centre of the axis system and the sand body is present between x = -24 and x = 10.1 m. The maximum depth of the model is 3 m and the sides slope with a 2.67:1 slope, so that the bottom of the model is 18 m long. The model is 5 m wide. Figure B.1 shows the model.

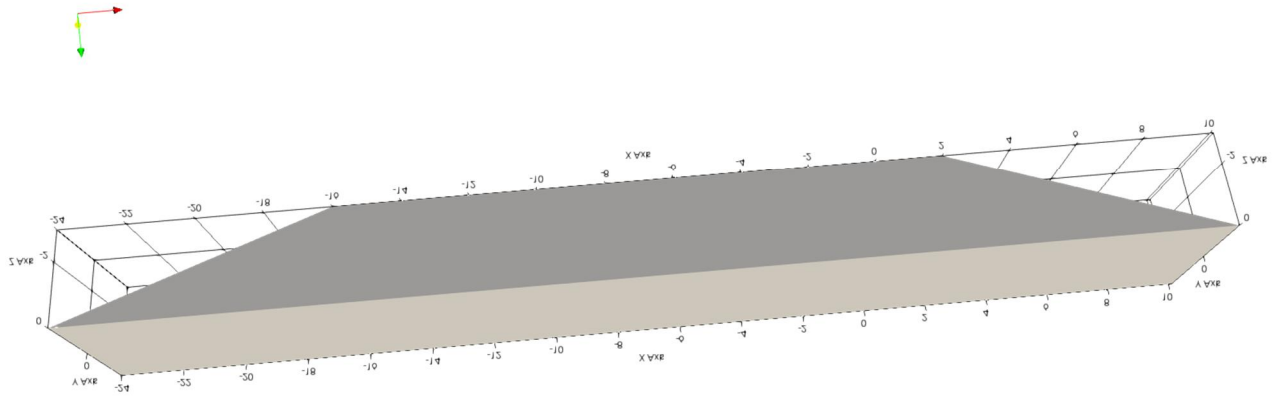

Figure B.1 Model of the sand body for the Delta Flume test.

B.2 Boundary conditions

The top at the location of the cover layer, the sides and bottom of the model have a no flow boundary. The ditch is modelled as a boundary condition at the surface of the sand based on the dimensions of the bottom of the ditch (0.5 m wide and from the downstream end of the model at x = +10.1 m, to x = 0 m). The upstream boundary condition is present at the surface

of the model between x = -24 m to x = -15 m. The boundary conditions are shown in Figure B.2.

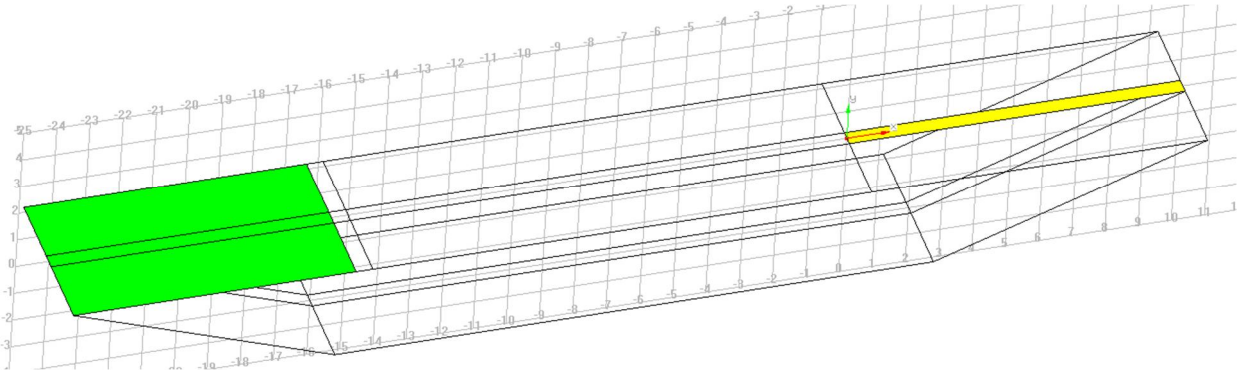

Figure B.2 Boundary conditions, upstream boundary (green) downstream boundary (yellow)

The upstream head, measured in DCTM01 is 0.8 m, the downstream head measured in transducer P15 near the tip of the ditch is 0.07 m.

B.3 Mesh

A preliminary mesh analysis shows that the computed flow rate is sensitive to the mesh refinement. Therefore, an unstructured mesh is used with a basis element size of 0.5 m, whereby the top surface of the model on the side of the upstream and the downstream boundary conditions is refined to have an element size of 0.1 m. The mesh is shown in Figure B.3.

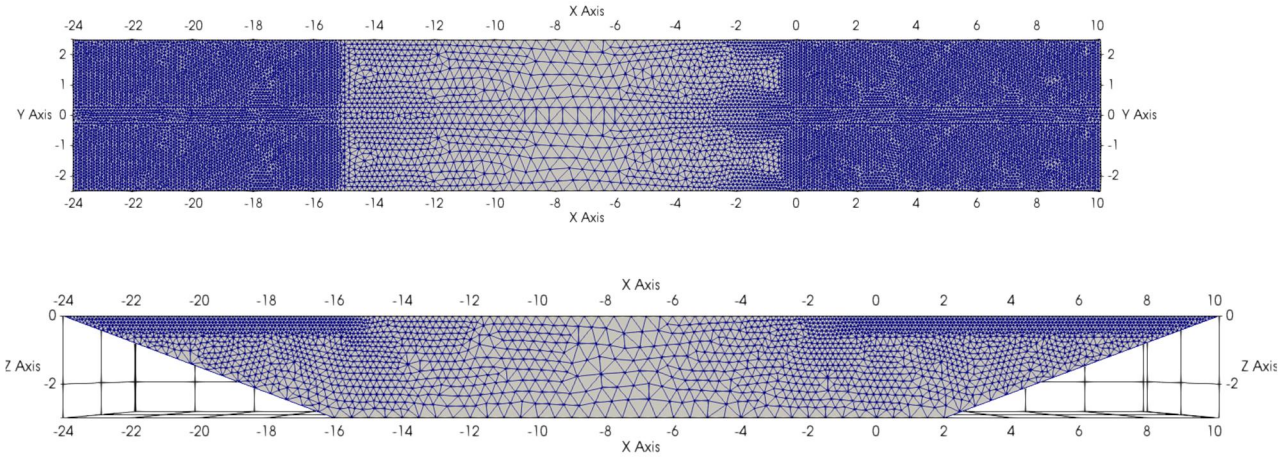

Figure B.3 Mesh of the 3D Delta Flume model, local refinements are on the surface on the sides of the upstream and downstream boundary conditions and the mesh gradually coarsens away from these surfaces

B.4 Results

B.4.1 Head profile

The modelled head profile is shown in Figure B.4 as well as the measurements in the centre of the model. The model matches the measurements well, indicating that the assumption that the barrier does not strongly affect the overall profile when there is no pipe is reasonable.

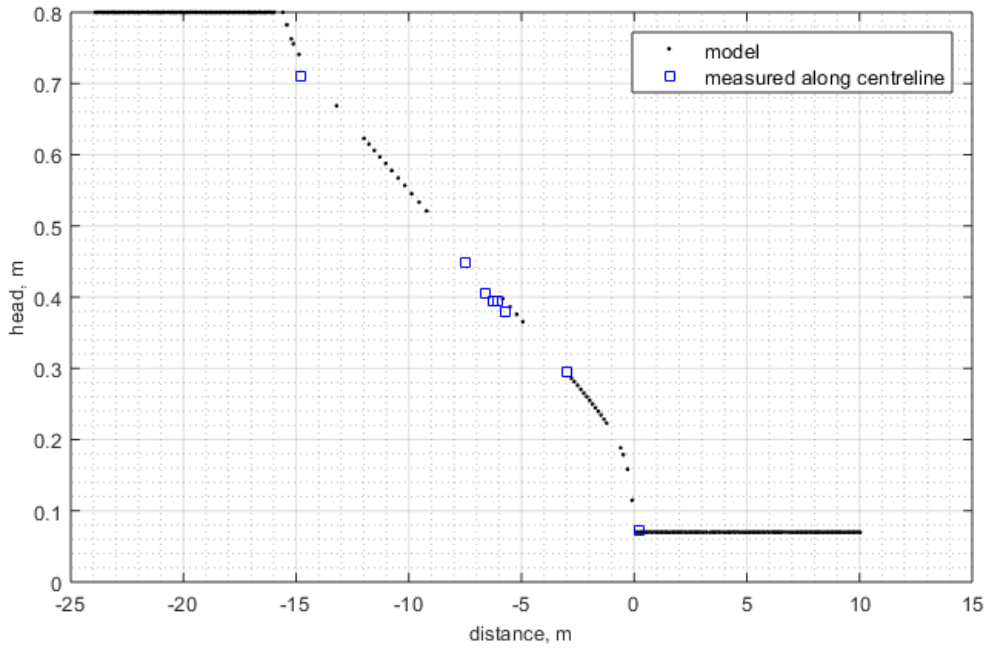

Figure B.4 Modelled head profile in the second Delta Flume test and measurements.

B.4.2 Hydraulic conductivity

The inflow rate in the model is computed by integrating the nodal flow rates over the inflow area. This yields the same result as integrating the nodal flow rates over the outflow area, which indicates the boundary conditions were applied correct. The hydraulic conductivity of the background sand is modified to match the measured inflow rate of 2.521 l/min. This results in an intrinsic permeability of 9.95 e-11 m/s, or a hydraulic conductivity of 7.69e-5 m/s (with fluid density of 999.6 kg/m^3, and viscosity of 1.2695 mPa.s for the temperature of 11^{o}C during this experiment).

The porosity and relative density of the background sand can then be computed by using the results from the column permeability experiments on the background sand. In those tests, a linear relation was fit between porosity and hydraulic conductivity: $k = 0.0025n - 0.0008$, this results in a porosity of the background sand of ca. 0.359, corresponding to a relative density (based on porosity with $n_{min} = 0.345$ and $n_{max} = 0.453$) of 87%.

There is some uncertainty involved in this estimate: it is assumed that the small sample that was tested in the column tests is representative for the entire sand body whereas there may be some variation in this, the hydraulic conductivity is assumed to be homogeneous and isotropic in the model, and there is measurement uncertainty in the transducers and in the flow rate measurement. Therefore, this computation can be considered as giving an indication that the relative density is in the order of 85 %.

B.4.2.1 Comparison to measurements at the start of the test

Samples of the background sand were taken at the start of the experiments to determine the relative density. Those indicated values of RD ranging from 0.35 to 0.65, this is significantly lower than the estimates of RD that were determined from samples at the start of the experiment. This discrepancy might be in part due to the uncertainty in those RD measurements. The material contains shell fragments and was difficult to sample.

Besides this it is possible that the saturation during the test was not 100%, which would also reduce the hydraulic conductivity. Another cause could be that there was a lower permeability at the upstream surface of the sand body, if a thin layer of finer material were present there. That would also account for the lower head that was measured in the transducer that is furthest upstream.

Therefore, the relative density of the background sand based on the modelled hydraulic conductivity is only an indication, the hydraulic conductivity does correspond to the flux and heads in the model, which is relevant for the analysis.

C Modelling only the pipe at the barrier

This appendix addresses the representation of the pipe downstream of the barrier. In the 2D medium-scale models, the pipe is modelled from the outlet hole to the barrier. This would correspond to an infinitely wide pipe in a 3D model. Especially on larger scales, such as the Delta Flume scale this would not be realistic. Therefore, the Delta flume test was modelled in this report with a pipe only over a limited distance of 0.3 m in front of the barrier. This would correspond to a pipe that had progressed parallel to the barrier in a 3D situation. Although excavations indicate that in the actual test, the pipe only progressed parallel to the barrier over a very limited distance, this approach is considered most appropriate. However, the width of the pipe parallel to the barrier is unknown. Therefore, this appendix analyses the effect of modelling a pipe over different distances in front of the barrier, i.e. varying the outflow distance in 2D models.

This sensitivity analysis addresses the effect of modelling a pipe of 0.10 m and 0.30 m downstream of the barrier, and of modelling a 16 m pipe from the barrier to the outflow hole. The model is similar to the model that was used in the main report, however, the length is smaller (the top length of the model is from +5 to -20 m (relative to the ditch) and the bottom of the model is from -1 to -14 m). Depth and dimensions and location of the barrier relative to the outlet hole are the same.
The pipe length inside the barrier is 4 cm. Results for two hydraulic conductivity contrasts are shown, of 7.0 (hydraulic conductivity of the background sand 1.0 e-4 m/s and hydraulic conductivity of the barrier 7 e-4 m/s) 11.3 (hydraulic conductivity background sand 1.0 e-4 m/s and hydraulic conductivity of the barrier 1.1 e-3 m/s.

The schematisation with the 0.3 m wide pipe is shown in Figure C.1.

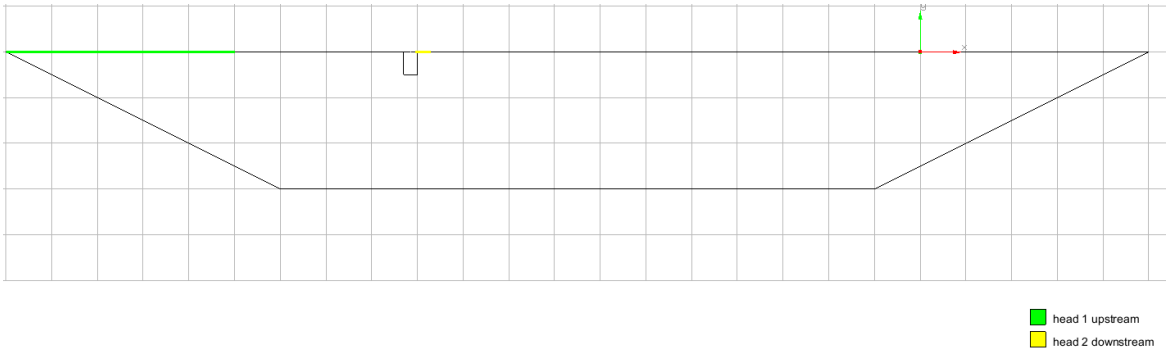

Figure C.1 Schematisation of Delta Flume model with 0.3 m pipe width in front of the barrier.

Due to the narrower pipe, the flow profile is different as shown in Figure C.2.

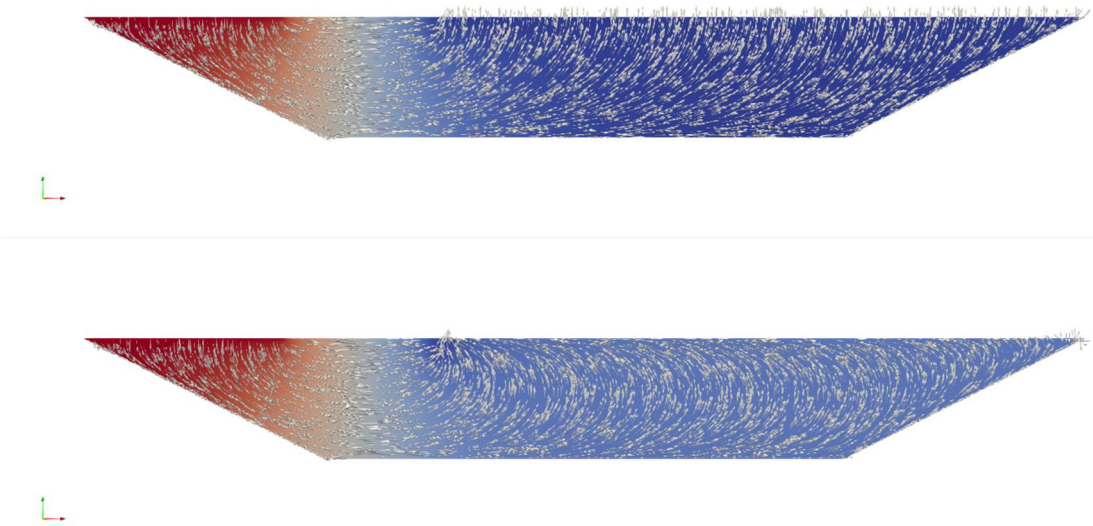

Figure C.2 Velocities indicate flow rate for models with hydraulic conductivity contrast of 11.3 with an outflow boundary from the ditch to the barrier (top) and with an outflow boundary of 0.3 m only at the barrier (bottom).

The modelled head profile inside the barrier is shown in Figure C.3. The modelled flow rates are shown in Figure C.4.

C.1 Conclusions

With a shorter downstream boundary condition, a higher hydraulic conductivity inside the barrier is required in order to achieve the same gradient inside the barrier. The flow rate modelled with a shorter outlet boundary is smaller than with the longer outlet boundary, however the effect on the modelled flow rates is relatively small. This means that when a field situation is modelled, with a given hydraulic conductivity of the barrier and therefore a fixed contrast, the modelled gradient inside the barrier will be higher when a shorter pipe is modelled in front of the barrier. This would give a more conservative result.

The effect of the pipe length inside the barrier was not analysed here, increasing this length will reduce the gradients in the barrier, and probably also the effect of the barrier length in front of the barrier, as the outflow area is increased.

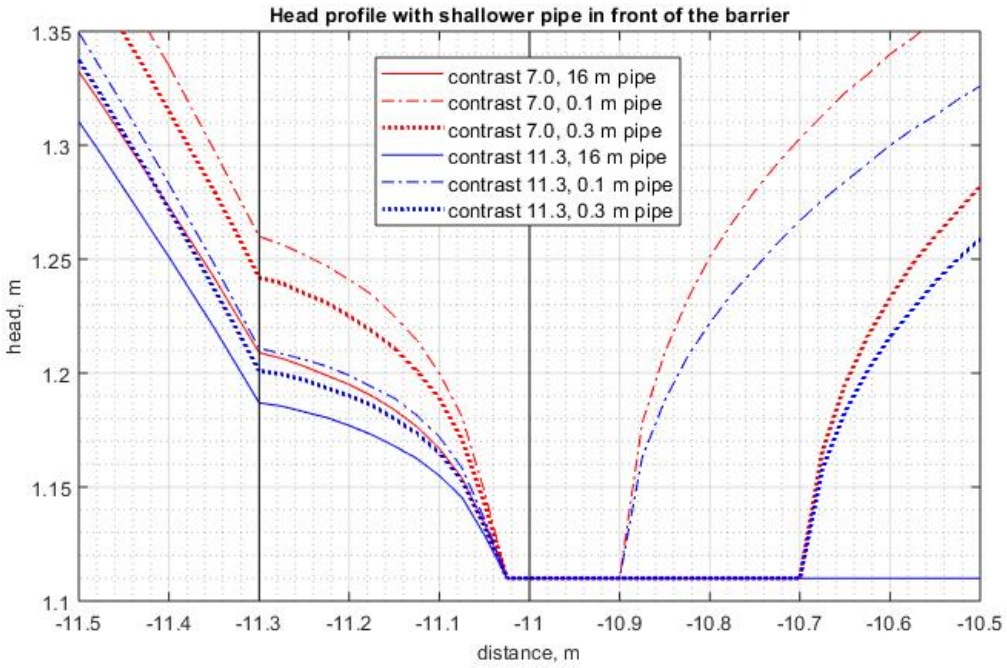

Figure C.3 Modelled head profiles for Delta Flume test 2 for barrier with 4 cm pipe length inside the barrier.

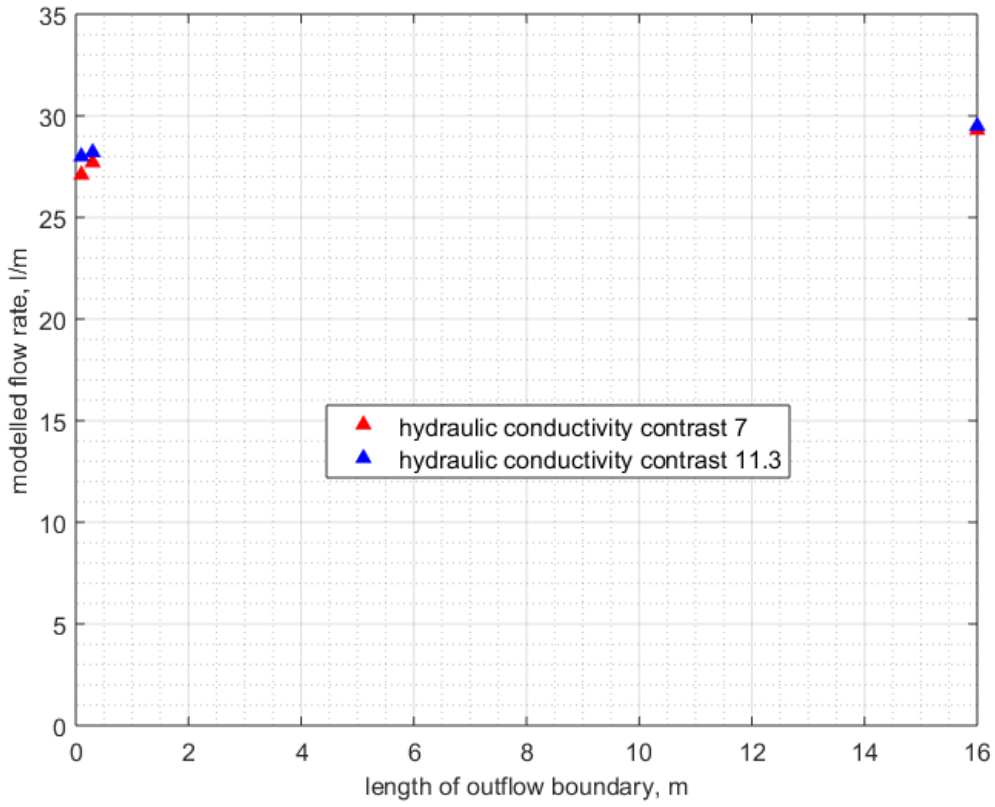

Figure C.4 Modelled flow rate with different lengths of outflow boundary,

D 3D model for Delta Flume test 2

This appendix presents the model schematisation for the 3D model of the second Delta Flume test.

D.1 Geometry schematisation

Only the sand body, not the cohesive cover layer, is modelled. As in the 2D models, the end of the ditch is the centre of the axis system and the sand body is present between x = -24 and x = 10.1 m. The maximum depth of the model is 3 m and the sides slope with a 2.67:1 slope, so that the bottom of the model is 18 m long. The model is 5 m wide. Figure B.1 shows the model.
The barrier is 0.5 m deep and 0.3 m thick.

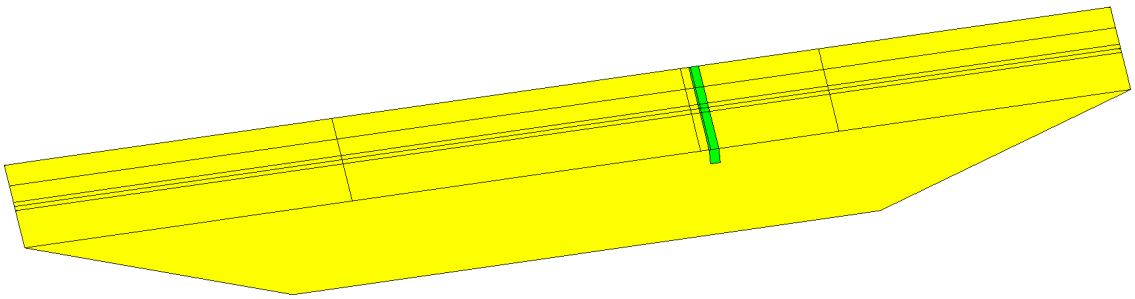

Figure D.1 Model of the sand body for the second Delta Flume test. Background sand (yellow) barrier (green)

D.2 Boundary conditions

The model is made for the critical point for pipe progression, based on measurements the pipe extent in front of the barrier was estimated to be approximately between the centre of the model and side #3 and not at sides #2 and #8. In terms of y coordinates this is from y = 0 to y = 1.25 m.
The extent of the pipe in the barrier is the same as in the 2D model, 0.05 m in the barrier, and 0.26 m in front of the barrier. This is from x coordinates x = -10.74 m to x=11.05 m.
The inflow area is from y = -24 m to y = -15.0 m as in the 2D model.
The ditch is 0.5 m wide, so from y coordinates y = 0.25 m to y = -0.25 m, and from x coordinates x = 10.1 m to x = 0 m.
Between the ditch and the pipe one straight pipe is assumed with a width of 0.25 m (running from y = 0 m to y = 0.25 m, and x = 0 m to x = -11.74 m).

The heads in the boundaries are the same as in the 2D model based on measurements for the critical point:

- Upstream 2.92 m (based on h99)
- Pipe at barrier and pipe from ditch to barrier 1.15 m (based on h43)
- Ditch 0.12 m (based on h09)

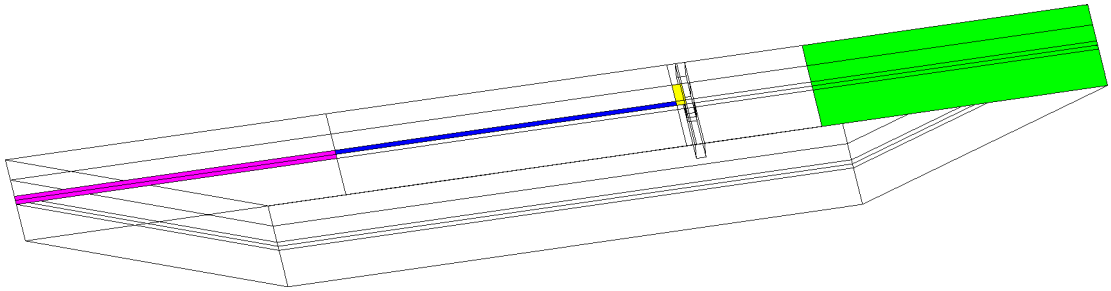

Figure D.2 Boundary conditions, upstream boundary (green) pipe at the barrier (yellow), pipe from the ditch to the barrier (blue) ditch (pink)

D.3 Mesh

Based on a preliminary mesh analysis, an unstructured mesh is used with a basis element size of 0.4 m, whereby a local refinement is applied on the top surface of the model on the elements that are in the barrier at the location where pipe progression occurred. (i.e. from x coordinates x = 0 m to x = 1.25 m and y = -11.0 m to y = 11.3 m). Here elements have a size of 0.02 m. There is a gradual transition from the zone of high mesh refinement to the rest of the model.

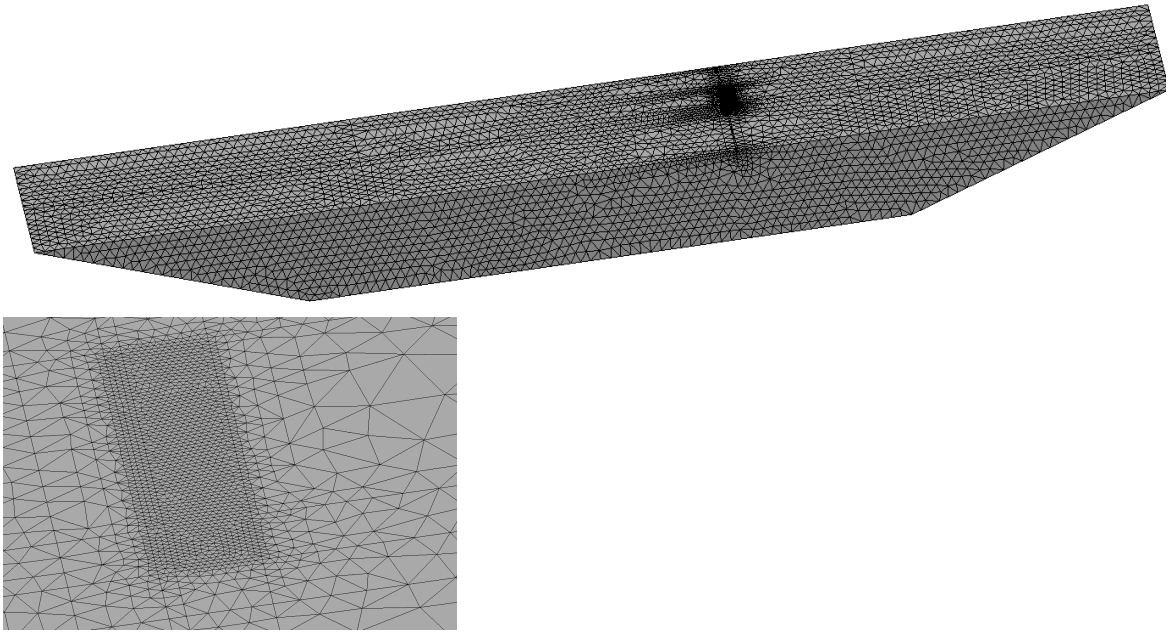

Figure D.3 Mesh for 3D model of second Delta Flume test, top overall view, bottom close-up of local refinement

D.4 Material parameters

The hydraulic conductivity of the background sand is the same as in the 2D model (based on a 3D model for the first Delta flume test), 8.57e-5 m/s. One computation is done with the same hydraulic conductivity that was found best in the 2D model, 6.85e-4m/s (i.e. contrast 8).
A second computation is done with a contrast of 20, a barrier conductivity of 1.69e-3 m/s. This would correspond to a barrier with RD 0.25 which is considered to be the lower limit that might be possible. As the barrier was densified, an of 0.74, as indicated by samples of the first Delta Flume test seems more realistic.